Fluid saturation and volatile partitioning between melts and hydrous fluids in crustal magmatic systems: The contribution of experimental measurements and solubility models

Don R. Baker, Marina Alletti

Fluid saturation and volatile partitioning between melts and hydrous fluids in crustal magmatic systems: The contribution of experimental measurements and solubility models

Don R. Baker[1] and Marina Alletti[2]

[1]Department of Earth and Planetary Sciences, McGill University
3450 rue University, Montreal, QC, CANADA H3A 2A7
phone: 1-514-398-7485, fax: 1-514-398-4680
don.baker@mcgill.ca
(corresponding author)

[2]Université d'Orléans, CNRS/INSU
Université François Rabelais - Tours
Institut des Sciences de la Terre d'Orléans - UMR 6113
Campus Géosciences, 1A, rue de la Férollerie
45071 Orléans cedex 2 FRANCE
marina.alletti@tin.it

Initial submission: 25 September 2010
Reviews on 1st draft received: 15 April 2011
Revision submission date: 10 September 2011
Reviews of 2nd draft received 15 June 2012
Final submission date: 16 June 2012

submitted to:
Earth-Science Reviews

Abstract

This work reviews the experimental constraints on the concentrations of volatiles that can be expected in melts found in the crust and the saturation of such melts with a separate fluid phase. After presenting evidence for volatile concentrations in magmatic source regions in the crust and upper mantle and discussing volatile concentrations in magmatic systems, experimental results on the solubility and partitioning of H_2O, CO_2, S, Cl, F and a few other minor volatiles at pressures up to 800 MPa are summarized. Many of the important models used to predict the solubility and partitioning of these volatiles are then introduced and two models, both easily available for use, are compared against experimental data. Finally, a model of isothermal, closed system ascent of a granitic composition magma with water, carbon dioxide and chlorine is presented to illustrate the evolution of volatiles in a crustal magmatic system and to demonstrate how this evolution may affect the formation of ore deposits and the vesiculation of ascending magmas.

Keywords: magmatic volatiles, solubility, water, carbon dioxide, sulfur, halogens

Table of Contents

1. Introduction

Magma ascent from depth to the near-surface, or eruption on the surface, is a fundamental transport mechanism of the volatiles H_2O, CO_2, S, and halogens in the Earth system. Magmas ascending from the mantle transport deeply stored volatiles to shallow levels and may also extract volatiles (and other components) from the crust and transport them to near-surface environments or the hydrosphere and atmosphere during volcanic eruptions. Melt extraction from high-temperature regions of the lower crust modifies residual rock compositions and removes volatiles, leaving behind volatile-poor, granulitic residues. Indeed, mantle volatiles have been proposed as a significant source of Earth's atmosphere and oceans (e.g., Brown, 1949; Rubey, 1951; Dauphas, 2003), and magmatic systems are the most important mechanisms responsible for mantle degassing. Thus, to fully comprehend the cycling of volatile elements in the Earth system it is essential that we understand the capabilities of magmatic systems to store and transport volatiles such as water, carbon dioxide, sulfur, and halogens.

An understanding of the composition and concentration of the volatiles in magmatic melts is also needed because of the profound influence of volatiles on melt properties. The concentrations of volatiles dissolved in silicate melts affect elemental diffusion (e.g., Baker, 1991) and the viscosities of silicate melts (e.g., Giordano et al., 2008). The concentration of some volatiles, in particular

water, affect the solubilities or partitioning of other volatiles, such as CO_2, Cl, S (e.g., Holloway, 1976; Carroll and Webster, 1994; Dixon et al., 1995; Burgisser et al., 2008), and as will discussed in Section 4.8 there are effects of some minor volatile concentrations on the partitioning of other volatiles. Understanding the changing concentrations of volatiles in silicate melts during ascent and exsolution will lead to better modeling of silicate melt properties, which affect both the rates of reactions in magmatic systems as well as the style of volcanic eruptions.

This review concentrates on the solubilities of volatile components in melts at crustal pressures and temperatures and the evolution of volatile-bearing melts and fluid phases during ascent from the lower crust to emplacement in the upper crust or eruption at a volcano. The rationale for concentrating on the crust is that most magmas generated in the mantle undergo fractionation and assimilation at crustal pressures, and most intermediate to silicic magmas are created in the crust. Additionally, it is at crustal pressures where the greatest changes in most volatile solubilities occur, especially between the surface and the first few kilometers depth. Understanding the effects of pressure, temperature and composition on the solubilities of volatiles in silicate melts will enhance our knowledge of processes ranging from the formation of ore deposits to the eruption of volcanoes. This understanding will improve our ability to model the fundamental biogeochemical cycles involving volatiles found in igneous systems, such as water,

carbon dioxide, sulfur, chlorine, fluorine, bromine and iodine, many of which significantly influence the global climate.

2. The volatile budget in upper mantle and crustal lithologies

2.1 The upper mantle

The average upper mantle rock contains low volatile concentrations because of its depleted nature due to crustal extraction and differentiation. Water stored in micas and amphiboles is limited by the low concentrations of alkalies in the average upper mantle, only 100's (K) to thousands (Na) of ppm (e.g., Salters and Stracke, 2004), which are necessary for stabilizing these phases at upper mantle pressures. Calculations of the water concentration by O'Neill and Palme (1998) yielded estimates of 250 ppm H_2O in the depleted mantle and 1160 ppm H_2O in the primitive mantle. Albarède (2009) estimated a similar value of 150 to 250 ppm water in Earth's mantle. Carbon dioxide concentrations in the average upper mantle are similar to those of water, 230 to 550 ppm (Zhang and Zindler, 1993; Jambon, 1994). Hirschmann and Dasgupta (2009) provided a range of mean mantle C concentrations of 20 to 300 ppm. Lyubetskaya and Korenaga (2007) estimated the concentrations of halogens and sulfur in the primitive, undepleted mantle to be only 18 ppm of F, 230 ppm of S, 1.4 ppm of Cl, 3.6 ppb of Br, and 10 ppb of I; the depleted upper mantle is expected to contain even lower concentrations of these volatile elements.

Dunai and Porcelli (2002) summarized measurements of ^{4}He in upper mantle minerals from xenoliths and demonstrated that its concentration ranges from 10^{-9} to 10^{-5} cm^3 STP g^{-1}, where cm^3 in the units refers to the volume in cubic centimeters of gas measured at standard temperature and pressure conditions, STP, from 1 gram of rock, g^{-1}; 1 cm^3 at standard temperature and pressure conditions is equivalent to 2.6868 x 10^{19} atoms. These ^{4}He concentrations convert to mass values of ~0.1 ppt to 1 ppb. Concentrations of ^{3}He are one million times lower. Although Dunai and Porcelli (2002) do not provide concentrations of heavier noble gases in mantle materials, they are known to be less abundant than He in almost all the solar system, the occasional exception is ^{40}Ar created by the decay of ^{40}K (Porcelli et al., 2002).

However, all of these estimates are for the average mantle. It has been known for many decades that the presence of metasomatized regions in the mantle indicate that locally larger concentrations of volatiles can be stored in the mantle (e.g., Smith, 1981; Smith et al., 1981). Although metasomatized regions are probably unimportant volatile sources for the dominant igneous systems on Earth, mid-ocean ridge volcanism, they quite possibly play a fundamental role in intraplate magmatism, but the spatial extent of metasomatized regions in the mantle is unknown. Nevertheless, the analyses of Smith (1981; Smith et al., 1981) combined with the stoichiometry of micas and amphiboles, constrain the volatiles present in metasomatized regions to be similar to the maximum concentrations in the crust.

2.2 The crust

Middle to deep crustal lithologies are dominated by amphibolites and granulites, with compositions broadly ranging from anorthositic to metapelitic (Rudnick and Fountain, 1995; Taylor and McLennan, 1985, 1995; Wedepohl, 1995; Rudnick and Gao, 2003). The middle and lower crust are heterogeneous, with more silicic compositions found in the upper and middle crust, and more mafic compositions in the deep crust (Rudnick and Gao, 2003). The concentrations of volatiles in the crust have been estimated by many authors. Although there is little to no evidence for a pervasive fluid phase dominated by water and carbon dioxide at depth, in local regions such a phase may be present (e.g.,Yardley, 1986; Marquis and Hyndman, 1992). But, in most cases the average volatile concentrations in the crust are determined by the mineralogy of the rocks.

The dominant volatile-bearing phases in crustal rocks near anatectic temperatures are amphiboles and micas, which nominally can contain up to approximately 2 and 4 wt.% water, respectively. The water present in hydroxyl sites of these minerals can be at least partially replaced by halogens. Given a suitable source of halogens, some of these minerals have the potential to be completely water-free (e.g., amphibole), however it is extremely doubtful that this occurs in nature. Additional sources of water and halogens are phosphate minerals (e.g., apatite), but the low abundance of phosphate in common crustal lithologies results in a very

small contribution of phosphate minerals to the volatile budget of these rocks. Halide minerals may also contribute to the halide budget of magma systems, but their low abundance also results in small average contributions, however this does not eliminate the possibility of significant local contributions. Carbon is found in the lower crust as graphite and in carbonates, dominantly calcite and dolomite. The temperature stability of these minerals is similar to crustal melting temperatures at pressures of 1.5 GPa or less. For example the reaction of calcite+quartz to produce wollastonite plus CO_2 occurs at approximately 800 °C at 200 MPa and 1000 °C at 800 MPa, the temperature range in which meta-pelitic rocks melt (Vielzeuf and Holloway, 1988). Sulfur is dominantly found as either sulfides, FeS and FeS_2, or as anhydrite, $CaSO_4$. Nitrogen can substitute into the feldspar structure and also into micas at NH_4^+ (e.g., Honma and Itihara, 1981), but this behavior is rarely reported.

Several researchers investigated the bulk volatile concentration of the crust. Wedepohl (1995) provided an estimate of 2 wt% H_2O and 1990 ppm carbon in the continental crust, but stated that the water is mostly found in upper crustal sedimentary rocks. Rudnick and Gao (2003) estimated the concentrations of fluorine in the crust to vary from 557 ppm in the upper crust, to 524 ppm in the middle crust and 570 ppm in the lower crust, with an average of 553 ppm for the entire crust. Chlorine concentrations provided by these authors were 294 ppm in the upper

crust, 182 ppm in the middle crust and 250 ppm in the lower crust; this yields an average of 244 ppm (Rudnick and Gao, 2003). These authors also estimated sulfur concentrations of 621, 249 and 345 ppm in the upper, middle and lower crust, respectively; their bulk crust contains 404 ppm S. Bromine and iodine were estimated by Rudnick and Gao (2003) to occur in the bulk crust at concentrations of 0.88 and 0.71 ppm, respectively; they estimated an average crustal concentration of 56 ppm N.

The source of noble gases in the lower crust is most probably due to degassing of the mantle and radioactive decay (e.g., Drescher et al., 1998). Ballentine and Burnard (2002) calculated the total production of noble gas isotopes in Earth's crust over the 4.5 Ga age of the Earth. Their calculations yield a crust with a He concentration of 2.5×10^{-3} cm^3 STP g^{-1}, a Ne concentration of 3.5×10^{-10} cm^3 STP g^{-1}, an Ar concentration of 1.2×10^{-3} cm^3 STP g^{-1}, a Kr concentration of 1×10^{-12} cm^3 STP g^{-1}, and a Xe concentration of 1.5×10^{-11} cm^3 STP g^{-1}. When converted into weight units the sum the concentrations of all of the noble gases is only approximately 1 ppm.

Rocks with these average volatile concentrations are most probably the source rocks for the anatectic melts forming in Earth's crust, however, just as in the upper mantle, locally the compositions of crustal rocks may be significantly different

from these averages.

2.3 Melting and volatile extraction

Most of the crust and mantle is considered to be fluid undersaturated, in such a case volatile-bearing minerals, particularly micas and amphiboles, melt at or near the solidus releasing their volatiles into the melt and possibly into a separate fluid phase (with a density near that of silicate melts) at high pressures or a gas phase (with a density significantly below silicate melts) at low pressures (e.g., Olafsson and Eggler, 1983; Clemens and Vielzeuf, 1987; Vielzeuf and Holloway, 1988; Patiño-Douce and Johnston , 1991; Skjerlie et al. 1993, Wolf and Wyllie, 1991; Rapp and Watson, 1995; *inter alia*). However, with increasing degrees of melting most of the volatile components discussed may be dissolved into the melt. However the presence of even relatively small quantities of CO_2 in the source rocks favor the existence of a separate fluid or gas phase into which all volatile components must partition at equilibrium conditions. On the other hand, in the absence of a separate fluid phase at high pressure the volatile components are transported by the melt to shallower depths where the solubilities become low enough that a separate fluid or gas phase exsolves from the melt. Detailed modeling of this process is delayed until section 6 of this paper, after the reader is introduced to the solubilities and partition coefficients that are necessary for quantitative

calculations.

3. Volatile components in igneous systems

Studies of melt inclusions trapped in silicate minerals and volcanic gases reveal that the volatile components in magmatic melts typically are dominated by those present in the system C-O-H (e.g., Johnson et al., 1994; Symonds et al., 1994; Hauri, 2002). In a C-O-H fluid phase, the species are predominantly H_2O and CO_2 at oxygen fugacities near the fayalite-quartz-magnetite buffer, FMQ, although CO, CH_4 and H_2 can be present in the fluid at some conditions of oxygen fugacity (Carroll and Holloway, 1994). In silicate melts, the components OH^-, H_2O^m (molecular water dissolved in a silicate melt), CO_2, CO_3^{2-}, CH_3^-, CH_4, and H_2 may be present (Carroll and Holloway, 1994). The concentration of total water (the sum of OH^- and H_2O^m species), H_2O^{total}, dissolved in terrestrial magmatic melts varies from the order of thousands of ppm in ocean-floor basalts to many weight percent in some granitic melts (e.g., Holtz et al., 2001; Hauri et al., 2002). Even some basaltic glasses from Earth's moon are estimated to contain 700 ppm total water (Saal et al., 2008). At low total water concentrations the dominant species is OH^-, but as water concentrations increase, the concentration of H_2O^m rapidly exceeds that of hydroxyl; the total water concentration at which this occurs as measured in quenched melts is approximately 3 wt% (e.g., Stolper, 1982; Acocella et al. 1984), although in-situ measurements demonstrate that ratio of OH^- to H_2O^m varies with

temperature and pressure (Nowak and Behrens 1995, 2001; Behrens and Nowak, 2003). There is an effect of melt composition on the relative proportions of the two species (Silver et al., 1990), but that effect remains under investigation and is complicated by changes in the proportion of the two species during quenching, as shown by the few in-situ measurements (e.g., Shen and Keppler, 1995; Nowak and Behrens 1995, 2001; Behrens and Nowak, 2003).

The concentration of total carbon as CO_2^{total} varies from only 10's of ppm to 10's of thousands of ppm in common igneous rocks (e.g., Hauri et al., 2002), but even greater concentrations are found in carbonatitic, kimberlitic, and associated alkalic rocks. In basaltic melts near the FMQ buffer, carbon was found as both CO_2 and CO_3^{2-} species (Fine and Stolper, 1985/86), but as melts become more silicic the CO_2 species become abundant and CO_3^{2-} species disappear (Fine and Stolper, 1985; Fogel and Rutherford, 1990; Brooker et al., 1999, 2001a,b). At oxygen fugacities orders of magnitude below the FMQ buffer where CH_4 may be present in a coexisting fluid, the melt dissolves very little or no methane (Jakobsson and Holloway, 1986; Morizet et al., 2010).

In addition to the species in the C-O-H system, magmas contain minor amounts (10's to 1 000's of ppm) of the volatile elements N, F, S, Cl, Br, I, and the noble gases (He, Ne, Ar, etc.). In some cases melts with these relatively low concentrations

coexist with fluids that contain substantial concentrations of these elements, up to 0.5 mole fraction, but more commonly the concentrations are below a mole fraction of 0.15 (Carroll and Holloway, 1994; Carroll and Webster, 1994; Symonds et al., 1994; Aiuppa et al., 2009). The concentrations of these minor elements in melts, especially Cl and S, may in some melts exceed those of CO_2 (e.g., Wallace, 2005). Although many of these elements are important in ore forming processes and affect the degassing behavior of silicate melts, we know much less about their behavior than the C-O-H system.

The concentrations of F and Cl in most igneous rocks are less than 5 000 ppm, whereas Br and I appear to only be present at concentrations near 100 ppm (Aiuppa et al., 2009 and references therein). Fluorine appears to substitute for oxygen in $(Si,Al)O_4^{4-}$ tetrahedral units or is associated with alkalies in aluminosilicate glasses, which are presumed to preserve melt structure (Kohn et al., 1991; Schaller et al., 1992; Zeng and Stebbins, 2000; Liu and Nekvasil, 2001; Mysen et al., 2004; Kiprianov and Karpukhina, 2006). The dissolution mechanisms of chlorine are poorly understood, but Cl appears to be associated with network-modifying cations (e.g., Na, K, Ca, Mg) in the melt (Chevychelov 1999; Chevychelov and Suk, 2003; Chevychelov et al., 2003; Sandland et al., 2004).

Sulfur concentrations in igneous rocks range from less than one hundred ppm (e.g.,

Jambon, 1994; Wallace, 2005) to many weight percent. Because of the ability of sulfur to form S-rich phases, such as immiscible sulfide droplets, sulfide minerals, or sulfate minerals, the concentrations of sulfur in igneous, ore-deposit rocks can reach values close to those of pyrrhotite, ~ 37 wt.% S, but such igneous rocks are clearly cumulate in origin (Naldrett, 1989) and do not represent silicate melts (although they may very well represent sulfide melts).

Sulfur concentrations in natural silicate melts (as opposed to rocks discussed in the preceding paragraph) range from 10's to 1000's of ppm (e.g., Jambon, 1994; Wallace, 2005) and are often controlled by the saturation of the silicate melt with crystalline or molten FeS (e.g., Haughton et al., 1974). Although the sulfur species in magmatic fluids are H_2S, SO_2 and S_2 (see Symonds et al., 1994; Clemente et al., 2004), sulfur is dissolved in silicate melts predominantly as sulfide, S^{2-}, at oxygen fugacities near the FMQ buffer and below; at oxygen fugacities approximately 2 orders of magnitude higher, most of the dissolved sulfur is found as sulfate, SO_4^{2-} (e.g., Fincham and Richardson, 1954; Katsura and Nagashima, 1974; Carroll and Rutherford, 1985, 1987, 1988; Carroll and Webster, 1994; Clemente et al., 2004; Jugo et al., 2005; Moretti and Baker, 2008; Wilke et al., 2011). At these high oxygen fugacities, commonly only found in subduction-related magmas, the concentrations of sulfur can reach the weight percent level before saturation with anhydrite occurs (Carroll and Rutherford, 1985, 1987, 1988; Luhr, 1990; Carroll and

Webster, 1994; Clemente et al., 2004; Jugo et al., 2005, Baker and Moretti, 2011).

Many measurements of the isotopic ratios of noble gases in igneous rocks and meteorites have been made, but the concentrations of the individual gases in igneous rocks are more rarely reported. This lack of concentration data stems from the incompatible nature of the noble gases that results in their loss during crystallization and incorporation into the fluid phase or post-crystallization loss due to weathering reactions (Porcelli et al., 2002). However rocks which have lost some of their noble gases can still yield useful noble gas isotope ratios, although it may be necessary to correct them for fractionation (e.g., Burnard, 2001). Noble gas isotopic ratios in fluids associated with igneous rocks can also be measured to constrain the ratios in the rocks (Hilton et al., 2002). Noble gas isotopic ratios can be extremely useful in the interpretation of petrogenetic processes, but they are not the subject of this paper; readers interested in this topic are referred the review edited by Porcelli et al. (2002). The best candidates for analyzing noble gas concentrations are rapidly cooled basalts quenched at high pressure that minimize volatile loss, typically found on the ocean floor as both normal mid-ocean ridge basalts and ocean island basalts.

Although dated, Sarda and Graham (1990) provide a concise summary of noble gas concentrations in ocean floor rocks. The average concentrations in mid-ocean ridge

basalts are lowest for ^{130}Xe, with a value of 4.6×10^{-14} cm^3 STP g^{-1}. With decreasing atomic number the average concentrations increase; the average for ^{84}Kr is 2.4×10^{-12}, for ^{36}Ar is 5.3×10^{-11}, for ^{20}Ne is 1.6×10^{-10}, and for ^{3}He is 1.8×10^{-10} cm^3 STP g^{-1}. Measurements of these isotopes concentrations in samples of Loihi seamount demonstrated enrichment in the heavier elements, but depletion in the lighter ones; noble gas concentrations in the "popping rocks" from the mid-Atlantic ridge were enriched by factors of 3.8 to 31.6 compared to the mid-ocean ridge average (Sarda and Graham, 1980). Carroll and Draper (1994) summarize noble gas analyses of igneous crystals and show that these concentrations vary from approximately 10^{-4} ppt to the ppb level. Recently Nauret et al. (2010) demonstrated that rocks from Arctic ocean spreading ridges contained ^{4}He and ^{40}Ar concentrations that varied from ~1 to ~9×10^{-6} cm^3 STP g^{-1}, whereas ^{22}Ne, ^{36}Ar, ^{84}Kr, and ^{130}Xe concentrations were typically 3 to 6 orders of magnitude less abundant in the rocks.

4. Melt/fluid saturation, solubility and partitioning measurements

Before the start of the presentation of experimental measurements on the behavior of volatiles in silicate melts it is necessary to explain a few terms that are repeatedly used in the literature.

The first term to consider is saturation. Saturation refers to the condition where

two phases coexist at equilibrium; a simple example relevant to this paper is a fluid-saturated melt. Note the use of terms that define phases (fluid and melt) rather than components (e.g., H_2O and SiO_2). (In general fluid will be used in the following review and discussion to save space, but the reader should realize that in most cases the term gas can be used at low pressures.) When the fluid is composed of pure H_2O the melt can be considered water-saturated, or if the fluid is pure CO_2 it can be considered CO_2-saturated, but this in not the case for a H_2O-CO_2 fluid. Nevertheless, such a melt is still defined to be fluid-saturated.

The second term to discuss is solubility. Solubility is the concentration of a substance that can dissolve into a solvent. This definition implicitly assumes the presence of two phases, one that is dissolving and the other that is the solvent. This paper reviews the solubilities of volatile species commonly present in relatively large concentrations in a fluid or gas (the dissolving phase) in a silicate melt (the solvent). When the fluid is pure, such as in the examples above, the solubility value is the same as the concentration in the melt at fluid saturation, but for impure fluids the solubility will be different than for pure fluids as demonstrated below. In the case of impure fluids, particularly when the volatile of interest is present at relatively low concentrations, the term partitioning is used to describe the behavior of the volatile component in the fluid and in the melt. This term is closely related to solubility and refers to

the relative distribution of a component between two phases (usually at equilibrium). Partitioning is commonly quantified by the Henrian partition, or distribution, coefficient, D, which is calculated by dividing the concentration of a species in one phase by its concentration in the coexisting phase. Thermodynamically, the distribution of each component between the fluid and the melt is driven by the requirement that the chemical potential of a component in a system at equilibrium must be equivalent in all phases within that system; this requirement controls the solubilities of all volatiles in silicate melts and their partitioning between the melt and the fluid phase.

4.1 Water

The solubility of water in silicate melts has been studied since the 1930's, when Goranson published his studies of water solubility in granitic and albitic ($NaAlSi_3O_8$) melts (Goranson, 1931, 1938). Since that time there have been hundreds of studies on water solubility in magmatic melts. Unfortunately there is not enough space to reference all of the available publications on volatile solubilities in silicate melts. Instead, only selected studies that measured volatile saturation and solubility in magmatic melt compositions found at crustal conditions of temperature and pressure will be cited.

Many of the early studies on compositionally simple melts demonstrated that the saturation concentration of water for silicate melts was linearly proportional to

the square root of the pressure (e.g., Tomlinson, 1956; Kurkjian and Russell, 1958) or the square root of the water fugacity. This behavior was interpreted to indicate the complete disproportionation of water in the melt to hydroxyl species:

$$H_2O^{fluid} + Si\text{-}O\text{-}Si^{melt} \rightleftharpoons 2\ Si\text{-}O\text{-}H^{melt}, \quad (1)$$

which implies that we can write the equation for the equilibrium constant, K, of this reaction as

$$K = \frac{\left(Si-O-H^{melt}\right)^2}{f_{H_2O}^{fluid}\left(Si-O-Si^{melt}\right)}, \quad (2)$$

where the parentheses represent the activities of the components and f represents fugacity. This equation can be approximated by substitution of the concentration of water in the melt, C_{H2O}, for the activity of $Si\text{-}O\text{-}H^{melt}$; the equilibrium constant and $(Si\text{-}O\text{-}Si^{melt})$ can be combined into an empirical constant, K', dependent upon the temperature and composition of the melt, and at high temperatures water can be approximated as an ideal gas resulting in the equivalence of fugacity and pressure. These substitutions and approximations can be applied to the equilibrium constant equation above to yield a simple equation relating the square root of the water pressure in the fluid with the concentration of water in the melt:

$$C_{H_2O} = K' \ P_{H_2O^{fluid}}^{1/2} . \quad (3)$$

This concept of complete water disproportionation into hydroxyl guided experiments

and theories of water dissolution in silicate melts for many decades until spectroscopic measurements by Stolper (1982) demonstrated the presence of molecular water in magmatic silicate melts even at low total water concentrations (discussed below in section 5.1).

Many studies on the solubility of water in albitic composition melts followed Goranson's classic papers. Albitic melts were often studied as a simple analogue for granitic, or rhyolitic, composition melts and because these hydrous melts can be readily quenched to glasses. Some of the important studies on the solubility of water in albitic melts are those of Burnham and Jahns (1962), Khitarov et al. (1963), Kadik and Lebedev (1968), Boettcher and Wyllie (1969), Burnham and Davis (1971, 1974), Bohlen et al. (1982, who included CO_2 in the fluid phase), Hamilton and Oxtoby (1986), and Paillat et al. (1992). Romano et al. (1996) investigated water solubility along the joins between albitic melt and potassium feldspar melts and between each of these melts and a lithium feldspar composition melt; they were the first to clearly demonstrate the compositional dependence of water solubility along each join and found that the solubility decreased as the ionic radius of the alkali cation increased. Behrens et al. (2001) performed a similar study and found similar results, although when they substituted the larger rubidium ion for the potassium ion water solubility increased, rather than decreased. These studies demonstrated that saturation of these melts in the deep crust and upper mantle

required greater than 10 to 15 wt% water, and even at relatively shallow depths of approximately 2.7 km, or 100 MPa, a water concentration of 4 wt% in the melt is required for saturation (Fig. 1). Although water solubility is only slightly sensitive to temperature, these studies demonstrated that it is retrograde at low pressures, i.e., solubility decreases with increasing temperature, and prograde at high pressures.

The classic study on the solubility of water in SiO_2 is that of Kennedy et al. (1962). They identified an upper critical end point in the system SiO_2-H_2O that has been the focus of many studies, most recently a series of papers by Newton and Manning (e.g., Newton and Manning, 2008). Some of the studies investigating water solubility in melts formed in the silica-water system have been performed by Boettcher (1984, who also studied the solubility of H_2O+CO_2 fluids), by Pichavant et al. (1992) and by Holtz et al. (2000); the latter two studies investigated quartzofeldspathic melts. These studies demonstrate that the solubility of water in silica melts is significantly less than in feldspar melts (Fig. 2). This observation led to various interpretations concerning the mechanism of water dissolution into silicate melts, the most famous, perhaps, being that of Burnham (1975, 1979a, 1981) discussed in section 5.1.

The solubility of water in melts of mafic mineral compositions has also been

measured, but these studies are much fewer, partially because of the difficulty of quenching melts of mafic compositions to glasses. Hodges (1974) measured the solubility of water at the melting temperatures of water-saturated diopside and olivine melts at 3.0 GPa. Eggler and Rosenhauer (1978) measured the solubility of water and carbon dioxide in diopside melt by differential thermal analysis to pressures of 4.0 GPa; Eggler and Burnham (1984) added a few more measurements of water solubility in diopside melt at 200 MPa and constructed a thermodynamic model for the prediction of water solubility. There appear to be no other data on the solubility of water in melts of mafic mineral compositions.

There are many measurements of the water solubility in haplogranitic (synthetic simplified granite composition) melt compositions, which are dominated by alkali feldspar and silica components but may be modified by the addition of alkalies or of alumina. The classic paper by Tuttle and Bowen (1958) investigating the magmatic origin of granitic rocks studied the solubility of water in haplogranitic melts. More recently, many studies on the solubility of water in haplogranitic melts have been performed by F. Holtz, H. Behrens and their colleagues. Holtz et al. (1993) studied the effects of fluorine, boron and phosphorus on water solubilities in haplogranitic melts. Holtz et al. (1995) demonstrated that a haplogranitic minimum melt composition ($Qz_{28}Ab_{38}Or_{34}$) saturates with water at concentrations from approximately 2 wt% at 50 MPa to 10 wt% at 500 MPa, and that

solubility is retrograde at low pressures and prograde at high pressures (Fig. 3). Dingwell et al. (1997) measured the effects of peralkalinity and peraluminousity on water solubility in haplogranitic melts. Schmidt et al. (1999) demonstrated that as oxygen fugacity decreased, and hydrogen fugacity increased, the mole fraction of water in the fluid decreased, resulting in a concomitant decrease of water solubility in a haplogranitic melt. The measured water solubility in most of these studies was well-explained by the model of Burnham (1975, 1979a, 1981), to be discussed in section 5.1.

The water solubility in synthetic versions of more basic rock compositions has also been studied. Benne and Behrens (2003) found that the water solubility in their haplobasaltic composition was similar to previous measurements in natural basalts (discussed in this section below), within approximately 0.5 wt%. Keppler (2003) measured the water solubility in a synthetic carbonatite melt from 25 to 250 MPa at 900 ° C. He found the water solubility significantly greater than that of silicate melts at similar temperatures and pressures and determined that the water solubility (in weight percent) could be expressed by the equation: Wt% water in melt = 8.705 $P^{0.635}$; the exponent in this equation is remarkably similar to that observed for the water saturation of silicate melts at low pressures, 0.5, in Equation 3.

The water saturation concentrations of silicic composition melts (granitic or rhyolitic) have been well studied. Many studies of the phase equilibria of granitic compositions define the water saturation values at the liquidus of the rock; indeed there exist too many studies of this type to reference, but for an excellent example of these works the reader is referred to the work of Naney (1983). Instead, only a selected group of studies whose goals were the measurement of volatile solubilities at crustal conditions will be discussed (Fig. 4). One of the first studies was that of Burnham and Jahns (1962) who measured the water solubility in a melt of the Harding pegmatitic. Shaw (1974) measured water solubilities at 850 ° C in a rhyolitic melt and demonstrated that they increased from 1.3 wt% at 10 MPa to 6.0 wt% at 200 MPa. Holtz et al.'s (1993) measurements of water solubility in peraluminous Macusani rhyolite are very similar to the results of Burnham and Jahns (1962) on a pegmatitic composition. Moore et al. (1998) determined water solubilities for normal and peralkaline rhyolitic melts. Yamashita (1999) was the first to clearly document a ~ 1 wt % decrease in water solubility in natural rhyolitic melts with increasing temperature from 800 to 1200 ° C at low pressures (Fig. 4). Behrens and Jantos (2001) studied the effect of anhydrous melt composition on water solubility in granitic melts at 50 to 500 MPa, 800 ° C . Tamic et al. (2001) measured water saturation in a rhyolitic melt, which varied from 6.1 wt% at 200 MPa, 800 ° C to 11 wt% at 500 MPa, 1100 ° C. These authors also constructed an empirical equation that described water saturation in

rhyolitic melts. Liu et al. (2005) measured water saturation in silicic melts at pressures from 0.1 to 25 MPa and confirmed the retrograde solubility documented by Yamashita (1999), whereas Tamic et al. (2001) demonstrated that by pressures of 500 MPa the solubility of water in rhyolitic melts increased with temperature. The measurements of water solubilities in various silicic melts demonstrate that at a given pressure the variation in water solubility at different temperatures is typically less than 1 wt%, similar to the observations Holtz et al. (1995) made on haplogranitic melts (Fig. 3).

The water solubility in common intermediate composition melts is less well known than in silicic ones (Fig. 5). Surprisingly only a few of measurements of water saturation in common andesitic melts are in the literature (Hamilton et al., 1964; Moore et al., 1998; Botcharnikov et al., 2006). More measurements have been made of water solubilities in alkali-rich intermediate melts such as phonolitic (Moore et al., 1995, 1998; Carroll and Blank, 1997; Schmidt and Behrens, 2008) and trachytic compositions (Moore et al., 1995, 1998; Di Matteo et al., 2004). Isobaric solubility measurements for intermediate melt compositions plot within a narrow band, within approximately 2 wt.% H_2O at its widest. The differences in water solubilities are due to both temperature and composition effects. Schmidt and Behrens (2008) demonstrated that the solubility in a phonolitic melt at low pressures decreases with increasing temperature, as seen in silicic melts. Water

saturation in these intermediate melts is clearly affected by the alkali concentration; the phonolitic melts display water solubilities measurably above those of the andesitic melts determined by Hamilton et al. (1964), Moore et al. (1998) and Botcharnikov et al. (2006).

The measurement of water solubilities in natural mafic melt compositions has not been neglected, even if it is generally agreed that few, if any mafic magmas on Earth are saturated with a pure-water fluid phase. Hamilton et al. (1964) published the first measurement of water solubility in a basaltic melt (Fig. 6). Kadik and co-workers confirmed these measurements and extended the data to higher pressures (Kadik and Lebedev,1968; Kadik et al., 1971; Khitarov and Kadik, 1973). The study of Dixon et al. (1995) was a major advance because it provided the data for their thermodynamic model for water solubility. In the same year, Moore et al. (1995) published their study of water solubility in various melt compositions, including mafic ones, together with their empirical model for the prediction of water solubility; these results were updated in Moore et al. (1998). Pineau et al. (1998) measured both the water solubility and the D/H fractionation between fluid and melt for basaltic andesite compositions at 50 to 300 MPa; their solubility results were similar to those of Hamilton et al. (1964). Berndt et al. (2002) measured the water solubility in a MORB basalt and further substantiated the previous solubility measurements on basaltic melts. Recently Shishkina et al.

(2010) measured the water saturation values of a tholeiitic basalt a pressures from 50 to 500 MPa; their results are consistent with all prior measurements on similar compositions (Fig. 6). Shishkina et al. (2010) demonstrated that water solubility in basaltic melts could be related to the pressure by a power law up to 500 MPa; the power-law exponent was 0.58, quite close to the theoretical value of 0.5 discussed above (Eqn. 3).

Water saturation in a few alkali-rich mafic magmas was measured by Moore et al. (1995, 1998). Comprehensive studies of water saturation in shoshonitic and latitic melts were performed by Di Matteo et al (2006), and Behrens et al. (2009) studied the water saturation of a phonotephritic melt (Fig. 6). The water saturation of shoshonitic melts was also studied by Vetere et al. (2011) whose results were similar to previous studies (Fig. 6) and agreed with the empirical equation for pure water solubility proposed by Tamic et al. (2001). Lesne et al. (2011a) studied the water saturation of three alkali basaltic melts (one each from Vesuvius, Etna and Stromboli) and demonstrated that these melts' water solubilities were higher than low-alkali basaltic melts (Fig. 6). Curiously, the water solubilities measured by Lesne et al. (2011a) are higher than some of those found by other researchers for more alkali-rich mafic melts.

Despite the compositional range in the mafic melts investigated, the water

concentrations at a given pressure only vary by a maximum of ~ 1.5 wt%. With only two exceptions, at pressures above 400 MPa, the addition of alkalies to mafic melts does not have a significant effect on water solubility. The exceptions are the alkali basaltic melts investigated by Lesne et al. (2011a) at 400 MPa and the phonotephritic melt studied by Behrens et al. (2009) at 500 MPa. However the latter authors suggested that their highest pressure results may not be reliable because of quench problems.

We currently have a good understanding of the water solubilities in most common igneous melts ranging from basaltic to rhyolitic, as well as in many more exotic compositions. The range of isobaric water saturation concentrations in the melts is rather small considering the varied compositions investigated. These experimental data form the basis for the various models available to predict the water solubility in magmatic melts discussed in Section 5.1.

4.2 Carbon dioxide

Carbon dioxide saturation concentrations at crustal pressures in most silicate magmas are one to two orders of magnitude below those of water. Consequently, measurement is much more difficult except at high pressures where the solubility of CO_2 becomes significant. The first experiments were at approximately 1.0 to 3.0 GPa and found CO_2 concentrations in saturated glasses at the weight percent level

(this early work is summarized and reviewed in Mysen, 1977). However, the analytical techniques used to measure carbon in some of the early studies in the 1970's appear to be problematic (Tingle, 1987). Although Fine and Stolper (1985) were the first to systematically apply infrared spectroscopy to the study of CO_2 solubility in compositionally simple aluminosilicate melts, Stolper and Holloway (1988) were the first to study CO_2 solubility in natural basaltic melt compositions at low pressures using infrared spectroscopy to characterize their quenched glasses (Fig. 7); this technique is now accepted as the most accurate available.

Infrared spectroscopic measurements indicate that the most abundant species of carbon in magmatic melts at common igneous oxygen fugacities are molecular carbon dioxide, CO_2^{melt}, and carbonate, $CO_3^{2-,\,melt}$ (e.g., Fine and Stolper, 1985, 1986/86; Stolper and Holloway, 1988; Brooker et al., 1999, 2001a,b; King and Holloway, 2002). These species abundances can be related through the reactions such as (see Fine and Stolper, 1985):

$$CO_2^{fluid} \Leftrightarrow CO_2^{melt} \tag{4a}$$

and

$$CO_2^{melt} + O^{2-,melt} \Leftrightarrow CO_3^{2-,melt}\,. \tag{4b}$$

The dominant carbon species in mafic melts is $CO_3^{2-,\,melt}$, with very little to no CO_2^{melt} present, but with increasing silica concentrations the molecular CO_2 species replaces carbonate as the most abundant one (Fine and Stolper, 1985, 1986/86;

Stopler and Holloway, 1988; Brooker et al., 1999, 2001a,b; King and Holloway, 2002).

Fogel and Rutherford (1990) measured CO_2 saturation values in a rhyolitic melt and discovered concentrations similar to those found by Stolper and Holloway (1988) in a basaltic melt. Mattey (1991) discovered that CO_2 solubilities in a basaltic melt at 1400 ° C were broadly consistent with previous studies and increased from 1600 ppm at 500 MPa to 1.5 wt% at 2.0 GPa. Pan et al. (1991) found that the solubility of CO_2 in a tholeiitic melt increased from 543 ppm at 100 MPa to 1.21 wt% at 1.5 GPa. Within their quoted analytical uncertainties of ± 15% relative concentration (Fig. 7), there is no evidence of a temperature effect on CO_2 solubility between 1400 and 1600 ° C. Pawley et al. (1992) studied the effect of oxygen fugacity on carbon species dissolution into a mid-ocean ridge basaltic melt at pressures from 50 to 150 MPa. They found that the mole fraction of dissolved CO_2 was linearly related to the fugacity of CO_2 and that at low oxygen fugacities (4 orders of magnitude below the nickel-nickel oxide buffer, NNO-4) the solubility decreased because the fluid is dominated by CO and the dissolution of CO into the melt requires reduction of another species in the melt, unlike CO_2 dissolution.

Brooker et al. (1999) demonstrated that although the solubility of carbon dioxide in anhydrous aluminosilicate melts increases with pressure (as known from earlier

studies), the fraction of dissolved molecular CO_2 decreases as pressure increases from 1.5 to 2.5 GPa. In contrast to Pan et al. (1991), Brooker et al. (1999) demonstrated that total CO_2 solubility decreased slightly with increasing temperature at the high pressures investigated. Brooker et al. (2001a) investigated carbon dioxide solubility under anhydrous conditions in a suite of simple compositions, as well as in 2 melilititic (one Ca-rich and the other Na-rich), 2 nephelinitic (one Ca-rich and the other Na-rich), an andesitic, and a phonolitic composition melt. They found that at saturation with a pure CO_2 fluid phase the concentration of total CO_2 in the natural melt compositions varied from a low of ~1 wt% in the andesite at 2.0 GPa and 1500 ° C to a high of ~19 wt% in the Ca-melilititic composition at 2.0 GPa, 1400 ° C. Brooker et al.'s (2001a) results for the andesitic and phonolitic melts are plotted in Figure 7; all of the CO_2 saturation values for the melilititic compositions plot at higher concentrations than shown in Figure 7. All natural melt compositions studied at pressures from 2.0 to 2.7 GPa demonstrated retrograde CO_2 solubility. Brooker et al. (2001a) demonstrated a positive correlation between the ratio of non-bridging oxygens to tetrahedral cations (NBO/T) to the carbon dioxide solubility at 2.0 GPa and proposed a quantitative relationship between this parameter and the concentration of total CO_2 dissolved in melts at saturation. Brooker et al. (2001b) used the same melt compositions as Brooker et al. (2001a) to intensively study local melt structure around carbonate groups by infrared spectroscopy and found that the

carbonate species in natural melts were preferentially associated with Ca^{2+} cations, rather than Fe cations.

King and Holloway (2002) compared the solubilities of molecular CO_2 to carbonate in anhydrous melts varying in composition from leucititic to rhyolitic with the Si+Al cation fraction in the melts. They corroborated previous results and demonstrated high concentrations of carbonate in leucititic melts with low Si+Al (or high NBO/T) and high concentrations of molecular CO_2 in rhyolitic melts with high Si+Al (or low NBO/T). The total solubility of carbon dioxide in these two end member melts is approximately equal, however intermediate melts of basanitic, tholeiitic, icelanditic and andesitic composition have lower solubilities of total CO_2. Andesitic melts were found to have sub-equal concentrations of molecular CO_2 and carbonate species dissolved in them at saturation with a pure CO_2 fluid phase. King and Holloway (2002) correlated the fraction of carbon dioxide dissolved as molecular CO_2 with the ionic porosity, or free space between the atoms of the melt, of andesitic and more Si+Al-rich melt compositions.

Tamic et al. (2001) studied the solubilities of CO_2 and H_2O in a rhyolitic melt at 200 and 500 MPa at 800 and 1100 ° C. The extrapolated CO_2 concentration in the melt saturated with a pure CO_2 fluid at 200 MPa is ~1100 ppm; no effect of temperature was measurable. At 500 MPa the effect of temperature was obvious and

the melt at 1100 ° C exhibited a CO_2 saturation value of 2750 ppm, whereas at 800 ° C the value found was ~2500 ppm, but is not well constrained by their data. This study demonstrates a prograde solubility of CO_2 in rhyolitic melts, but is the only one to do so. Nevertheless the results are consistent with those of Fogel and Rutherford (1990).

Morizet et al. (2002) measured the solubility of CO_2 in a synthetic Fe-free phonolitic melt at pressures between 1000 and 2500 MPa and temperatures between 1300 and 1550 ° C. They found that the solubility of CO_2 follows a positive correlation with pressure and a negative correlation with temperature. Their results are in excellent agreement with the CO_2 solubilities in a phonolitic melt measured by Brooker et al. (2001b). Morizet et al. (2002) also used bulk CO_2 analyses to calibrate infra-red extinction coefficients for carbonate groups, but concluded that infra-red spectroscopy may not be a reliable method for the analysis of dissolved CO_3 in intermediate melt compositions.

Nowak et al. (2004) investigated diffusion of CO_2 in Fe-free analogues of natural melts varying in composition from hawaiitic to rhyolitic. Although they could not directly measure the concentration of CO_2^{melt} species in the more basic compositions, their diffusion modeling indicated the presence of significant concentrations of this species in all melts. Behrens et al. (2004) measured the

solubility of total CO_2 by ion microprobe in a dacitic melt with 1.5% H_2O at 500 MPa, 1250 ° C. They found a concentration of 2900 ppm. Botcharnikov et al. (2006) argued that the similar solubility of carbon dioxide in melts ranging in composition from tholeiitic to rhyolitic indicates that as the amount of free oxygen in the melt, $O^{2-,\,melt}$, that reacts to produce carbonate in Equation 4b decreases with increasing SiO_2 concentrations, the ionic porosity (or free space within the melt structure) increases enough to accommodate the CO_2^{melt} species dissolved in the melt. Behrens et al. (2009) studied the solubility of CO_2 in a phono-tephritic melt coexisting with a C-O-H fluid and extrapolated their measurements to fluids of pure CO_2. They estimated that the solubility is 3000 ppm at 1250 ° C , 200 MPa and increases to 8250 ppm at 500 MPa, whereas decreasing the temperature to 1200 ° C was shown to increase the solubility to 9250 ppm at 500 MPa. The concentrations of dissolved carbon dioxide, CO_2^{total}, in the melt are significantly greater than measured in other melt compositions at similar conditions of temperature and pressure (Fig. 7). Experiments conducted at 200 MPa, 1200 ° C with high hydrogen fugacities, creating correspondingly low oxygen fugacities, resulted in a 1000 ppm increase in the CO_2 solubility, similar to the temperature effect observed at 500 MPa. Lesne et al. (2011b) investigated the solubility of carbon dioxide in three alkali basalt melts with approximately 1 wt% dissolved H_2O at 1200 ° C, and pressures from 26 to 200 MPa; their concentrations of CO_2 reached a maximum of 2000 ppm at 200 MPa, only slightly higher than values

measured in common, low-to-moderate alkali concentration melts (Fig. 7). However, they clearly demonstrated that augmenting the alkali concentrations in basaltic melts increased the solubility of CO_2. Vetere et al. (2011) measured the solubility of CO_2 in a shoshonitic melt coexisting with a C-O-H fluid at 1250 ° C, 50 to 400 MPa, and estimated that the solubility of pure CO_2 varied from ~400 ppm at 50 MPa to ~3000 ppm at 400 MPa (Fig. 7).

These measurements of the concentrations of CO_2 in silicate melts saturated with a pure CO_2 fluid are similar for most melt compositions at pressures of 500 MPa or less. Indeed the maximum difference between the solubility of pure CO_2 in a tholeiitic melt and a rhyoltic melt is ~500 ppm, with the rhyolite displaying a higher saturation concentration. However, many of the measurements of CO_2 solubility in rhyolitic and basaltic melts are within uncertainty of each other. At 500 MPa, or less, increasing the alkali concentration in basic melts, as shown by the results of Lesne et al. (2011b) on alkali basalt melts and Behrens et al. (2009) on alkali-rich phono-tephritic melts, increases the concentration of dissolved CO_2 (Fig. 7), as does increasing the silica concentration of the melt. At pressures above 500 MPa the effect of composition is much more evident where the effect of adding alkalies and lowering the silica concentration enhances CO_2 solubilities (Fig. 7).

Although the earliest studies of CO_2 saturation concentrations in silicate melts were performed with a pure, or nearly pure, CO_2 fluid, during the 1990's the focus of research changed to the investigation of both CO_2 and H_2O solubilities in silicate melts coexisting with C-O-H fluids (as exemplified by some of the studies discussed above). This change occurred because of the improvement of infrared and ion microprobe techniques that allowed rapid and accurate determination of volatile concentrations in silicate glasses quenched from melts. But more importantly, the determination of CO_2 and H_2O solubilities in melts coexisting with a C-O-H fluid is a better approximation of Nature than the solubilities of either pure H_2O or CO_2.

4.3 Water and carbon dioxide

The importance of mixed volatiles, particularly H_2O and CO_2, in the evolution of magmatic systems was already realized and measured in the laboratory by the early 1970's. Khitarov and Kadik (1973) present a summary of their research into the individual and combined solubilities of water and carbon dioxide in silicate melts. Holloway (1976) discussed the effect of the low solubility of CO_2 in melts on the evolution of a granitic magma containing both H_2O and CO_2. And, although Eggler and Rosenhauer (1978) studied the saturation of diopside melt with a mixed-volatile fluid phase composed of H_2O and CO_2, similar studies on natural melt compositions at crustal pressures did not become abundant until approximately a decade later.

The first recent study on the solubilities of water and carbon dioxide in a

silicate melt coexisting with a mixed volatile fluid was that of Blank et al. (1993) who studied CO_2 and H_2O dissolution into rhyolitic melts at 75 MPa and 850 °C. Other notable studies of the behavior of rhyolitic melts and H_2O-CO_2 fluids are those of Tamic et al. (2001) and Liu et al. (2005). Tamic et al. (2001) studied the saturation of a rhyoltic melt with a CO_2- and H_2O-bearing fluid phase from 200 to 500 MPa and 800 to 1100 °C. Tamic et al. (2001) provide an excellent example of the effects of a mixed-volatile phase on the solubility of water and carbon dioxide in silicate melts (Fig. 8).

Figures 8a and 8b, whose design was originally conceived by either Holloway and Blank (1994) or by Dixon et al. (1995), demonstrates that only if the fluid is either pure CO_2 or pure H_2O will the melt contain a single volatile. Similarly, if the melt contains two, or more, volatiles so must the fluid, as required by the equivalence of chemical potentials in all phases coexisting at thermodynamic equilibrium. The curves plotted in Figure 8 for the pressures of 200 and 500 MPa define the concentration of H_2O and CO_2 in melts at saturation with a mixed-volatile fluid phase. At volatile concentrations below the curves the melts are undersaturated, above the curves a separate fluid phase coexists with the melt at equilibrium. Note how the total amount of H_2O and CO_2 necessary to saturate melts increases with increasing pressure. Beginning with a fluid composed of pure water, Figure 8 demonstrates that saturation of a rhyoltic melt with H_2O^{fluid} at 200 MPa

occurs at approximately 5.5 wt% bulk water dissolved in the melt. However, if the fluid is a CO_2-H_2O mixture, for example with a mole fraction of water in the fluid of 0.8, or X_{H2O}^{fluid} = 0.8, the rhyolitic melt at 200 MPa must contain ~4.5 wt% H_2O and ~ 400 ppm CO_2 at equilibrium. At 500 MPa the rhyolitic melt coexisting with the same composition fluid will contain ~8 wt% H_2O and ~ 1450 ppm CO_2 (Fig. 8).

A number of other studies investigated the saturation of basic, intermediate and silicic melts with a H_2O-CO_2 mixed-volatile phase. Some of the notable studies are those of King and Holloway (2002) who investigated an andesitic melt. They found that the concentration of CO_2 species dissolved in an andesitic melt coexisting with a C-O-H fluid was positively correlated with the mole fraction of CO_2 in the coexisting fluid and corresponding total water concentration in the melt, whereas the carbonate species abundance decreases. Behrens et al. (2004) studied saturation in the system dacitic melt-H_2O-CO_2. These authors confirmed the effect of the mole fraction of CO_2 in the fluid on the relative fraction of CO_2^{melt}/CO_2^{total} seen by King and Holloway (2002); they also demonstrated that CO_2^{melt}/CO_2^{total} was positively correlated with the concentration of total dissolved CO_2. Behrens et al.'s (2004) comparison of their results to those of previous studies on CO_2 solubilities in rhyoltic melts coexisting with a CO_2-H_2O mixed fluid demonstrated broad agreement. Botcharnikov et al. (2005, 2006, 2007) measured and compared mixed volatile solubilities in both synthetic and natural ferrobasaltic to rhyolitic

melts at crustal pressures. Botcharnikov et al. (2007) is notable for its measurement of the solubilities of H_2O, CO_2 and Cl in an andesitic melt coexisting with a C-O-H-Cl fluid at 1050 and 1200 ° C , 200 MPa. Vetere et al. (2011) investigated the solubilities of H_2O and CO_2 in a shoshonitic melt at 1250 ° C and pressures from 50 to 400 MPa; their values are similar to those measured by Tamic et al. (2001), as demonstrated in Figure 8.

Studies on the saturation of a basaltic melts with a mixed-volatile fluid phase progressed in parallel with studies on silicic and intermediate compositions. Dixon et al. (1995) measured the solubilities of H_2O and CO_2 in a basaltic melt at 1200 ℃ and pressures of 20 to 99 MPa and used those data as calibration points for their model (discussed in section 5.1). Jakobsson (1997) studied the solubility of CO_2 and H_2O in an icelandite (similar in composition to a basaltic andesite) at 1400 ℃ and 1000 MPa. Behrens et al. (2009) investigated the solubility of H_2O-CO_2 fluids in a phonolitic melt at pressures to 500 MPa. Shishkina et al. (2010) and Morizet et al. (2010) measured the solubilities of mixed CO_2-H_2O fluids in basaltic melts at crustal pressures. Shishkina et al. (2010) studied solubilities at relatively oxidized conditions whereas Morizet et al. (2010) worked at reduced conditions. The solubilities of CO_2 and H_2O in the basaltic melt studied by Shishkina et al. (2010) are quite similar to those found in a rhyoltic melt at similar conditions of pressure, temperature and oxygen fugacity (Fig. 8). Morizet

et al. (2010) demonstrate that decreasing the oxygen fugacity results in lower concentrations of CO_2^{total} in the melt due to lower CO_2 fugacities in the fluid, as seen in previous studies.

It is instructive to use the data to calculate simple Henrian partition coefficients for CO_2^{total} between the fluid and the melt, $D^{fluid/melt}$ to investigate its variability and applicability. For example, using the data of Tamic et al. (2001) displayed in Figure 8 the $D^{fluid/melt}$ for CO_2^{total} at 200 MPa varies from 1050 at X_{H2O}^{fluid} = 0.8 to 900 at X_{H2O}^{fluid} = 0.2. At 500 MPa this value increases from 270 to 350 as X_{H2O}^{fluid} varies from 0.8 to 0.2. Even for fluids of pure CO_2 the calculated partition coefficient is 950 at 200 MPa and 360 at 500 MPa (Fig. 8). Although the pressure effect is evident in the partition coefficients, it is striking that effects of volatile composition on $D^{fluid/melt}$ for CO_2^{total} are small, less than ~ 10 relative percent. On the other had the $D^{fluid/melt}$ for H_2O^{total} as a function of the fluid composition varies by a factor of 3*x* at both 200 and 500 MPa. Thus to a first approximation the distribution of CO_2 between fluids and melt can be determined using a simple Henrian partition coefficient, but that of water cannot.

These studies on the solubilities of H_2O and CO_2 demonstrated the significant control of pressure on their concentrations in silicate melts and the weaker effect of temperature and melt composition. In particular, the solubility studies using

mixed H_2O-CO_2 fluids have provided the fundamental data needed for the creation and assessment of complex thermodynamic models that better describe silicate melt-fluid phase interactions (to be discussed in Section 5, below) than the simple partition coefficients discussed above.

4.4 Sulfur

Our knowledge of sulfur saturation in melts and partitioning between melts and geologically important fluids (dominated by H_2O and CO_2) remains woefully inadequate, especially considering the importance of sulfur in ore formation processes, volcanic monitoring and global climate change. Many studies were performed on the partitioning of sulfur between slags and C-O-S gases at 1 bar (e.g., Fincham and Richardson,1954; Katsura and Nagashima, 1974), but they are not directly applicable to magmatic systems because of the absence of H_2O in the system. Additionally, many studies on the saturation of natural silicate melts with sulfide (either molten or solid) or sulfate (molten or solid) have been performed (the reader interested in this topic is referred to the review by Baker and Moretti, 2011), but these sulfide and sulfate saturation studies do not provide partition coefficients between melts and typical magmatic fluids. Only a few studies have measured these important values. Because a dedicated review of this topic was recently published (Webster and Botcharnikov, 2011), only a brief summary of sulfur partitioning between silicate melts and aqueous fluids will be presented.

Scaillet et al. (1998) present a summary of partition coefficients for sulfur between magmatic melts and hydrous gases estimated from measurements of natural volcanic gases; their summary shows fluid/melt partition coefficients varying from 50 to 2600. In their experiments on a metaluminous rhyolitic melt near 780 ° C, 224 MPa, Scaillet et al. (1998) demonstrated that as the oxygen fugacity increased from the nickel-nickel oxide buffer (NNO), where S^{2-} is the stable sulfur species in the melt, to approximately 2 log units higher, where SO_4^{2-} is the stable melt species, the fluid/melt partition coefficient increased from 1 to almost 1600. The partition coefficient was shown to decrease with increasing pressure or increasing temperature at constant oxygen fugacity. Scaillet and MacDonald (2006) expanded on Scaillet et al. (1998) and studied sulfur partitioning between peralkaline rhyolitic melts of different compositions and an aqueous fluid phase. All peralkaline rhyolitic melts studied by Scaillet and MacDonald (2006) had significantly higher partition coefficients than metaluminous rhyolites, except at the highest oxygen fugacities studied. They found that the fluid/melt partition coefficient of approximately 270 was relatively insensitive to pressure for mildly peralkaline rhyolitic melts, but that the melt with the highest peralkalinity and iron concentration increased its partition coefficient to in excess of 500 at oxygen fugacities more that one log unit above NNO. However, over the temperature range of 800 to 900 ℃ they found only a weak temperature influence.

Keppler (1999, 2010) studied the partitioning of sulfur between a haplogranitic melt and an aqueous fluid phase. In particular, Keppler (2010) studied the partitioning from 50 to 300 MPa, 750 to 850 °C, at various oxygen fugacities. Keppler (2010) found that in his iron- and calcium-free melts at 200 MPa, 850 °C as the oxygen fugacity increased from the cobalt-cobalt oxide buffer to NNO the fluid/melt partition coefficient dropped from 468 to 47 and did not change at the even higher oxygen fugacity of the magnetite-hematite buffer. Note that this finding of an inverse correlation between the partition coefficient and the oxygen fugacity is the opposite of that reported by Scaillet et al. (1998) and Scaillet and MacDonald (2006). At 850 °C and an oxygen fugacity between 0.5 to 1 log unit above NNO, Keppler measured a fluid/melt partition coefficient of 58 at 50 MPa and 94 at 100 MPa, indicative of a significant positive correlation between pressure and the partition coefficient, but at 750 °C, 200 MPa the partition coefficient was 51. Some of the differences between Keppler's study and previous results are no doubt due to his use of an iron- and calcium-free system, however whether or not that explains all of the differences remains for future research to discover.

Botcharnikov et al. (2004) studied the partitioning of sulfur between a rhyodacitic melt and a fluid containing water and chlorine at 850 °C, 200 MPa. These experiments contained a significant amount of minerals, which made the calculation of the fluid composition challenging. Their three measurements made in the absence

of Cl yield a weight-based, fluid/melt partition coefficient of sulfur at 200 MPa, 850 ° C of 1500 ± 400. Alternatively, if each of these experiments is considered individually the partition coefficient varies from 840 to 1700. (The effect of Cl on the partitioning of sulfur in this system will be discussed in section 4.8.)

Few published measurements of sulfur partitioning between hydrous fluids and basaltic melts are available. Most of these measurements are reported in the review of Webster and Botcharnikov (2011) and are based upon personal communications concerning the experimental results of Moune et al. (2009), Lesne et al. (2011c), Webster et al. (2011) and studies currently only published as abstracts or a thesis (Beermann et al., 2009; Beermann, 2010). Webster and Botcharnikov's (2011) compilation of the data demonstrate a strong effect of the water concentration in the melt on the partitioning of sulfur at 1050 ° C , 300 MPa and oxygen fugacities within ½ a log unit of the FMQ buffer (i.e., where sulfide is expected to be the dominant sulfur species in the melt, see Baker and Moretti, 2011); as the water concentration in the melt increases from 0 to 4 wt% the partition coefficient of sulfur drops from ~500 to between ~ 50 and 25, and remains at these values for higher water concentrations. These authors also demonstrated that decreasing the pressure to 200 MPa does not have a significant effect on the partition coefficient, however at pressures below 100 MPa and temperatures of 1150

° C they indicate that fluid/basaltic melt partition coefficients for sulfur reach values of 3000. Webster and Botcharnikov (2011) report that Beermann (2010) found that at oxidizing conditions of FMQ+3.2 (where the dominant sulfur species in the melt is sulfate, see Baker and Moretti, 2011) the partition coefficient is 30 to 40 at 200 MPa and 70 at 100 MPa. Two reconnaissance experiments by D.R. Baker at McGill University have yielded two fluid/melt partition coefficients for sulfur between an Mt. Etna alkali basaltic melt with 0.15 wt% dissolved H_2O and a hydrous fluid at 1260 °C, NNO, and 1 MPa: 57 and 52. As Webster and Botcharnikov (2011) clearly state, many more measurements on the partitioning of sulfur between magmatic melts of all compositions and hydrous fluids must be performed before we fully understand this process.

4.5 Chlorine

Because of its importance as a ligand for ore metals, the study of chlorine partitioning between fluids and silicate melts has been actively pursued by many research groups. One of the early, if not the earliest, experimental measurement of chlorine partitioning between magmatic melts and fluids was that of Kilinc and Burnham (1972). However, over the past 20 years it is J.D. Webster who has made the single most important set of contributions to our knowledge of chlorine partitioning between silicate melts and aqueous fluids. Some, and only some, of the more important papers on this topic by Webster and colleagues are: Webster and

Holloway (1988), Webster (1992a, 1992b), Carroll and Webster (1994), Webster et al. (1999), Webster and De Vivo (2002), Webster et al. (2009a, 2009b), Webster and Mandeville (2007). These papers demonstrate the complexity of the interactions between chlorine and water in the fluid and melt phases. The most important complication is that continued addition of chlorine to a system composed of a silicate melt and an aqueous fluid will eventually result in the saturation of the system with a Cl-rich brine, similar to what is seen in the simple system H_2O-NaCl (e.g., Chou, 1987), although the exact conditions at which this occurs depends upon the bulk composition of the system, temperature and pressure (see Webster and Mandeville, 2007). Because most magmatic systems probably do not contain a separate brine this review will concentrate on relations between silicate melts and the Cl-bearing aqueous fluid.

Figure 9a demonstrates how for a given melt composition (e.g., andesitic melt) the addition of Cl to the melt at low concentrations has little or no measurable effect on the water solubility; at these conditions a Henrian fluid melt partition coefficient for chlorine, $D^{fluid/melt}_{Cl}$ can be defined (Fig. 9b). However, given sufficient addition of Cl the fluid phase will exsolve into two phases, a lower density hydrous fluid and a high density brine (Fig. 9b). The three phases coexist stably only at one point in these diagrams where a distinct singularity, a kink in the curve (Fig. 9a), is present. However, for some conditions the fluid phase is

supercritical and does not intersect a singular three-phase point; in these cases there is a smooth progression from the low Cl, hydrous fluid to a high-Cl brine as the bulk Cl concentration in the system is increased, as exemplified by the basaltic composition in Figure 9a (see Webster et al., 1999, and Webster and Mandeville, 2007, for further details). Studies by Webster and colleagues demonstrate that saturation of silicate melts with a Cl-brine at 200 MPa varies from ~3000 ppm for granitic melts to in excess of 2.5 wt% for basaltic melts. However, these diagrams are not useful in the portrayal of the partition coefficients of chlorine between silicate melts containing only 100's to 1000's of ppm of Cl and hydrous fluids. Instead, partition coefficients need to be calculated from the chlorine concentrations of coexisting melts and aqueous fluids (e.g., Signorelli and Carroll, 2000).

The behavior of Cl in the silicate melt and in the fluid are schematically illustrated for two cases in Figure 9b, each at constant pressure and temperature. In the first case the system is at subcritical conditions and in the second case at supercritical conditions. At low Cl concentrations in both cases the system will show Henrian behavior and the chlorine partition coefficient between the fluid and the melt can be defined. However, with increasing addition of Cl at subcritical conditions the system will eventually saturate in a brine phase creating a three phase system and further addition of Cl will eliminate the fluid phase (Fig. 9b).

At supercritical conditions there exists a smooth transition from the water-dominated fluid phase to the Cl-dominated brine phase (Fig. 9b). The details of the behavior depicted in Figure 9 depend upon pressure, temperature and the composition of the system. Nevertheless, in most magmatic systems experimentally investigated the chlorine partitioning displays Henrian behavior (i.e., a constant partition coefficient) at concentrations less than about 5000 ppm in basic to intermediate melt compositions and less than about 500 ppm in silicic compositions. This review concentrates on this region of chlorine concentrations because these are common ranges in magmatic systems (Aiuppa et al., 2009) and measurements of fluid/melt partitioning of chlorine indicate that at low concentrations a simple partition coefficient can be defined. However, at higher concentrations of Cl (as shown in Fig. 9b) the chlorine partition coefficient increases with the Cl concentration in the melt and in the fluid. All of the studies discussed below present measurements of fluid/melt partitioning for chlorine at high concentrations where a constant partition coefficient for Cl does not exist; the reader interested in such the behavior of chlorine in melts at such high concentrations is referred to the original sources.

Experimental data from published studies of chlorine partitioning between aqueous fluids and silicate melts have been compiled and in most cases plotted on figures similar to Fig. 9b to calculate the chlorine partition coefficient between fluids

and melts at low concentrations (approximately less than 5000 ppm in basic to intermediate melts and less than 500 ppm in silicic melts). This technique is useful for investigating the partitioning of an element at low concentrations where it follows Henrian behavior, but fails at higher concentrations where the activity coefficient becomes a complex function of the phase composition. Figure 10 presents the partition coefficients of chlorine between aqueous fluids and silicate melts as a function of pressure from 1 to 600 MPa. The partitioning measurements were conducted over a temperature range of approximately 800 to 1250 ° C, but the results demonstrate only a weak effect of temperature.

Shinohara et al. (1989, see also Shinohara 2009) studied the behavior of a haplogranitic melt coexisting with hydrous, Cl-bearing fluids and brines at 810 °C and pressures from 60 to 600 MPa. At 60 and 120 MPa they found evidence that their melts became saturated with both an aqueous fluid and a chloride brine, but at higher pressures only a single-phase, Cl-bearing fluid was present in their experiments. They demonstrated that their fluid/melt partition coefficients increased with pressure from 3 to almost 250 as the pressured increased from 60 to 600 MPa (Fig. 10). Webster and Holloway (1990) also measured fluid/haplogranitic melt partitioning of chlorine and found values approximately ½ of those that can be estimated from Shinohara et al.'s (1989) data (Fig. 10).

Kravchuk and Keppler (1994) built upon the work of Malinin et al. (1989) and Malinin and Kravchuk (1994) and reported experimental results on the partitioning of chlorine between feldspathic, quarzofeldspathic and haplogranitic melts and an aqueous fluid. They demonstrated that the method by which chlorine was introduced into the system had an effect on the partition coefficient at 800 °C, 200 MPa. If chlorine was added as HCl the partitioning of Cl between the hydrous fluid and either albitic or potassium feldspar melts behaved in a Henrian manner and the chlorine partition coefficient between fluid and melt was ~ 25, although the partition coefficient in the presence of potassium was a little higher than in the case of sodium. If the Cl was added as a salt the partitioning depended upon the amount of salt added. For example, when Cl was added as NaCl to an albite-quartz melt the partition coefficient of Cl between fluid and melt was ~ 12 at infinite dilution of Cl in the fluid and increased to about 200 when ~ 28 mols of Cl/kg H_2O were present in the fluid. Kravchuk and Keppler (1994) found that when Cl was added as NaCl to the haplogranitic melt the fluid/melt partition coefficient for Cl was 32 at 200 MPa, very similar to the previous results of Webster and Holloway (1990), as demonstrated in Figure 10.

Métrich and Rutherford (1992) studied the partitioning of Cl between rhyolitic, phonolitic, pantelleritic, as well as synthetic melts, and hydrous fluids. They clearly demonstrated saturation of the studied melts with a chloride brine at high

concentrations, similar to the earlier studies discussed above. The concentration of chlorine in the brine-saturated melts at 830 to 850 °C, 100 MPa varies from ~3000 ppm in the rhyolitic melt to ~7000 in the phonolitic melt to ~9000 in the pantelleritic melt. They demonstrated that the chlorine concentration in the brine-saturated, pantelleritic melt increased with pressure. Their measurements at low chlorine concentrations in the pantelleritic melt can be used to define a Henrian partition coefficient of 7 at 830 °C, 100 MPa (Fig. 10). Botcharnikov et al. (2004) measured the partitioning of Cl between a rhyodacitic melt and hydrous fluids; at 200 MPa, 850 ° C they measured a fluid/melt partition coefficient of 2. These values of the partition coefficients between fluids and natural silicic melts are 1/3rd to 1/10th those measured for haplogranitic melts by Shinohara et al. (1989) and Kravchuck and Keppler (1994). Webster et al.'s (2009b) measurements of chlorine partitioning between a Mt. Mazama rhyodacitic melt with between 2900 and 5700 ppm and hydrous fluid produce a higher partition coefficient of 16 ± 6, in between the value Botcharnikov et al.'s (2004) results and those determined for haplogranitic compositions.

Chevychelov (1999), Chevychelov and Suk (2003), Chevychelov et al. (2003) and Chevychelov et al. (2008a) performed numerous studies on the interaction of halogens and silicate melts, but only the most recent study will be discussed. Chevychelov et al. (2008a) measured ~ 5 000 ppm chlorine in a K-phonolitic melt

(from Vesuvius) in equilibrium with a Cl-brine at 200 MPa, NNO, and 845 to 860 °C , and at 200 MPa, 1000 ° C and NNO+3.5. Using fluorine-free experiments with chlorine concentrations in the melt below 5 000 ppm (i.e., not in equilibrium with a brine) a fluid/melt partition coefficient for chlorine of 7.9 at 845-860 ° C can be calculated from one measurement, and at 1000 ° C and NNO+3.5 the partition coefficient is 4.3 ± 1.3 (Fig. 10).

Signorelli and Carroll (2000) measured the partitioning of chlorine between aqueous fluids and two phonolitic melts, one peraluminous (from Vesuvius) and one peralkaline (from Montaña Blanca, Tenerife) at 860 to 890 ° C and pressures from 25 to 250 MPa. They found that both melts saturated with a brine at pressures below 200 MPa, but that the chlorine concentration in the melt coexisting with the brine decreased from ~ 9 000 ppm at 25 MPa to ~7 000 at 150 MPa. They demonstrated that although the fluid-melt partition coefficients for Cl at brine-undersaturated conditions were slightly different for each melt, they increased from near 1 at the lowest pressured investigated to a high of 25 at 250 MPa (Fig. 10). Signorelli and Carroll (2002) extended their previous study by investigating the interactions between trachytic melts and Cl-bearing aqueous fluids and brines at 860 to 930 ° C and 25 to 250 MPa. They found no significant effect of the alkali/alumina ratio on the concentration of chlorine necessary to saturate the trachytic melts with a brine, unlike phonolitic melts that have a minimum in this value near an

alkali/alumina ratio of 1. They also found that the concentration of chlorine in trachytic melts coexisting with a brine decreased with increasing pressure, as they previously observed in phonolitic melts, from near 8 000 ppm at 25 MPa to ~4 000 ppm at 250 MPa. The partitioning of chlorine between hydrous fluids and andesitic melts was studied by Webster et al. (1999) and Botcharnikov et al. (2007); the measurements of both of these studies are similar and yield a Cl fluid/melt partition coefficient 2.8±0.6 and 3.6±0.6, respectively, at 200 MPa for melts with less than 5000 ppm Cl in them.

Stelling et al. (2008) and Alletti et al. (2009) studied the partitioning of Cl between hawaiitic basaltic compositions from Mt. Etna and aqueous fluids (Fig. 10). Stelling et al. (2008) investigated the effects of temperature and Alletti et al. (2009) investigated the effects of pressure on the chlorine partition coefficient. The results of Stelling et al. (2008) and Alletti et al. (2009) at low total chlorine concentrations yield fluid/melt partition coefficients that are generally between 3 and 8. Alletti et al. (2009) provide an equation for the prediction of the hydrous fluid/melt chlorine partition coefficient at 1200 °C, NNO over the range of 1 to 200 MPa:

$$D_{Cl}^{fluid/melt} = 12.732 P^{-0.0853} \quad . \qquad (5)$$

Interestingly, there are some important differences in the measured partition coefficients between Stelling et al. (2008) and Alletti et al. (2009), even at the

same conditions of temperature and pressure. These differences are not easily reconciled as discussed in Alletti et al. (2009). Additionally, unlike the studies on haplogranitic and phonolitic melts discussed above, Alletti et al. (2009) found that the partition coefficient of Cl aqueous fluid and melt decreased slightly with increasing pressure.

Alletti et al. (2009) is the only study to investigate the partitioning of Cl between and aqueous fluid and a magmatic melt at 1 MPa, where the Cl dissolved in the fluid phase should be dominantly complexed as HCl, rather than as alkali chlorides (Shinohara, 2009). This change in the dominant form of complexing in the fluid may be responsible for the small increase in the partition coefficient from 10.8 to 13.9 as the pressure increases from 1 to 25 MPa, whereas at higher pressures the partition coefficient decreases. However, as Shinohara (2009) pleads, we need much more partitioning data at low pressures to better understand how changes in Cl complexing affect its distribution between silicate melts and coexisting fluids.

Beerman (2010) in his Ph.D. thesis reports data on the partitioning of chlorine between hydrous fluids and either a dacitic melt or a hawaiitic melt at 1050 ° C , 200 MPa and an oxygen fugacity of approximately FMQ+ 0.8. The hawaiitic melt was similar in composition to that used by Stelling et al. (2008) and Alletti et al.

(2009). Using his data with Cl concentrations of 1 wt% or less in the melt, a partition coefficient between the fluid and the hawaiitic melt of 6.4 can be calculated, and between the fluid and the dacitic melt the value is 8.7 (Fig. 10).

The chlorine partitioning data in Figure 10 display a range of almost 2 orders of magnitude at 200 MPa. However, most of the measured fluid/melt partition coefficients for Cl at low concentrations in natural compositions ranging from basalt to rhyolite only vary from approximately 2 to 8 and therefore allow us to model the evolution of Cl in most common magmatic systems at 200 MPa. The exceptions to this tight clustering of partition coefficients include experiments on a haplogranitic, and F-bearing rhyolitic and phonolite melt compositions, whose partition coefficients are higher. Some of these differences in partition coefficients are no doubt related to the different temperatures of the various experiments, but currently there are insufficient data available to constrain the effect of temperature on the chlorine partition coefficient.

Almost no measurements exist at pressures above 200 MPa. But the few data that exist at lower pressures suggests that for common compositions there does not seem to be a significant pressure effect; once again the phonolites are the exception. Nevertheless, Figure 10 clearly demonstrates the need for additional measurements on chlorine partitioning at pressures both above and below 200 MPa.

4.6 Other halogens

Measurements of fluorine partitioning between melts and fluids are rare because of the difficulty of analyzing fluorine by the electron microprobe. On the other hand fluorine does not form a separate brine, as does chlorine, at concentrations similar to those found in magmatic systems (Aiuppa et al., 2009). Nevertheless, as shown by many of the papers cited below, systems containing both chlorine and fluorine at high, but still natural, concentration levels can form brines. This review concentrates on partition coefficients of halogens at low concentrations between silicate melts and aqueous fluids, as done above for Cl..

Webster (1990) measured the partitioning of fluorine between a fluid and a peraluminous rhyolitic melt and found that for melts with approximately1 wt.% F at pressures of 200 MPa its value varied from 0.13 at 775 ° C to 0.37 at 994 ° C. There was no significant influence of pressure on the partition coefficient over the range of 200 to 500 MPa. Increasing the the F concentration in the melt resulted in partition coefficients reaching values as high as 1.11, which occurred for a melt containing 6.8 wt% F. Webster (1990) also demonstrated that diluting the fluid with CO_2 such that the mole fraction of water in the fluid was ~ 0.5 resulted in an order of magnitude decrease in the fluorine fluid/melt partition coefficient. Webster and Holloway (1990) measured fluid/melt partitioning of

fluorine for melts of both peraluminous rhyolitic and haplogranitic compositions at 200 MPa and temperatures near 800 ° C. The fluorine partition coefficient for the rhyolitic melt was found to be 0.3 ± 0.06 at F concentrations less than ~ 2 wt% and for the haplogranitic composition the value of the partition coefficient was almost identical, 0.4 ± 0.09.

Borodulin et al. (2009) investigated the partitioning of F between haplosilicic (67 to 74% SiO_2 and composed of only SiO_2, Al_2O_3, Na_2O and K_2O) melts that varied from peralkaline to peraluminous and hydrous fluids at 100 MPa and temperatures from 650 to 850 ° C. They found that the fluorine partition coefficients between fluids and peralkaline melts with 0.6 to 2.1 wt.% dissolved F increased from 0.7 at 650 ° C to 3.8 at 850 ° C, and for peraluminous melts with 4.8 to 6.2 wt% F the partition coefficient decreased from 0.15 to 0.04. Metaluminous melts with 4 wt% F displayed relatively constant fluid melt fluorine partition coefficients of 0.3.

Chevychelov et al. (2008a) provide the results of fluorine partitioning measurements between a phonolitic melt and F- and Cl-bearing aqueous fluids and brines at 200 MPa, 845-860 ° C, NNO, and also at 200 MPa, 1000 ° C, NNO+3.5. The maximum fluorine concentration in the K-phonolitic melt saturated with a Cl- and F-bearing brine was 7 000 ppm. Although they found that the capsule material (either Au or Pt) affected the F concentrations of the melt, their results indicate that

the fluid/melt partition coefficient for fluorine is always greater than 1. Combining their data from both capsule types for melts that coexist with only an aqueous fluid, not a brine, yield a partition coefficient of 14.8 ± 4.3 at 845-860 ° C and of 7.6 ± 5.3 at 1000 ° C. Chevychelov et al. (2008b) investigated the fluid/basaltic melt partition coefficient for F in the presence of only small amounts of Cl (0.11 wt.% in the melt) and measured a value of 28±5.

Alletti (2008) measured partition coefficients of fluorine between aqueous fluids and a melt of an Etna hawiitic basalt. At 1 MPa the fluid/melt partition coefficient was ~3 based upon forward and reversal experiments. However, higher pressure, unreversed experiments yielded fluid-melt partition coefficients for fluorine of 19 at 1200 °C, 25 MPa and 38 at 1200 °C, 100 MPa (Alletti, 2007). These values are remarkably similar to those of Chevychelov et al. (2008b) measured at similar conditions.

Bureau et al. (2000) investigated the partitioning of chlorine, bromine and iodine between an albitic melt and an aqueous fluid at 900 °C, 200 MPa and found that the partition coefficients increased from 8 for Cl, to 18 for Br, and to 104 for I. They demonstrated a linear relationship between the logarithm of the partition coefficient and the ionic radius of the anion, but could not find a physical explanation for this relationship. Bureau and Métrich (2003) investigated the

maximum bromine concentrations (i.e., saturation with a Br-brine) in a series of iron-free synthetic glass compositions at 100 to 200 MPa and 900 to 1080 °C. They found that bromine concentrations increased from haplogranitic (2 800 to 3 900 ppm, low temperature to high temperature) to rhyolitic (4 300 to 5 900 ppm) to albitic (5 400 to 7 900 ppm) to pantelleritic melts (9700 to 11 300 ppm). Bureau et al. (2010) studied bromine partitioning between a fluid and a haplogranitic melt at in situ conditions using a heated diamond anvil and demonstrated the utility of this technique for fluid/melt partitioning studies. Experimental temperatures varied from 590 to 890 ° C and pressures 650 MPa to 1.7 GPa. They found that the Br fluid/melt partition coefficient varied from near 9 at the 900 MPa and 660 ° C to approximately 2 at the highest combination of temperature and pressure, however Bureau et al. (2010) argue for little influence of temperature on their results and ascribe the differences to the effect of pressure. Interestingly, Bureau et al. (2010) demonstrate the changes in Br concentrations in their samples between the in situ conditions and after quenching to room temperature and pressure.

The paucity of data on fluid/melt partitioning for halogens other than chlorine limits our understanding of their storage and transport in magmatic systems. Understanding the degassing behavior of halogens is becoming more critical as these elements become tools for the prediction of volcanic eruptions and as we learn about their detrimental effects on Earth's atmosphere (e.g., Aiuppa et al.,

2009). Although we now have in hand some very useful partition coefficients, the current experimental results raise some very interesting and potentially important questions. For example, fluid/melt partition coefficients for fluorine significantly greater than 1 are surprising because fluorine is generally considered to be a compatible element in fluid-saturated melts (e.g., Dolejš and Baker, 2008) and not lost into the volatile phase until very low pressures (e.g., Aiuppa et al., 2009). However, at the present time there is no explanation for the remarkably high partition coefficients measured in experiments on basaltic melts by different research groups (Alletti, 2008; Chevychelov et al., 2008b). Clearly there is the need for further experiments to investigate the partitioning of all halogens between silicate melts an coexisting aqueous fluids.

4.7 Noble gases and nitrogen

Our knowledge of the behavior of noble gases and nitrogen in magmatic systems is limited. However, at crustal pressures their solubilities are in the range of a few thousand ppm and they appear to be dissolved as atoms in the free-space (the ionic porosity) of the silicate melts (Jambon et al., 1986; Carroll and Stolper, 1993; Carroll and Webster, 1994; Carroll and Draper, 1994; Paonita, 2005). Paonita (2005) provides a table of noble gas solubilities; their values range from near 6 x 10^{-6} to 8.6 x 10^{-3} cm3 g^{-1} bar^{-1}, where the bar^{-1} unit indicates that the concentration is normalized to the pressure of the gas at saturation. Consistent

with the ionic porosity model, the solubilities of these gases increase with increasing ionic porosity, which to a first order approximation increases with the silica concentration in the melt, and decreases with increasing atomic radius. More recently Iacono-Marziano et el. (2010) demonstrated that both Ar and Ne solubilities in basaltic and rhyolitic melts followed Henry's law, i.e., they found a linear relationship between the concentration of these gases in the melt and the gas pressure. Combining their data with previous experimental results they were able to construct an empirical model to predict the solubilities of He, Ne and Ar in a wide range of igneous melt compositions.

Our knowledge of nitrogen's behavior in magmatic systems is fragmentary, at best. Unpublished experiments by D.R. Baker and D.H. Eggler at the Pennsylvania State University in the 1980's demonstrated that nitrogen saturation reduced the solidus temperature of diopside by less than 100 ℃ at 2.5 GPa, indicating that little nitrogen dissolved in the melt. Libourel et al. (2003) demonstrated that at 1 atmosphere basaltic melts dissolve nitrogen only at the ppb level, unless the oxygen fugacity is extremely low, below that estimated for lunar rocks. Both studies indicate the relative unimportance of nitrogen in terrestrial magmatic processes. Mysen et al. (2008) and Mysen and Fogel (2010) studied the solubility of nitrogen in sodium silicate binary melts far removed from natural compositions. These studies found little effect of oxygen fugacity on nitrogen solubility, but

Mysen and Fogel (2010) determined that increasing the Na/Si ratio of the melt resulted in higher solubilities. Mysen and Fogel (2010) determined that at the reducing conditions of the iron-wustite buffer, nitrogen was present as NH_3, NH_2^-, and minor N_2; no evidence of azide or nitride formation was found in either of these studies. The presence of nitride minerals in reduced meteorites (e.g., Russell et al., 1995) hints at its possible importance somewhere in the history of our solar system, but such nitrides are probably not associated with most terrestrial igneous processes.

4.8 Multicomponent fluids and the partitioning of trace volatiles

4.8.1 Chlorine, fluorine and water

Webster and Holloway (1990) studied the partitioning of F and Cl between fluids and a haplogranitic melt and between fluids and a rhyoltic melt. They found that addition of F at 1 to 2 wt.% in a haplogranitic melt resulted in a substantial decrease in the fluid/melt partition coefficient for chlorine; at 200 MPa the Cl partition coefficient in the presence of F is about one-half of the value for haplogranitic systems in which Cl is the only halogen (Fig. 10). They also demonstrated that the combination of increasing temperature and increasing concentrations of F in the system resulted in a decrease in the Cl fluid/melt partition coefficient such that at 200 MPa, 1000 ° C for a melt with almost 8 wt.% F, chlorine was partitioned into the melt rather than the fluid ($D^{fluid/melt}_{Cl}$ = 0.8).

Webster and Holloway's (1990) measurements of the chlorine fluid/melt partition coefficient for F-bearing topaz rhyolitic melt produced results almost identical to those obtained for the haplogranitic composition.

Webster and Rebbert's (1998) measurement of the chlorine partition coefficient between an F-bearing peraluminous rhyolitic melt at 200 MPa and fluid, $D^{fluid/melt}_{Cl}$ = 10.8 ± 2.2, similar to fluid/melt partition coefficients for similar rhyolitic melts in which chlorine is the only halogen (Fig. 10). Their $D^{fluid/melt}_{Cl}$ of 12 ± 4 at 50 MPa is similar to measurements for hawaiitic melts and fluids (Alletti et al., 2009) and approximately 1/3 of the value measured between fluids and a peralkaline phonolite (Signorelli and Carroll, 2000).

Chevychelov et al.'s (2008a) 845-860 ° C , 200 MPa data indicate that the chlorine fluid/melt partition coefficient in the presence of 0.1 to 0.7 wt % F is 3.3 ± 2.7, or approximately one half of that measured in the absence of fluorine. The fluorine fluid/phonolitic melt partition coefficient measured in the presence of 0.3 to 0.7 wt% Cl was, 7.3 ± 1.0, was also approximately one half of the value measured in chlorine free experiments. On the other hand, the measurements at 1000 ° C indicate no measurable effect of F on the Cl fluid/melt partition coefficient and almost no effect of Cl on the F fluid/melt partition coefficient, 4.4 ± 1.9 in the presence of 0.36 to 0.82 wt% Cl in the melt versus 7.6 ± 5.3 in the absence of

chlorine.

Chevychelov et al. (2008b) investigated partitioning of both Cl and F at 1200 °C, 200 MPa between a fluid and a hawaiitic melt. Their data defines a Cl partition coefficient of 2.7 when the fluorine concentration in the melt varies from 0.5 to 0.79 wt%. This value is quite similar to other values for the Cl partition coefficient between fluids and basaltic melts in F-free systems (Fig. 10). Chevychelov et al.'s (2008b) determination of the F fluid/melt partition coefficient in the presence of 0.4 to 2.67wt% Cl in the melt was 23.7 ± 2.7, virtually indistinguishable from the value determined with only 0.11 wt% Cl in the system of 28.1 ± 5.4. The results suggest the independence of the Cl and F fluid/melt partition coefficients from the presence of the other halogen in this system at concentrations similar to those studied (Fig. 10).

4.8.2 Chlorine, carbon dioxide and water

The effect of diluting the fluid with CO_2 on the partition coefficient of chlorine has been studied by two groups. Botcharnikov et al. (2007) investigated the difference in the fluid/andesitic melt partitioning of chlorine with fluids containing only water and chlorine at 1200 ° C , 200 MPa, where $D^{fluid/melt}_{Cl}$= 3.6±0.6, and fluids with water, chlorine and CO_2, where X_{H2O}^{fluid} = 0.85 and $D^{fluid/melt}_{Cl}$= 2.0±0.1 (Fig. 10). Although the decrease of the partition coefficient with the addition of

CO_2 is consistent with previous studies, the effect is minor at the conditions investigated. Botcharnikov et al. (2007) proposed that the chlorine partitioning between the fluid and andesitic melt was most-probably controlled by activity-composition relationships in the fluid phase composed of H_2O, Cl and CO_2. However, some of the variation they measured may have been due to the different melt compositions found in various experiments.

Alletti et al. (2009) measured partitioning of Cl between a hawaiitic melt and a C-O-H-Cl fluid and compared their results to a fluid only containing O-H-Cl. They found that at the addition of CO_2 measurably decreased the chlorine fluid/melt partition coefficient at 25 and 50 MPa, but had only a small effect at 100 MPa (Fig. 10). These effects of CO_2 on the partition coefficient of Cl were attributed by Alletti (2008) to the lower bulk dielectric constant of CO_2-H_2O fluids compared to pure H_2O fluids.

4.8.3 Chlorine, sulfur and water

Botcharnikov et al. (2004) investigated the partitioning of S and Cl between a hydrous fluid and a rhyodacitic melt. Their results demonstrated that as sulfur was added to the system the Cl concentration in the melt decreased for equivalent concentrations in the fluid. The total concentration of S in the melt and in the fluid increased from 60 ppm to 200 ppm as the chlorine concentration in the melt

varied from 0 to 8100 ppm. The effect of S on the partition coefficient of Cl was impressive. Using results from experiments whose melts contained 800 to 2300 ppm Cl and 60 to 160 ppm S, the calculated Cl partition fluid/melt coefficient is 10.3 ± 0.9 (Fig. 10), a fivefold increase over the partition coefficient determined in the absence of sulfur, ~2 (cf. Section 4.5). Botcharnikov et al.'s (2004) measurements yield a sulfur partition coefficient of 1500±400 in the absence of Cl, but this value drops to 260±36 when 0.22 to 0.23 wt.% Cl is present in the melt. This dramatic decrease in the partition coefficient was attributed to non-ideal mixing in the fluid by Botcharnikov et al. (2004).

Webster et al. (2009a) investigated the partitioning of chlorine and sulfur between phonolitic to trachytic melts and a hydrous fluid at 200 MPa and ~ 900 to 1000 °C and oxygen fugacities greater than NNO. Calculating the Cl partition coefficient for melts with 0.16 to 0.5 wt% Cl and approximately 1000 ppm S yields a fluid/melt partition coefficient of Cl equal to 14.5 ± 5.4 when measured Cl concentrations in the fluid are used or 11.9 ± 6.4 if the calculated fluid concentrations are used (see Webster et al., 2009a). This value is slightly higher than the Cl fluid/melt partitioning values found by Chevychelov et al. (2008) for a similar composition melt, but in the absence of sulfur (Fig 10.). No obvious dependence of the chlorine partition coefficient on the sulfur concentration can be observed in the data. The range in the fluid/melt partition coefficients of sulfur for most of the

experiments was 50 to 300, with most clustering near 200, but one was as low as 2 and another exceeded 1000. These authors found a clear dependence of the S partition coefficient on the calcium concentration of the melt and noted that this partition coefficient increased with increasing S in the system. The results of Webster et al. (2009a) display a weak dependence of the sulfur fluid/melt partition coefficient on the concentration of Cl in the melt over a range of Cl concentrations between 0.2 and 0.8 wt. %.

Beerman's (2010) thesis presents a comprehensive study of S and Cl partitioning between a hawaiitic melt and fluid, as well as similar data for a dacitic melt. Because this data is currently only available in the thesis only a short summary of it will be given; the interested reader should look for a full publication of the results by Beerman and his colleagues. Beerman's (2010) data demonstrate that at 1050 ° C, 200 MPa, and oxygen fugacities approximately 0.4 log units above the FMQ buffer the fluid/melt partition coefficient of sulfur between a hawaiitic melt and a Cl-bearing aqueous fluid is 180, and independent of the Cl concentration in the melt over the range of 0.06 to 2.23 wt%. However at oxygen fugacities of 2 log units above FMQ and higher, the partitioning of sulfur is complex and clearly dependent upon the Cl concentration in the system. At low Cl concentrations, below ~ 0.6 wt% in the melt, the sulfur fluid/melt partition coefficient is approximately 6 when sulfur concentrations in the melt are less than ~ 0.6 wt%, but as Cl

concentrations increase to values as high as 2.2 wt% in the melt the partition coefficient increases to 34. Beerman's (2010) measurements of Cl in the hawaiitic melt and in the fluid in the same S-bearing experiments at approximately FMQ + 0.5 and FMQ+2 demonstrate that the fluid/melt partition coefficient of Cl is ~2, if only experiments with melts containing up to 0.5 wt% Cl are used for the calculation. The value of 2 is approximately 1/3 of the partition coefficient of 6.4 calculated from Beerman's S-free experiments for the same melt, but at FMQ+0.8 (see Section 4.5). Beerman (2010) observed that at higher Cl concentrations in the melt the partition coefficient increases and that the partitioning was affected by the dissolution of cations into the fluid.

4.8.5 Sulfur, chlorine, carbon dioxide and water

Lesne et al. (2011c) experimentally simulated the degassing of two basaltic melts containing water, carbon dioxide, sulfur and chlorine at 1150 ° C and pressures from 300 to 25 MPa. The concentrations of sulfur in the experimental melts varied from 40 to 3 200 ppm and the concentration of chlorine from 1 200 to 2 400 ppm. At pressures between 100 and 300 MPa most of the measured partition coefficients for sulfur fall in the range between 10 and 100 when expressed in weight units. At lower pressures the partition coefficients increased to 100 to 300 at 50 MPa and up to 2800 at 25 MPa. The sulfur partition coefficients measured at and above 100 MPa are consistent with previous

determinations, but the lower pressure values are extremely high compared to other measurements, discussed in Section 4.4. The chlorine partition coefficient appeared insensitive to pressure; most measurements yielded values between 1 and 30 (in weight units), although some measurements were as high as 200. Although somewhat scattered, these measured partition coefficients are broadly consistent with others for basaltic melts (Fig. 10).

4.8.6 Sulfur, carbon dioxide and water

Webster et al. (2011) studied the partitioning of sulfur between haplogranitic melts and C-O-H fluids at 900 ° C , 200 MPa; the oxygen fugacities of the experiments ranged from 0.4 log units below the NNO buffer to 1.45 log units above it. They found that a linear correlation between sulfur in the melt and in the fluid independent of the CO_2 concentration in the system. This result is consistent with Henrian behavior of the sulfur and the insensitivity of the partition coefficient to CO_2. Although there was scatter in the data, the average sulfur fluid/melt partition coefficient measured by Webster et al. (2011) is 185. Webster et al. (2011) also discovered that at the lower oxygen fugacities they studied, but still only slightly below NNO, the addition of sulfur to the system lowered the solubility of CO_2 in the melt. Incidentally, it appears that Webster et al. (2011) were the first authors to consider calculating a simple partition

coefficient between fluid and melt for CO_2. Webster and Botcharnikov's (2011) analysis of experimental results lead them to note that the presence of CO_2 in the system had little to no effect on sulfur partitioning, but stressed the need for more studies.

Although our knowledge of the partitioning of volatile elements between multicomponent fluids and melts has increased in the past decade, we are only at the beginning of understanding their combined behavior. At relatively high concentrations of H_2O and low concentrations of the other volatiles (F, S, Cl, CO_2) the partitioning of any minor volatile between the melt and fluid seems little affected (less than a factor of 10*x*) by the presence of other volatiles, however differences of a factor of 3*x* do not seem uncommon. There is also a clear effect of melt and fluid compositions on the partitioning, that has not yet been well quantified (cf., Webster and Botcharnikov, 2011). This state of affairs can only be improved by more experiments and analysis at magmatic pressures and temperatures.

5. A brief history of silicate melt-volatile species interaction models for crustal pressures

In order to extend the partitioning measured at specific conditions of temperature,

pressure, melt and fluid composition, a model of the interactions between the volatile species in the fluid and in the melt must be constructed. Often geological models of element behavior are based upon the statistical fitting of a few thermodynamic parameters (e.g., P and T) and many empirical parameters (e.g., melt composition in terms of weight percent oxides). Although such models can be very useful and reproduce their calibration data sets accurately, extrapolation beyond, and sometimes even interpolation between, the calibrating points may produce nonsensical results. On the other hand, thermodynamics provides a firm foundation upon which to base models for volatile behavior in magmatic systems; a good thermodynamic model should accurately interpolate between calibration points and extrapolate, at least a little, beyond the calibration. However, often the uncertainties in the results calculated by a thermodynamic model are greater than those of an empirical model. The following sections provide information on some of the more well-known models of both types that can be used to investigate the behavior of volatile species in magmatic systems at crustal pressures.

5.1 Water

The first thermodynamic investigation of the dissolution of water in silicate melts was that of Wasserburg (1957), which was subsequently extended by Shaw (1964). And although Spera (1974) proposed a thermodynamically based model for water dissolution into silicate melts, the first widely used model for the behavior of water in silicate melts was that of Burnham (e.g., Burnham, 1975, 1979a, 1981;

Burnham and Nekvasil, 1986). This model is based upon Burnham's measurements of the molar volumes of water in the fluid phase and dissolved in albite melt (Burnham and Davis, 1971, 1974), the linear relationship between fugacity of H_2O and the square of the mole fraction of water dissolved in silicate melts at low pressures, and upon the observation by Burnham and co-workers that when melt compositions are expressed using an equi-oxygen molecular formula (in this case 8 oxygens) the water solubilities for all melts are similar. This model can be considered a classical thermodynamic model in that the actual species involved in the model are not correlated with species measured spectroscopically. Burnham's (1975, 1979a, 1981) model proposes that at $X_{H2O} \leq 0.5$ all water is dissolved as OH^- because as molecular water dissolves into the melt it immediately reacts with a bridging oxygen to form hydroxyl groups by the reaction

$$H_2O^{fluid} + Si\text{-}O\text{-}Si^{melt} \rightleftharpoons 2\ Si\text{-}O\text{-}H^{melt}, \qquad (1)$$

which can also be expressed as

$$H_2O^{melt} + O^{melt} \rightleftharpoons 2\ OH^{melt}. \qquad (6)$$

Based upon Burnham's studies of albitic melts, where at $X_{H2O} = 0.5$ equimolar proportions of H_2O^{bulk} and Na^+ exist in the melt, he proposed that for water concentrations above $X_{H2O} = 0.5$, and also in melts without exchangeable cations such as Na^+ (e.g., SiO_2 melts), another dissolution reaction occurs, but the nature of this reaction was unclear. Burnham explained the lower water solubility in pure silica melts, compared to feldspar melts (Fig. 2), by the absence of exchangeable

cations such as Na^+. Although the Burnham model successfully calculates water solubilities in many common silicate melts and can be used to model the phase relations in granitic systems, it has been largely replaced by more recent models based upon the measured concentrations of both dissolved molecular H_2O species at low concentrations of total water and the disproportionation of water into OH^- species in silicate melts.

In the 1980's, E. Stopler and associates (e.g., Stolper, 1982) used infrared spectroscopy to demonstrate the presence of OH^- and molecular H_2O dissolved in silicate melts and quantitatively measure their abundance in quenched glasses. In contrast to Burnham's model, dissolved molecular water was found to coexist with hydroxyl at low total water concentrations (less than approximately 1 wt%) in quenched silicate melts (i.e., glasses). With the insight gained from these measurements Stolper and colleagues could calibrate the equilibrium constants for the reactions :

$$H_2O^{fluid} \blacksquare H_2O^{melt} \qquad (7)$$

and Equation 6.

In a series of papers Stolper and coworkers built upon the original model and applied it to melt compositions ranging from basaltic to rhyolitic (Stolper, 1982; Silver and Stolper, 1985, 1989; Silver et al. 1990; Dixon et al., 1995). These

models rely upon the thermodynamic equilibrium requirement that the chemical potential of molecular water in the melt be equivalent to that of water in the fluid, $\mu_{H2O}^{melt} = \mu_{H2O}^{fluid}$, to calculate the activity of water in the melt relative to reference conditions:

$$a_{H_2O}^{melt}(P,T) = a_{H_2O}^{melt}(P_o,T_o)\frac{f_{H_2O}(P,T)}{f_{H_2O}(P_o,T_o)}\exp\left(\frac{-V_{H_2O}^{o,melt}(P-P_o)}{RT_o} + \frac{-\Delta H_{H_2O}^{o}}{R}\left[\frac{1}{T}-\frac{1}{T_o}\right]\right), \quad (8)$$

where T_o and P_o are the reference temperature (e.g., 1200 °C) and pressure (e.g., 1 bar or 0.1 MPa), the f_{H2O} terms refer to the fugacity of water, $V_{H2O}^{o,melt}$ is the molar volume of water in the melt that was found to be a constant for basaltic melts, 12 ± 1 cm^3 mol^{-1} (Dixon et al. 1995), and ΔH_{H2O}^{o}, the enthalpy of water dissolution, can be treated as a constant. Silver and Stolper (1989) and Dixon et al. (1995) demonstrated that dissolved molecular water followed Henry's law and therefore a simple linear relationship linked X_{H2O}^{melt} to a_{H2O}^{melt}. Once the concentration of molecular water dissolved in the melt is known, the hydroxyl concentration can be calculated from the equilibrium disproportionation reaction and the water concentration (in mol fraction) by

$$X_{H2O}^{total} = X_{H2O}^{melt} + \tfrac{1}{2} X_{OH^-}^{melt}, \quad (9)$$

which can be converted to weight percent.

These papers, in particular Silver and Stolper (1989) and Dixon et al. (1995),

demonstrated the success of the model and its ability to calculate water concentration in silicate melts saturated with a H_2O or H_2O-CO_2 fluid. Subsequently, Dixon (1997) published a model for water solubility in basaltic melts of differing compositions that was integrated into the software package VOLATILECALC (Newman and Lowenstern, 2002), which calculates water and CO_2 solubilities in basaltic and rhyoltic melts; an Excel® spreadsheet for this model can be downloaded from http://volcanoes.usgs.gov/yvo/aboutus/jlowenstern/other/software_jbl.html.

At the same time Stolper's group was constructing their models, more classical thermodynamic (i.e., macroscopic) models were under development by other researchers. Nicholls (1980) proposed a symmetrical regular solution model for the estimation of water solubility in silicate melts and demonstrated its utility. Ghiorso's regular solution model for the thermodynamics of anhydrous silicate melts (e.g., Ghiorso et al., 1983) was used to describe hydrous melts through the addition of one term in the expressions used to calculate the activity coefficient of the components in silicate melts:

$$RT\ln\gamma_w = \sum W_{w,i} X_i - \frac{1}{2}\sum\sum W_{i,j} X_i X_j + RT\ln X_w , \qquad (10)$$

and

$$RT\ln\gamma_k = \sum W_{k,i} X_i - \frac{1}{2}\sum\sum W_{i,j} X_i X_j + RT\ln(1 - X_w), \qquad (11)$$

where R is the gas constant, T is the temperature, the subscript w on the activity

coefficient γ, the Margules parameter W, and the mole fraction X, represents H_2O, which is modeled as the undissociated molecule, and the subscripts i, j, and k represent the anhydrous components in the melt (e.g., Mg_2SiO_4, $NaAlSi_3O_8$, $CaMgSi_2O_6$, etc.). Although this model neglects the disproportionation of dissolved molecular water into hydroxyl groups, it is nonetheless thermodynamically consistent and with calibration accurately describes the macroscopic behavior of water in silicate melts. Ghiorso et al. (1983) successfully reproduced the measured water solubilities available to them at that time using this model. Ghiorso and Sack (1995) updated and recalibrated the MELTS model using the same expressions for the chemical potentials of the components. The MELTS model can either be run from the website (http://melts.ofm-research.org/) as a java applet, or downloaded for use on a personal computer. Kirschen and Pichavant (2001) modeled the system albite-orthoclase-silica-water in a similar manner, but with additional Margules-like interaction parameters.

Papale (1997) used the regular solution formalism and Ghiorso et al.'s (1983) Margules parameters for the interactions of anhydrous components in silicate melts to calibrate a model for the solubility of H_2O (and a separate one for CO_2) in silicate melts using experimental data. Similar to Ghiorso et al. (1983) and Ghiorso and Sack (1995), the disproportionation of dissolved molecular water into hydroxyl was not included in the model. This model was updated in 1999 (Papale,

1999) and in 2006 (Papale et al. 2006) to also calculate the partitioning of water between silicate melts and an H_2O-CO_2 fluid. As Papale (1999) discussed, addition of a second volatile component to the system creates conditions such that the concentration of a volatile in the melt depends not only upon pressure and temperature, but also upon the fluid composition, i.e., the partial pressure of the volatile component in the fluid at P and T, as seen in Figure 8. The latest version of this model is accessible for online use at the website: http://vmsg.pi.ingv.it/index.php/en/software/interactiveArea/sw_id/4.

Other researchers took a more empirical approach to modeling solubility in melt compositions spanning most found in Nature. Moore et al. (1995, 1998) presented a successful semi-empirical model for the solubility of water in melts from basaltic to rhyolitic at pressures up to 300 MPa. This model is based upon the temperature, water fugacity, and the weighted sum of the mole fractions of SiO_2, FeO^{total} and Na_2O multiplied by the pressure divided by the temperature (Moore et al., 1998).

Many authors instead chose to model water solubility over only a limited range of melt compositions. The advantage of this philosophy is that it typically reproduces the experimental data much better than models designed for a wide compositional range. Examples of such models are those for rhyoltic melts from

Zhang (1999) and Tamic et al. (2001), and Liu et al. (2005). Lesne et al. (2011a) followed the approach of Dixon et al. (1995) to investigate the solubility and speciation of water in basaltic melts of varying alkalinity.

5.2 Carbon dioxide

Because all known CO_2-bearing, natural silicate melts also contain water, many of the models used for the calculation of carbon dioxide solubility and partitioning were previously discussed in the context of models for water. However, a few models that predict only CO_2 solubility were created. One of the earliest (if not the earliest) was Spera and Berman (1980), who based their model on the few high-pressure (mantle conditions) measurements available at that time. Stolper and Holloway (1988) applied infrared spectroscopy to investigate carbon dioxide dissolution into basaltic melts at low pressures and modeled it by the reaction:

$$CO_2^{\ fluid} + O^{2-,\ melt} \blacksquare CO_3^{2-,\ melt} . \qquad (4b)$$

They used the same type of equations as applied to water solubility model in other papers by Stolper and his group (*op sit.*). Pawley et al. (1992) used a similar model to explain CO_2 solubility in tholeiitic melts. Based upon their extensive study of CO_2 solubilities and infrared spectra, Brooker et al. (2001a) presented an empirical model for the solubility of CO_2 as a function of the ratio of non-bridging oxygens to tetrahedral cations in the melt. Behrens et al. (2004) presented a model for the solubility of CO_2 in rhyolitic and dacitic melts, and Lesne et al. (2011b) created a model for CO_2 solubility in basaltic melts following

Dixon (1997). Lesne et al. (2011b) compared their measured CO_2 saturation pressures with those predicted by VolatileCalc (Newman and Lowenstern, 2002) and by the model of Papale et al. (2006). They found that VolatileCalc overestimated the saturation pressure by up to ~150 MPa, whereas the Papale et al. (2006) model overestimated the pressures by less than 50 MPa.

5.3 Water and carbon dioxide

Dixon et al. (1995) and Dixon (1997) built upon the results of Stolper and Holloway (1988) to model both CO_2 and H_2O solubility (discussed above) in basic silicate melts; the Dixon et al. (1997) model is available in the program VolatileCalc (Newman and Lowenstern, 2002). Papale's model (Papale, 1999; Papale et al., 2006) calculates both H_2O and CO_2 concentrations in melts coexisting with C-O-H fluids for compositions ranging from basaltic to rhyolitic.

Tamic et al. (2001) present an empirical model for calculating the water concentration in silicic melts as a function of the mole fraction of water in the coexisting CO_2-H_2O fluid based upon their experiments. Behrens et al. (2004) present another model to predict the interactions of dacitic and rhyoltic melts with CO_2 and H_2O. The Liu et al. (2005) model for rhyolitic melts calculates the solubilities of H_2O and CO_2 in silicic melts saturated with a H_2O-CO_2 fluid phase.

Witham et al. (2011) created a model for the solubilities of H_2O, CO_2, S, and Cl in basaltic melts over the pressure range of 0.5 to 400 MPa; these researchers combined the approach of Dixon et al. (1995) and Dixon (1997) for water and CO_2, and the S and Cl partitioning measurements of Lesne et al. (2011c). Although VolatileCalc (Newman and Lowenstern, 2002) is similarly based upon Dixon et al. (1995) and Dixon (1997), Witham et al. (2011) include the effects of melt composition in their model. The Witham et al. (2011) model yields similar water and CO_2 solubilities for a normal MORB composition at 400 MPa to those calculated using VolatileCalc (Newman and Lowenstern, 2002). However, for an alkali-enriched, ocean island basalt at the same conditions the Witham et al. (2011) model predicts a concentration of 2200 ppm rather than the 1400 ppm predicted by VolatileCalc and the 2500 ppm predicted by the Papale et al. (2006) model.

5.4 Comparison of two H_2O and CO_2 solubility models with experimental measurements

The solubilities of H_2O and CO_2 calculated by both VolatileCalc for basaltic and rhyolitic melts (Newman and Lowenstern, 2002) and the Papale et al. (2006) model for melts ranging in composition from basaltic to rhyolitic are compared against the experimental data in Figures 4 through 8. The success of these models for the prediction of water solubilities in silicic and intermediate composition melts is demonstrated in Figures 4 and 5, where the difference between modeled and measured

solubilities is typically less than 0.5 wt.%. Note that only the Papale et al. (2006) model is applicable to the intermediate composition melts. The differences between measured and modeled water solubilities for mafic melts is greater (Fig. 6), about 1 to 1.5 wt%. The solubility of CO_2 in magmatic melts predicted by the models agrees excellently with the experimental data at pressures of 500 MPa and below, but with increasing pressure the predicted solubilities become increasingly greater than the measured values (Fig. 7). Comparison of both models with H_2O and CO_2 solubilities measured in rhyoltic melts coexisting with an H_2O-CO_2 fluid at 500 MPa (Tamic et al., 2001) demonstrates agreement to within ~ 1 wt% H_2O and 0.07 wt%, or 700 ppm, CO_2 (Fig. 8a). As shown in Figure 8b, H_2O and CO_2 solubilities predicted by VolatileCalc for a basaltic melt with 49 wt.% SiO_2 and those measured in a basaltic melt at 500 MPa (Shishkina et al., 2010) differ by up to 1.5 wt.% H_2O and 0.15 wt.% CO_2. The newer model of Witham et al. (2011) produces similar results to VolatileCalc (discussed above).

Two basaltic compositions were investigated with the Papale et al. (2006) model. The first is the rather normal MORB composition used by Dixon et al. (1995), which the Papale et al. (2006) model predicts to have H_2O and CO_2 solubilities, similar to those for the rhyolitic melt, and at most only ~0.1 wt% more enriched in CO_2 than predicted by VolatileCalc (Fig. 8b). The second composition is that used by Shishkina et al. (2010) for their experiment results plotted in Figure 8b. Although

the Papale et al. (2006) model and the experimental data are in good agreement at water-rich conditions, the model over-predicts CO_2 solubilities at low water conditions. At water concentrations below approximately 6 wt.% in the melt the Papale et al. (2006) model begins to over-predict the CO_2 solubility by up to ~0.13 wt% for the most water-poor experiment (Fig. 8b). Some of the differences between the experimental measurements and the Papale et al. (2006) model may be a function of the ferric/ferrous ratio of the melt, which is influenced by the oxygen fugacity (Papale et al., 2006). Vetere et al.'s (2011) comparison of their measured solubilities and those predicted by the Papale et al. (2006) model demonstrated that the ferric/ferrous ratio has a significant effect on the calculated CO_2 solubility at low water concentrations; they showed that changing the Fe^{2+}/Fe^{total} from 0.5 to 0 increases CO_2 solubility by up to ~ 0.08 wt%.

Although neither model perfectly fits the experimental measurements and both tend to underestimate measured water saturation concentrations in silicic melts and overestimate them in mafic melts, as well as VolatileCalc tending to underestimate CO_2 solubilities for melts coexisting with H_2O-CO_2 fluids and the Papale et al. (2006) model overestimating them, the accuracy of the models is sufficient for the investigation of water and carbon dioxide behavior in magmatic systems. Both models are based upon measurements at normal magmatic temperatures, ~ 800 to 1200 ° C, and typical experimental oxygen fugacities, within a few log units of the

nickel-nickel oxide buffer. Choosing between the models for application at pressures of 500 MPa or less appears to be a matter of personal preference, however because the maximum pressure limit of VolatileCalc is 500 MPa, only the Papale model can be used for investigations of volatile behavior at higher pressures (as exemplified in Section 6, below).

5.5 Sulfur

Modeling the partitioning of sulfur between aqueous fluids and silicate melts lags far behind water and carbon dioxide, due almost certainly to the paucity of experimental measurements. Most models for the behavior of sulfur in silicate melts involve the saturation of the melts with a sulfide or sulfate phase, pyrrhotite or anhydrite, respectively, and are not explicitly developed to predict sulfur partitioning between the melt and a fluid phase. In comparison to water and carbon dioxide, sulfur has the possibility of existing in multiple oxidation states (-2, +6) in magmatic environments (Wilke et al., 2011, Baker and Moretti, 2011). Additionally, because magmatic fluids are never pure sulfur, a model needs to predict the partitioning of sulfur between a C-O-H-S fluid and a silicate melt. Moretti and Papale (2004); presented a thermodynamic model that calculates the equilibrium behavior of species in a C-O-H-S fluid and their dissolution into melts ranging in composition from shoshonitic to rhyolitic. This model demonstrates the complexity of volatile partitioning between fluids and melts and how changing the

oxygen fugacity affects the partitioning of all volatile components in the system. Scaillet and Pichavant (2005) presented an empirical model to calculate the concentration of sulfur in a melt based upon the pressure, temperature, oxygen and sulfur fugacities, and melt composition. The molar partitioning of S between the fluid and melt, $K_S^{fluid/melt}$, in the Witham et al. (2011) model is given as a function of pressure, P:

$$\log K_S^{fluid/melt} = 431.69P^{-0.0074946} - 410.49 + 2.7426x10^{-3}P - 1.4891x10^{-7}P^2 \quad . \quad (12)$$

5.6 Chlorine and fluorine

Despite the abundance of chlorine partitioning studies between silicate melts and aqueous fluids there is no general model for Cl partitioning applicable to magmatic systems. Webster and DeVivo (2002) presented a model to calculate the solubility of Cl-brine in melt compositions from basaltic to rhyolitic, however it was limited to a single pressure of 200 MPa. Shinohara (2009) presented a polybaric model for the partitioning of chlorine between a hydrous fluid and melt, but it is limited to felsic melts. Both of these models are classified as empirical, although they contain a thermodynamic foundation. Although there are no experimentally based models currently available for fluorine partitioning between aqueous fluids and silicate melts, Villemant and colleagues (Villemant and Boudon, 1998, 1999; Villemant et al. 2003) have constructed some models based upon measurements of natural volcanic products. The Witham et al. (2011) model for C-O-H-S-Cl

partitioning considers the molar partitioning of chlorine, $K_{Cl}^{fluid/melt}$, between the melt and fluid to be constant at 0.31.

6. Evolution of fluids during partial melting and ascent

6.1 Melt and fluid compositions during partial melting

Initial experiments on hydrous phase equilibria in the crust concentrated on the water-saturated melting and crystallization behavior of crustal lithologies and synthetic equivalents (e.g., Tuttle and Bowen, 1958). However the importance of fluid-absent, dehydration melting became widely accepted and studied in the 1980's and 1990's, in particular due to the experiments of Vielzeuf and co-workers (e.g., Clemens and Vielzeuf, 1987; Vielzeuf and Holloway, 1988), as well as studies by Patiño-Douce, Johnston and their colleagues (e.g., Patiño-Douce and Johnston , 1991; Skjerlie et al. 1993). However, many other research groups were also actively studying dehydration melting and their work substantially contributed to our understanding of this process (e.g., Wolf and Wyllie, 1991; Rapp and Watson, 1995; *inter alia*). These experimental studies demonstrate that melting reactions during either dehydration melting or fluid-saturated melting at the solidus, which varies from near 700 °C for metapelitic compositions (Vielzeuf and Holloway, 1988) to near 1000 °C for metabasic compositions (Rapp and Watson, 1995) in the mid- to lower-crust, involve the melting of hydrous phases, amphibole and/or micas.

The amount of granitic melt produced near the solidus is typically on the order of 10 wt% and within 100 °C above the solidus can increase to 40% (e.g., Vielzeuf and Holloway, 1988; Patiño-Douce and Johnston, 1991). If the protolith undergoing melting contains 20% mica with 4 wt% H_2O, or 0.8 % water in the rock, as the only source of volatiles, a 10% melt would contain 8 wt% H_2O and be undersaturated with water at pressures above approximately 300 MPa (Fig. 4). However the melting of a pure amphibolite, with a bulk concentration of 2 wt% H_2O, to produce 10 % melt would yield a separate fluid phase at pressures below approximately 1 000 MPa. Such a scenario seems unlikely, but even if this case, approximately doubling the percentage of melt to 20% would result in the absorption of the water into the melt and elimination of the fluid phase at pressures of 300 MPa or greater (Fig. 4). However, when carbonates are also present in the rock and during anatexis the carbonate stability is exceeded, the system behaves very differently. Even if a pelitic source rock contains only 5 wt% carbonate mineral, thermodynamic calculations of dehydration and melting demonstrate that at temperatures near 800 °C the fluid may contain 0.8 mol fraction H_2O and 0.2 CO_2 (calculations by J. Connolly, pers. comm. 2010).

If CO_2 is present in the fluid phase, dehydration and melting reactions occur at higher temperatures and some of the water liberated during dehydration and melting is partitioned into the fluid phase due to the requirement that at equilibrium the

chemical potential of all components must be equal in all phases. Thus, the melts produced in this scenario are fluid saturated, but may contain less water than melts produced by fluid-absent, dehydration melting. Furthermore, addition of CO_2 to a hydrous fluid generally reduces the partition coefficients of elements between silicate crystals and melts and CO_2-H_2O fluids with the result that the fluids are less enriched than if they were composed of pure water (see discussion in Schneider and Eggler, 1986) .

The behavior of a magmatic system can be investigated using the H_2O-CO_2-melt model of Papale et al. (2006) and a melt similar in composition to that produced in experiments at 800 °C, 800 MPa by Vielzeuf and Holloway (1988), shown in Table 1. With this composition and model, the concentration of dissolved volatiles in the silicate melt and the composition of the coexisting fluid phase as a function of the total concentration of H_2O and CO_2 in the system melt+fluid can be calculated. If this system contains approximately 0.5 wt% CO_2, or less, no fluid phase is present unless the total amount of water is greater than approximately 9.5 wt% (Fig. 11). Once the carbon dioxide concentration in the melt+fluid system reaches 1 wt% the system is always fluid saturated, thus only a small amount of carbonate in the source rock can lead to the saturation of the melt with an H_2O-CO_2 fluid. The fluid composition is controlled dominantly by the total concentration of water in the system and only weakly affected by the carbon dioxide concentration (Fig.

11), at least up to a total of 4 wt% CO_2 in the melt+fluid system.

The concentration of water in the melt was calculated for two bulk CO_2 concentrations at 800 MPa; the first was 0.5 wt%, where a fluid phase is not present except in systems with 10 wt% H_2O, and the second was 2.0 wt%, where a fluid phase is always present. A crustal rock with an average concentration of 1900 ppm CO_2 (Wedepohl, 1995) that is 10% molten produces a melt+fluid system with 1.9 wt% CO_2, if no carbon-bearing minerals are stable. As expected, the higher the water concentration in the system, the higher the concentration of water dissolved in the melt (Fig. 12). Systems with ~2.0 wt% CO_2 contain less water in the melts than systems with lower concentrations, also as expected because the formation of a mixed-volatile fluid phase requires the partitioning of water between the fluid and the melt, but this effect on the concentration of water in the melt is minor except at the highest concentrations (Fig. 12). The calculated concentrations of carbon dioxide in these melts are all approximately 5 000 ppm.

6.2 Fluid exsolution and changes in fluid composition during ascent

Separation of the magma (melt+fluid) from the residuum and ascent through the crust will affect the volatile concentrations in both the melt and the fluid phase. However the effects depend upon whether the fluid and melt remain in thermodynamic equilibrium throughout the ascent (modeled as closed system behavior), or if the

equilibrium fluid at each pressure and temperature can separate from the melt (open system behavior), as well as processes such as magma mixing and assimilation. Both of these behaviors can be modeled in a stepwise manner, however in this contribution only a demonstration of the volatile evolution in a closed system at isothermal conditions and constant melt composition will be considered. The justification for these simplifications is founded upon the evidence that most granitic melts are transported through the crust in dikes over short time scales (Clemens and Mawer, 1992; Petford et al., 1993). Thus, changes in temperature and composition between the source region and emplacement can be modeled as minor, and for the case of the present discussion ignored. The compositions of coexisting melts and fluids are calculated at 50 MPa intervals from 800 to 50 MPa; the coexisting fluid and melt compositions were also calculated at 25 MPa (Figs. 12, 13). Because of the dominance of H_2O and CO_2 in the magmatic volatile budget we will concentrate on their behavior, with only a short discussion of chlorine and sulfur. Similar models have been previously presented by Holloway (1976) and by Burgisser et al. (2008) and interested readers are strongly encouraged to look at those papers to increase their understanding of the complexity of melt degassing during magma ascent.

Considering the case where H_2O is the only volatile in the system, the ascent of an undersaturated melt only creates a separate volatile phase once the pressure of the

system is below the saturation pressure (Figs. 4, 5, 6). As the pressure of the water-saturated system decreases, the concentration of water in the melt also decreases. However, water-saturated melts formed at the solidus (i.e., without superheat) cannot ascend without intercepting their solidus and suffering thermal death, because water-saturated solidi for magmatic systems exhibit a negative slope on pressure-temperature diagrams (e.g., Luth, 1969).

In cases where two or more volatiles are present in the system the behavior is much more complex because the magmatic solidi under such conditions have a positive slope on pressure-temperature diagrams. During ascent, the compositions of the melt and of the coexisting fluid evolve toward a melt with less water and CO_2 and a fluid that is richer in H_2O than that initially present at melting (Figs. 12, 13). The CO_2 concentrations in the melts decline from near 5 000 ppm at 800 MPa to a few 10's of ppm at 25 MPa. The changes in the fluid composition are most pronounced for melts with water concentrations that were initially low.

The change in the H_2O and CO_2 concentrations in the fluid during ascent and degassing has a significant effect on the partitioning of minor and trace elements between the melt and the fluid. The effects of pressure, temperature, and fluid composition of the fluid-melt partition coefficient of chlorine can be estimated using the Cl fluid/melt partitioning data determined for a haplogranitic melt

(Shinohara et al., 1989) , as weighed by the mole fraction of water in the fluid (Alletti, 2008). These estimated partition coefficients range from 375 for the most water-rich bulk compositions investigated to 125 for the water-poor ones. The effects of the changing partition coefficients for chlorine were studied for a system in which the melt initially contained 1 000 ppm chlorine. The results are rather surprising (Fig. 14) in that whenever a fluid phase is present the melt is significantly depleted in chlorine (from 1 000 ppm in the melt to a maximum of 10 ppm) and that the effect of the changes in the partition coefficient with pressure and fluid composition are weak. This weakness is due to the high partition coefficient of chlorine between the melt and the fluid which is sufficient to effectively strip chlorine from the melt.

The high fluid/melt partition coefficients for sulfur, on the order of 500 to 1000, discussed in Section 4.4 will result in significant depletion of the melt and corresponding enrichment of the fluid. Given a system with 1000 ppm total sulfur the melt is only calculated to contain less than 10 ppm S once a separate fluid phase becomes stable. Thus, virtually all of the sulfur is expected to be contained in the fluid phase.

The amount of fluid in equilibrium with the melt during closed system ascent scales with the total mass of water and carbon dioxide in the system. As pressure

decreases the amount of the fluid phase in these closed system models increases as the melt exsolves volatiles (Fig. 15). Only systems that originally contained significant amounts of volatiles can exsolve large amounts of fluid. For systems initially containing 8 and 10 wt% water, much of the fluid phase is exsolved at pressures in the range of 100 to 200 MPa, whereas for systems with 2 and 4 wt% water most exsolution occurs below 100 MPa.

The volume of the magmatic system (silicate melt + fluid) was calculated using the density-composition relationships for individual oxides in the silicate melt (Lange and Carmichael, 1987 for TiO_2 and the TiO_2*x*Na_2O term; Ochs and Lange, 1997 for SiO_2, Al_2O_3, MgO, CaO, and Na_2O ; Ochs and Lange, 1999 for H_2O; Liu and Lange, 2006 for Fe_2O_3, FeO and K_2O) and the modified Redlich-Kwong equation of state for the fluid (Holloway, 1977; Flowers, 1979). The effect of the small amount of CO_2 dissolved in the melt on its density was neglected. The volume of 100 g of the granitic melt + fluid magmatic system does not change significantly as its pressure decreases from 800 to ~200 MPa and is between 40 and 60 cm^3 (Fig. 16). However, at lower pressures the volume increases up to 200 cm^3 for systems with the highest water concentrations; this large volume increase is due to the exsolution of the fluid phase because the molar volume of water in the fluid is much larger than when dissolved in the melt.

6.3 Effect of volatiles on vesicularity

The calculations of fluid density and melt density can be used to investigate the volume fraction of the fluid phase in the magma, the vesicularity. As expected, the vesicularity increases with decreasing pressure as more volatiles partition into the fluid phase (Fig. 17). For the volatile-rich compositions modeled, 8 and 10 wt% water in the magma, significant increases in vesicularity occur at pressures below 200 MPa and these magmas achieve vesicularities greater than 75% at 25 MPa. Such a large fraction of fluid might separate from the melt and ascend independently, leading to open system behavior (but this is not modeled here). The exsolution of carbon dioxide and its partitioning into the fluid phase has a significant effect on the vesicularity of water-rich magmas at high pressures, but because of the small concentrations of CO_2 the effect is minor at low pressures near Earth's surface. Even magmas with 2 and 4 wt% water achieve significant vesicularities, between 25 and 62 volume percent at 25 MPa, and the effect of CO_2 on increased vesicularity is clearly evident at both high and low pressures (Fig. 17).

All but the most volatile-poor compositions modeled achieve greater than 30% vesicularity at pressures between 50 and 180 MPa (Fig. 17). This vesicle fraction is potentially an important parameter because percolation theory predicts that spherical vesicles will form a connected network at this point allowing relatively

easy and rapid gas transport (Lorenz and Ziff, 2001). Such a network may be important in allowing degassing from depths to the surface, or if there is an impermeable cap on the top of the magma the transport may allow the build up of significant amounts of gas near the upper, and potentially weaker, portions of a magma chamber or volcanic conduit system.

The modeled magmas with lower volatile concentrations increase their vesicularities from below 10% to greater than 30% over a much smaller pressure interval, ~ 25 MPa (or a distance of less than 1 km of depth), than magmas with higher water concentrations that require 200 MPa (~6 km of depth) or more decompression to achieve this critical threshold. Thus, given equal ascent rates to shallow depths, the growth of vesicles in the water-poor melts is expected to occur more rapidly and potentially result in more rapid acceleration of these magmas than the water rich ones. This potentially creates the possibility where volcanic eruptions created by magmas with low-to-moderate volatile concentrations may be more explosive than those created by volatile-rich magmas.

6.4 Magmatic fluids and ore deposits

These results indicate that whenever a fluid phase first forms it will not only strip Cl and S from the melt, but also metals associated with chlorine (e.g., Cu and Au) as discussed by Williams-Jones and Heinrich (2005) and/or with sulfur

(e.g., Au, Cu, Ni, Pd) as demonstrated by Baker et al. (2001) and extensively reviewed by Simon and Ripley (2011). Such a fluid may be the precursor to an ore deposit (Candela, 1997). The calculations in Section 6.2 strongly suggest that melts are fluid saturated at high pressures in many cases, where the fluid-melt partition coefficients are greatest. Additionally, at high pressures the solubility of water in granitic melts is prograde, higher temperatures lead to greater concentrations of water dissolved in the melt and higher solubilities of melt components (probably dominated by silica) in the fluid phase (e.g., Holloway, 1971; Schneider and Eggler, 1986; Ayers and Eggler, 1995). Thus, fluids in equilibrium with melts in the mid- to deep crust are expected to be rich in silica, chlorine, sulfur and metals; these fluids may be excellent sources of ore deposits.

During closed system ascent this fluid will remain in contact with the melt and not lose significant amounts of chlorine and sulfur (and presumably metals) into the melt, although there is minor Cl resorption evident at pressures below about 300 MPa (Fig. 14). The concentration of silica in the fluid will drop with decreasing pressure (Kennedy et al., 1962; Boettcher, 1984). If during ascent the system became open and the fluid escaped from the melt, the chlorine and metals are expected to precipitate out in cooler rocks.

The large increase in volumes of the magmatic systems at pressures below 200 MPa

may also play a role in ore deposit formation. The volume increase of 200% for magmas with 4% bulk water to 400% for magmas with 8 and 10 % bulk water (Fig. 16) could be responsible for fracturing of rocks and the possible formation of ore deposits as discussed by Burnham (1979b). Clearly, magmas with higher water contents have larger volumes at low pressure and are more likely mechanisms for fracturing country rocks.

The available information on fluid saturation, partitioning and the physical properties of magmas allows the construction of many possible scenarios for the formation of ore deposits, but the construction of such scenarios is far beyond the scope of this contribution.

7. Conclusions

Our current state of measurements and models for the interaction of water with natural silicate melts, particularly silicic compositions, is very good. However, our knowledge of the solubilities in silicate melts of CO_2, S and halogens, whether individually or in mixed fluids, needs substantial improvement if we want to fully understand the interaction of silicate melts with multicomponent fluids in magmatic systems. Many more experiments and improved models are needed. Nevertheless, the models that are currently available can be used to constrain the behavior of volatiles in many magmatic systems and can be used to predict the saturation of

melts with multicomponent fluids and the partitioning of volatiles between melts and coexisting fluids. These constraints can provide insights into important ore forming processes, magmatic degassing and volcanic eruption mechanisms.

Acknowledgments

This paper is dedicated to the former professors who introduced the senior author to the importance of volatiles in igneous systems: Peter J. Wyllie, David H. Eggler and A.T. (Fred) Anderson. Many thanks also go to R. Moretti, P. Papale, R. Rudnick, F. Spera, J.D. Webster and particularly E. Stolper for their time spent in discussions while preparing this article. Oliver Beerman was kind enough to provide us with a copy of his Ph.D. Dissertation. J. Connolly is thanked for his calculations. An anonymous reviewer and R. Botcharnikov are thanked for their detailed reviews that resulted in a significantly improved paper. Obviously, any omissions or errors are solely the responsibility of the authors.

References

Acocella, J., Tomozawa, M., Watson, E.B., 1984. The nature of dissolved water in sodium silicate glasses and its effect on various properties. J. Non-Cryst. Solids 65:355-372.

Albarède, F., 2009. Volatile accretion history of the terrestrial planets and dynamic implications. Nature 461:1227-1233.

Aiuppa, A., Baker, D.R., Webster, J.D., 2009. Halogens in volcanic systems. Chem. Geol. 263:1-18.

Alletti, M., 2008. Experimental investigation of halogen diffusivity and solubility in Etnean basaltic melts. Ph.D. Thesis. Univ. of Palermo.

Alletti, M., Baker, D.R., Scaillet, B., Aiuppa, A., Moretti, R., Ottolini, L., 2009. Chlorine partitioning between a basaltic melt and H2O-CO2 fluids at Mount Etna. Chem. Geol. 263:37-50 .

Ayers, J.C., Eggler, D.H., 1995. Partitioning of elements between silicate melt and H_2O-NaCl fluids at 1.5 and 2.0 GPa pressure: Implications for mantle metasomatism. Geochim. Cosmochim. Acta 59:4237-4246.

Baker, D.R., 1991. Interdiffusion of hydrous dacitic and rhyolitic melts and the efficacy of rhyolite contamination by dacitic enclaves. Contrib. Mineral. Petrol. 106:462-473.

Baker, D.R., Moretti, R., 2011. Modeling the solubility of sulfur in magmas: a 50-year old geochemical challenge. In: H. Behrens, J.D. Webster (Editors), Sulfur in Magmas and Melts: Its Importance for Natural and Technical Processes, Rev. Mineral. Geochem. 73:167-213.

Baker, D.R., Barnes, S.-H., Simon, G., Bernier, F., 2001. Fluid transport of sulfur and metals between sulfide melt and basaltic melt. Can. Min. 39:537-546.

Barnes, H.L. (Editor), 1979. Geochemistry of Hydrothermal Ore Deposits 2nd ed. Wiley, New York, 798 pp.

Beermann, O., 2010. The solubility of sulfur and chlorine in H_2O-bearing dacites of Krakatau and basalts of Mt. Etna. PhD Thesis, 109 p, Hannover.

Beermann, O., Botcharnikov, R.E., Nowak, M., Holtz, F., 2009. Redox control on S and Cl partitioning between basaltic melts and coexisting fluids: Experimental constraints at 1050 °C and 200 MPa. Eos Trans. AGU:90, Fall Meet. Suppl. Abstract V43B-2230

Behrens, H., Jantos, N., 2001. The effect of anhydrous composition on water solubility in granitic melts. Am. Mineral. 86:14-20.

Behrens, H., Nowak, M., 2003. Quantification of H_2O speciation in silicate glasses

and melts by IR spectroscopy - in situ versus quench techniques, Phase Transitions, 76:45-61. DOI: 10.1080/01411590310000076048

Behrens, H., Meyer, M., Holtz, F., Benne, D., Nowak, M., 2001. The effect of alkali ionic radius, temperature, and pressure on the solubility of water in $MAlSi_3O_8$ melts (M = Li, Na, K, Rb). Chem. Geol. 174:275-289.

Behrens, H., Misiti,V., Freda, F., Vetere, F., Botcharnikov R., Scarlato, P., 2009. Solubility of H_2O and CO_2 in ultrapotassic melts at 1200 and 1250 ° C and pressure from 50 to 500 MPa. Am. Mineral. 94:105-120.

Behrens, H., Ohlhorst, S., Holtz, F., Champenois, M., 2004. CO_2 solubility in dacitic melts equilibrated with H_2O-CO_2 fluids: Implications for modeling the solubility of CO_2 in silicic melts. Geochim. Cosmochim. Acta 68:4687-4703.

Benne, D., Behrens, H., 2003. Water solubility in haplobasaltic melts. Eur. Jour. Mineral. 15:803-814.

Berndt, J., Liebske, C., Holtz, F., Freise, M., Nowak, M., Ziegenbein, D., Hurkuck, W., Koepke, J., 2002. A combined rapid-quench and H_2-membrane setup for internally heated pressure vessels: Description and application for water solubility in basaltic melts. Am. Mineral. 87:1717-1726.

Blank, J.G., Stolper, E.M., Carroll, M.R., 1993. Solubilities of carbon dioxide and water in rhyolitic melt at 850 ° C and 750 bars. Earth Planet. Sci. Lett. 119:27 - 36.

Boettcher, A.L., 1984. The system SiO_2-H_2O-CO_2: melting, solubility mechanisms of carbon, and liquid structure to high pressures. Am. Mineral. 69:823-833.

Boettcher, A.L., Wyllie, P.J., 1969. Phase relationships in the system $NaAlSiO_4$-SiO_2-H_2O to 35 kilobars pressure. Am. Jour. Sci. 267:875-909.

Bohlen, S.R., Boettcher, A,L., Wall, V.J., 1982. The system albite-H_2O-CO_2: a model for melting and activities of water at high pressures. Am. Mineral. 67:451-462.

Borodulin, G.P., Chevychelov, V.Yu., Zaraysky, G.P., 2009. Experimental study of partitioning of tantalum, niobium, manganese, and fluorine between aqueous fluoride fluid and granitic and alkaline melts. Doklady Earth. Sci. 427:868-873.

Botcharnikov, R., Behrens, H., Holtz, F., Koepke, J.,Sato, H., 2004. Sulfur and chlorine solubility in Mt. Unzen rhyodacitic melt at 850 ° C and 200 MPa. Chem. Geol. 213:207-225.

Botcharnikov, R., Freise, M., Holtz, F., Behrens, H., 2005. Solubility of C-O-H mixtures in natural melts: new experimental data and application range of recent models. Ann. Geophys. 48:633-646.

Botcharnikov, R.E., Behrens, H., Holtz, F., 2006. Solubility and speciation of C-O-

H fluids in andesitic melt at T =1100-1300 ° C and P = 200 and 500 MPa. Chem. Geol. 229:125-143.

Botcharnikov, R., Holtz, F., Behrens, H., 2007. The effect of CO_2 on the solubility of H_2O-Cl fluids in andesitic melt. Eur. Jour. Mineral. 19:671-680.

Brimhall, G.H., Crerar, D.A., 1987. Ore fluids; magmatic to supergene. Rev. Mineral. Geochem. 17:235-321.

Brooker, R.A., Kohn, S.C., Holloway, J.R., McMillan, P.F., Carroll, M.R., 1999. Solubility, speciation and dissolution mechanisms for CO_2 in melts on the $NaAlO_2$-SiO_2 join. Geochim. Cosmochim. Acta 63:3549-3565.

Brooker, R.A., Kohn, S.C., Holloway, J.R., McMillan, P.F., 2001a. Structural controls on the solubility of CO_2 in silicate melts: Part I: Bulk solubility data. Chem. Geol. 174:225-239.

Brooker, R.A., Kohn, S.C., Holloway, J.R., McMillan, P.F., 2001b. Structural controls on the solubility of CO_2 in silicate melts: Part II: IR characteristics of carbonate groups in silicate glasses. Chem. Geol. 174:241-254.

Brown, H., 1949.Rare gases and the formation of the Earth's atmosphere. In: Kuiper GP (editor), Atmospheres of the Earth and the planets, University of Chicago Press, Chicago, pp. 258-266.

Bureau, H., Métrich, N., 2003. An experimental study of bromine behaviour in water-saturated silicic melts. Geochim. Cosmochim. Acta 67:1689-1697.

Bureau, H., Keppler, H., Métrich, N., 2000. Volcanic degassing of bromine and iodine: experimental fluid/melt partitioning data and applications to stratospheric chemistry. Earth Planet. Sci. Lett. 183:51-60.

Bureau, H., Foy, E., Raepsaet, C., Somogyi, A., Munsch, P., Simon, G., Kubsky, S. 2010. Bromine cycle in subduction zones through in situ Br monitoring in diamond anvil cells. Geochim. Cosmochim. Acta. 74:3839-3850.

Burgisser, A., Scaillet, B., and Harshvadhan, 2008. Chemical patterns of erupting silicic magmas and their influence on the amount of degassing during ascent. Jour. Geophys. Res. 113: B12204, doi:10.1029/2008JB005680.

Burnard, P., 2001. Correction for volatile fractionation in ascending magmas: Noble gas abundances in primary mantle melts. Geochim. Cosmochim. Acta 65:2605-2614.

Burnham, C.W, 1975. Water and magmas: a mixing model. Geochim. Cosmochim. Acta 39:1077-1084.

Burnham, C.W., 1979a. The importance of volatile constituents. In: H.S. Yoder

(Editor), The Evolution of Igneous Rocks, Fiftieth Anniversary Perspectives, Princeton Univ. Press, Princeton, NJ, pp. 439-482.

Burnham, C. W., 1979b. Magmas and hydrothermal fluids. In: H.L. Barnes (Editor), Geochemistry of Hydrothermal Ore Deposits 2nd edn. Wiley, New York, NY, pp. 71-136.

Burnham, C.W., 1981. The nature of multicomponent aluminosilicate melts. In: D.T. Rickard, F.E. Wickman (Editors), Chemistry and Geochemistry at High temperatures and Pressures, Pergammon Press, New York, NY, pp. 197- 229.

Burnham, C.W., Davis, N.F., 1971. The role of H_2O in silicate melts; I, P-V-T relations in the system $NaAlSi_3O_8$-H_2O to 10 kilobars and 1000 degrees C. Am. J. Sci. 270:54-79.

Burnham, C.W., Davis, N.F., 1974.The role of H_2O in silicate melts; II, Thermodynamic and phase relations in the system $NaAlSi_3O_8$-H_2O to 10 kilobars, 700 degrees to 1100 degrees C. Am. J. Sci. 274: 902-940

Burnham, C.W., Jahns, R.H., 1962. A method for determining the solubility of water in silicate melts. Am. J. Sci. 260:721-745.

Burnham, C.W., Nekvasil, H., 1986. Equilibrium properties of granitic magmas. Am. Mineral. 71:239-263.

Candela, P.A., 1997. A review of shallow, ore-related granites: textures, volatiles, and ore metals. J. Petrol. 38:1619-1633.

Carroll, M.R., Blank, J.G., 1997. The solubility of H_2O in phonolite melts. Am. Mineral. 82:549-556.

Carroll, M.R., Draper, D.S., 1994. Noble gases as trace elements in magmatic processes. Chem. Geol. 117:37-56.

Carroll, M.R., Holloway, J.R. (Editors), 1994. Volatiles in Magmas. Rev. Mineral. Geochem. 30.

Carroll, M.R., Rutherford, M.J., 1985. Sulfide and sulfate saturation in hydrous silicate melts. J. Geophys. Res. 90:601-612

Carroll, M.R., Rutherford, M.J., 1987. The stability of igneous anhydrite: Experimental results and implications for sulfur behavior in the 1982 El Chichon trachyandesite and other evolved magmas. J. Petrol. 28:781-801

Carroll, M.R., Rutherford, M.J. 1988. Sulfur speciation in hydrous experimental glasses of varying oxidation state: results from measured wavelength shifts of sulfur X-rays. Am. Mineral. 73:845-849

Carroll, M.R., Stolper E.M., 1993. Noble gas solubilities in silicate melts and glasses: New experimental results for argon and the relationship between solubility and ionic porosity. Geochim. Cosmochim. Acta 57:5039-5051

Carroll, M.R., Webster, J.D., 1994 Solubilities of sulfur, noble gases, nitrogen, chlorine, and fluorine in magmas. In: M.R. Carroll, J.R. Holloway (Editors), Volatiles in Magmas, Rev. Mineral. Geochem. 30:231-279.

Chevychelov, V.Y., 1999. Chlorine dissolution in fluid-rich granitic melts: the effect of calcium addition. Geochem. Internat. 37:456-467.

Chevychelov, V.Y., Suk, N.I., 2003. Influence of the composition of magmatic melt on the solubility of metal chlorides at pressures of 0.1-3.0 kbar. Petrol. 11:62-74.

Chevychelov, V.Y., Simakin, A.G., Bondarenko, G.V., 2003. Mechanism of chlorine dissolution in water-saturated model granodiorite melt: applications of IR spectroscopic methods. Geochim. Internat. 41:395-409.

Chevychelov, V.Y., Botcharnikov, R.E., Holtz, F., 2008a. Partitioning of Cl and F between fluid and hydrous phonolitic melt of Mt. Vesuvius at ~850-1000 °C and 200 MPa. Chem. Geol. 256:172-184.

Chevychelov, V.Y., Bocharnikov, R.E., Holtz, F. 2008b, Experimental Study of Chlorine and Fluorine Partitioning between Fluid and Subalkaline Basaltic Melt. Doklady Earth Sci. 422:1089-1092.

Chou, I-M., 1987. Phase relations in the system NaCl-KCl-H_2O. III: Solubilities of halite in vapor-saturated liquids above 445° C and redetermination of phase equilibrium properties in the system NaCl-H_2O to 1000° C and 1500 bars. Geochim. Cosmochim. Acta 51:1965-1975.

Clemens, J.D., Mawer, C.K., 1992. Granitic magma transport by fracture propagation. Tectonophysics 204:339-360.

Clemens, J.D., Vielzeuf, D., 1987. Constraints on melting and magma production in the crust . Earth Planet. Sci. Lett. 86:287-307.

Clemente, B., Scaillet, B., Pichavant, M. 2004. The solubility of sulfur in hydrous rhyolitic melts. J. Petrol. 45:2171-2196

Dauphas, N., 2003. The dual origin of the terrestrial atmosphere. Icarus 165:326-339.

Di Matteo, V., Carroll, M.R., Behrens, H., Vetere, F., Brooker, R.A., 2004. Water solubility in trachytic melts. Chem. Geol. 213:187-196.

Di Matteo, V., Mangiacapra, A., Dingwell, D.B., Orsi, G., 2006. Water solubility and speciation in shoshonitic and latitic melt composition from Campi Flegrei Caldera (Italy). Chem. Geol. 229:113-124.

Dingwell, D.B., Holtz, F., Behrens, H., 1997. The solubility of H_2O in peralkaline and peraluminous granitic melts. Am. Mineral. 82:434-437.

Dixon, J.E., 1997. Degassing of alkalic basalts. Am. Mineral. 82:368-378.

Dixon, J.E., Stolper, E.M., and Holloway, J.R., 1995. An experimental study of water and carbon dioxide solubilities in mid-ocean ridge basaltic liquids. Part I: Calibration and solubility models. J. Petrol. 36:1607-1631.

Dolejš, D., Baker, D.R., 2007. Liquidus equilibria in the system K_2O-Na_2O-Al_2O_3-SiO_2-F_2O_{-1}-H_2O to 100 MPa: II. Differentiation paths of fluorosilicic magmas in hydrous systems. J. Petrol. 48:807-828.

Drescher, J., Kirsten, T., Schäfer K., 1998. The rare gas inventory of the continental crust, recovered by the KTB continental deep drilling project. Earth Planet. Sci. Lett. 154:247-263.

Dunai, T.J., Porcelli, D., 2002. Storage and transport of noble gases in the subcontinental lithosphere. Rev. Mineral. Geochem. 47: 371-409.

Eggler, D.H., Burnham, C.W., 1984. Solution of water in diopside melts - a thermodynamic model. Contrib. Mineral. Petrol. 85:58-66.

Eggler, D.H., Rosenhauer, M., 1978. Carbon-dioxide in silicate melts. 2. Solubilities of CO2 and H20 in CaMgSi2O6 liquids and vapors at pressures to 40 Kb. Am. J. Sci. 278:64-94.

Fincham, C.J., Richardson, F.D., 1954. The behavior of sulfur in silicate and aluminate melts. Proc. R. Soc. London 223A:40-61.

Fine, G., Stolper, E., 1985. The speciation of carbon dioxide in sodium aluminosilicate glasses. Contrib. Mineral. Petrol. 91:105-121.

Fine, G., Stolper, E., 1985/86. Dissolved carbon dioxide in basaltic glasses: concentrations and speciation. Earth Planet. Sci. Lett. 76:263-278.

Flowers, G., 1979. Correction of Holloway's (1977) adaptation of the modified Redlich-Kwong equation of state for calculation of the fugacities of molecular species in supercritical fluids of geological interest. Contrib. Mineral. Petrol. 69:315-318.

Fogel, R.A., Rutherford, M.J., 1990. The solubility of carbon dioxide in rhyolitic melts: A quantitative FTIR study. Am. Mineral. 75:1311-1326.

Ghiorso, M.S., Sack, R. O., 1995. Chemical mass transfer in magmatic processes. IV. A revised and internally consistent thermodynamic model for the interpolation and extrapolation of liquid-solid equilibria in magmatic systems at elevated temperatures and pressures. Contrib. Mineral. Petrol. 119:197-212.

Ghiorso, M.S., Carmichael, I.S.E., Rivers, M.L., Sack, R.O., 1983. The Gibbs Free Energy of mixing of natural silicate liquids; an expanded regular solution approximation for the calculation of magmatic intensive variables. Contrib. Mineral. Petrol. 84:107-145.

Giordano, D., Russell, J.K., Dingwell, D.B., 2008. Viscosity of magmatic liquids: a model. Earth Planet. Sci. Lett. 271:123-134.

Goranson, R.W., 1931. The solubility of water in granitic magma. Am. J. Sci. 22:481-502.

Goranson, R.W., 1938. Silicate-water systems: phase equilibria in the $NaAlSi_3O_8$-H_2O and $KAlSi_3O_8$-H_2O systems at high temperatures and pressures. Am. J. Sci. 35A:71-91.

Hamilton, D.L., Oxtoby, S., 1986. Solubility of water in albite-melt determined by the weight-loss method. J. Geol. 94: 626-630

Hamilton, D.L., Burnham, C.W., Osborn, E.F., 1964. The solubility of water and effects of oxygen fugacity and water content on crystallization in mafic magmas. J. Petrol. 5:21-39.

Haughton, D.R., Roeder, P.L., Skinner, B.J., 1974. Solubility of sulfur in mafic magmas. Econ. Geol. 69:451-467

Hauri, E., 2002. SIMS analysis of volatiles in silicate glasses, 2: isotopes and abundances in Hawaiian melt inclusions. Chem. Geol. 193:115-141.

Hauri, E., Wang, J., Dixon, J.E., King, P.L., Mandeville, C., Newman, S., 2002. SIMS analysis of volatiles in silicate glasses 1. Calibration, matrix effects and comparisons with FTIR. Chem. Geol. 193:99-114.

Hilton, D.R., Fischer, T.P., Marty, B., 2002. Noble gases and volatile recycling at subduction zones. Rev. Mineral. Geochem. 47:319-370.

Hirschmann, M.M., Dasgupta, R., 2009. The H/C ratios of Earth's near-surface and deep reservoirs, and consequences for deep Earth cycles. Chem. Geol. 262:4-16.

Hodges, F.N., 1974. The solubility of H_2O in silicate melts. Carnegie Inst. Washington Yearbook 73:251-255.

Holloway, J.R., 1971. Composition of fluid phase solutes in basalt-H_2O-CO_2 system. Geol. Soc. Am. Bull. 82:233-238.

Holloway, J.R., 1976. Fluids in the evolution of granitic magmas: consequences of finite CO_2 solubility. Geol. Soc. Am. Bull. 87:1513-1518.

Holloway, J.R., 1977. Fugacity and activity of molecular species in supercritical fluids. In: D.G. Fraser (Editor), Thermodynamics in Geology, D. Reidel, Dortrecht, pp. 161-180.

Holloway, J. R., 1987. Igneous fluids. Rev. Mineral. Geochem. 17: 211-233.

Holloway, J.R., Blank, J.G., 1994. Application of experimental results to C-O-H species in natural melts. In: M.R. Carroll, J.R. Holloway (Editors), Volatiles in Magmas, Rev. Mineral. Geochem. 30:187-230.

Holtz, F., Dingwell, D.B., Behrens, H., 1993. Effects of F, B_2O_3 and P_2O_5 on the solubility of water in haplogranite melts compared to natural melts. Contrib. Mineral. Petrol. 113:492-501.

Holtz, F., Johannes, W., Tamic, N., Behrens, H., 2001. Maximum and minimum water contents of granitic melts generated in the crust: a reevaluation and implications. Lithos 56:1-14.

Holtz, F., Behrens, H., Dingwell, D.B., Johannes W., 1995. H_2O solubility in haplogranitic melts: Compositional, pressure, and temperature dependence. Am. Mineral. 80:94-108.

Holtz, F., Roux, J., Behrens, H., Pichavant, M., 2000. Water solubility in silica and quartzofeldspathic melts. Am. Mineral. 85:682-682.

Honma, H., Itihara, Y., 1981. Distribution of ammonium in minerals of metamorphic and granitic rocks. Geochim. Cosmochim. Acta 45:983-988.

Jakobsson, S., 1997. Solubility of water and carbon dioxide in an icelandite at 1400 ° C and 10 kilobars. Contrib. Mineral. Petrol. 127:129-135.

Jakobsson, S., Holloway, J.R., 1986. Crystal-liquid experiments in the presence of a C-O-H fluid buffered by graphite+iron+wustite: Experimental method and near-liquidus phase relations in basanite. J. Volcan. Geotherm. Res. 29:265-291.

Jambon, A., 1994. Earth degassing and large-scale geochemical cycling of volatile elements. In: M.R. Carroll and J.R. Holloway (Editors) Volatiles in Magmas. Rev. Mineral. Geochem. 30:479-517.

Jambon, A., Weber, H., Braun, O., 1986. Solubility of He, Ne, Ar, Kr and Xe in a basalt melt in the range 1250-1600 oC. Geochemical implications. Geochim. Cosmochim. Acta 50:401-408.

Johnson, M.C., Anderson, A.T., Jr., Rutherford, M.J., 1994. Pre-eruptive volatile contents of magmas. In: M.R. Carroll, J.R. Holloway, (Editors) Volatiles in Magmas. Rev. Mineral. Geochem. 30:281-330.

Jugo, P.J., Luth, R.W., Richards, J.P., 2005. An experimental study of the sulfur content in basaltic melts saturated with immiscible sulfide or sulfate liquids at 1300 degrees C and 1.0 GPa, J. Petrol. 46:783-798.

Kadik, A.A., Lebedev, YeB., 1968. Temperature dependence of the solubility of water in an albite melt at high pressures. Geochem. Int. 5:1172-1181.

Kadik, A.A., Lebedev, E.B., Khitarov, N.I., 1971. The water in magmatic melts. Nauka Publishing House, Moscow.

Katsura, T., Nagashima, S., 1974. Solubility of sulfur in some magmas at 1 atmosphere. Geochim. Cosmochim. Acta 38:517-531.

Kennedy, G.C., Wasserburg, G.J., Heard, H.C., Newton, R.C., 1962. The upper three-phase region in the system SiO_2-H_2O. Am. J. Sci. 260:501-521.

Keppler, H., 1999. Experimental evidence for the source of excess sulfur in explosive volcanic eruptions. Science 284:1652-1654.

Keppler, H., 2003. Water solubility in carbonatitic melts. Am. Mineral. 88:1822-1824.

Keppler, H., 2010. The distribution of sulfur between haplogranitic melts and aqueous fluids. Geochim. Cosmochim. Acta 74:645-660.

Khitarov, N.I., Kadik, A.A., 1973. Water and carbon dioxide in magmatic melts. Contrib. Mineral. Petrol. 41:205-215.

Khitarov, N.I., Kadik, A.A., Lebedev YeB., 1963. Estimation of the thermal effects of the separation of water from felsic melts based on data for the system albite-water. Geochem. 7:637-649.

Kilinc, I.A., Burnham, C.W., 1972. Partitioning of chloride between a silicate melt and coexisting aqueous phase from 2 to 8 kilobars. Econ. Geol. 67:231-235.

King, P.L., Holloway, J.R., 2002. CO_2 solubility and speciation in intermediate (andesitic) melts: The role of H_2O and composition. Geochim. Cosmochim. Acta 66:1627-1640.

Kiprianov, A.A., Karpukhina, N.G., 2006. Oxyhalide silicate glasses. Glass Phys. Chem. 32:1-27.

Kirschen, M., Pichavant, M., 2001. A thermodynamic model for hydrous silicate melts in the system $NaAlSi_3O_8$ -$KAlSi_3O_8$ -Si_4O_8 -H_2O. Chem. Geol. 174:103-114.

Kohn, S.C, Dupree, R. Mortuza, M.G., Henderson, C.M.B., 1991. NMR evidence for five- and six-coordinated aluminum fluoride complexes in F-bearing aluminosilicate glasses. Am. Mineral. 76:309-312.

Kravchuk, I. F., Keppler, H., 1994. Distribution of chloride between aqueous fluids and felsic melts at 2 kbar and 800 ° C. Eur. J. Mineral. 6:913-923.

Kurkjian, C.R., Russell, L.E., 1958. Solubility of water in molten alkali silicates. J. Soc. Glass. Techn. 42:130T-144T.

Lange, R.A., Carmichael, I.S.E., 1987. Densities of Na_2O-K_2O-CaO-MgO-FeO-Fe_2O_3-Al_2O_3-TiO_2-SiO_2 liquids: New measurements and derived partial molar properties. Geochim. Cosmochim. Acta 51:2931-2946.

Lesne, P., Scaillet, B., Pichavant, M., Iacono-Marziano, G., Beny, J.-M., 2011a. The H_2O solubility of alkali basaltic melts: an experimental study. Contrib. Mineral. Petrol. 162:133-151.

Lesne, P., Scaillet, B., Pichavant, M., Beny, J.-M., 2011b. The CO_2 solubility in alkali basaltic melts: an experimental study. Contrib. Mineral. Petrol. 162:153-168.

Lesne, P., Kohn, S.C., Blundy, J., Witham, F., Botcharnikov, R.E., Behrens, H., 2011c. Experimental Simulation of Closed-System Degassing in the System Basalt-H_2O-CO_2-S-Cl. J. Petrol. 52:1737-1762.

Libourel, G., Marty, B., Humbert, F., 2003. Nitrogen solubility in basaltic melt. Part I. Effect of oxygen fugacity. Geochim. Cosmochim. Acta 67:4123-4135.

Liu, Q., Lange, R.A., 2006. The partial molar volume of Fe_2O_3 in alkali silicate melts: Evidence for an average Fe^{3+} coordination number near five. Am. Mineral. 91:385-393.

Liu, Y., Nekvasil, H., 2001. Ab initio study of possible fluorine-bearing four- and five-fold coordinated Al species in aluminosilicate glasses. Am. Mineral. 86, 491-497.

Liu, Y., Zhang, Y., Behrens, H., 2005. Solubility of H_2O in rhyolitic melts at low pressures and a new empirical model for mixed H_2O-CO_2 solubility in rhyolitic melts. J. Volcan. Geotherm. Res. 143:219-235.

Lorenz, C.D., Ziff, R.M., 2001. Precise determination of the critical percolation threshold for the three-dimensional "Swiss cheese" model using a growth algorithm. J. Chem. Phys. 114:3659-3661.

Luhr, J.F., 1990. Experimental phase relations of water- and sulfur-saturated arc magmas and the 1982 eruptions of El Chichón volcano. J. Petrol. 31:1071-1114.

Luth,W.C., 1969. The systems $NaAlSi_3O_8$-SiO_2 and $KalSi_3O_8$-SiO_2 to 20 kb and the relationship between H_2O concentration, P_{H2O}, and P_{total} in granitic magmas. Am. J. Sci. 267A:325-341.

Lyubetskaya, T., Korenaga, J., 2007. Chemical composition of Earth's primitive mantle and its variance: 1. Methods and results. J. Geophys. Res. 112:doi:10.1029/2005JB004223.

Malinin, S.D., Kravchuk, I.F., 1994. Estimation of the activity coefficient of NaCl in aqueous fluid. Geokimiya, 1:75-88 (in Russian).

Malinin, S.D., Kravchuk, I.F., Delbove, F., 1989. Chloride distribution between phases in hydrated and dry chloride-aluminosilicate melt systems as a function of phase composition. Geochem. Intern. 26:32-38.

Marquis, G., Hyndman, R.D., 1992. Geophysical support for aqueous fluids in the deep crust: seismic and electrical relationships. Geophys. Jour. Intern. 110:91-105.

Mattey, D.P., 1991. Carbon dioxide solubility and carbon isotope fractionation in basaltic melt. Geochim. Cosmochim. Acta 55:3467-3473.

Métrich, N., Rutherford, M.J., 1992. Experimental study of chlorine behavior in hydrous silicic melts. Geochim. Cosmochim. Acta 56:607-616.

Moore, G., Vennemann, T., Carmichael, I.S.E., 1995. Solubility of water in magmas to 2 kbar. Geology 23:1099-1102.

Moore, G., Vennemann, T., Carmichael, I.S.E., 1998. An empirical model for the

solubility of H_2O in magmas to 3 kilobars, Am. Mineral. 83:36-42.

Moretti, R., Baker, D.R., 2008. Modeling the interplay of fO_2 of fS_2 along the $FeS_{MSS\ or\ liq}$-silicate melt equilibrium. Chem. Geol. 256:286-298.

Moretti, R., Papale, P., 2004. On the oxidation state and volatile behavior in multicomponent gas-melt equilibria. Chem. Geol. 213:265-280.

Morizet, Y., Brooker, R.A., Kohn, S.C., 2002. CO_2 in haplo-phonolite melt: solubility, speciations and carbonate complexation, Geoch. Cosmochim. Acta 66: 1809-1820.

Morizet, Y., Paris, M., Gaillard, F., Scaillet, B., 2010. C-O-H fluid solubility in haplobasalt under reducing conditions: An experimental study. Chem. Geol. 279:1-16.

Moune, S., Holtz, F., Botcharnikov, R., 2009. Sulphur solubility in andesitic to basaltic melts: implications for Hekla volcano. Contrib. Mineral. Petrol. 157:691-707.

Mysen, B.O., 1977. The solubility of H_2O and CO_2 under predicted magma genesis conditions and some petrological and geophysical implications, Rev. Geophys. Space Phys. 15:351-361.

Mysen, B.O., Fogel, M.L., 2010. Nitrogen and hydrogen isotope compositions and solubility in silicate melts in equilibrium with reduced (N+H)-bearing fluids at high pressure and temperature: Effects of melt structure. Am. Mineral. 95:987-999.

Mysen, B.O., Cody, G.D., Smith, A., 2004. Solubility mechanisms of fluorine in peralkaline and meta-aluminous silicate glasses and in melts to magmatic temperatures. Geochim. Cosmochim. Acta 68:2745-2769.

Mysen, B.O., Yamashita, S., Chertkova, N., 2008. Solubility and solution mechanisms of NOH volatiles in silicate melts at high pressure and temperature-amine groups and hydrogen fugacity. Am. Mineral. 93:1760-1770.

Naldrett, A.J., 1989. Magmatic sulfide deposits. Clarendon Press, Oxford University Press, Oxford. 186 pp.

Naney, M.T., 1983. Phase-equilibria of rock-forming ferromagnesian silicates in granitic systems. Am. J. Sci. 283:993-1033.

Nauret, F., Moreira, M., Snow, J.E., 2010. Rare gases in lavas from the ultraslow spreading Lena Trough, Arctic Ocean, Geochem. Geophys. Geosyst. 11:Q0AC04, doi:10.1029/2010GC003027.

Newman, S., Lowenstern, J.B., 2002. VolatileCalc: a silicate melt-H_2O-CO_2 solution model written in Visual Basic for excel. Comput. Geosci. 28:597-604.

Newton, R.C., Manning, C.E., 2008. Thermodynamics of SiO_2-H_2O fluid near the upper

critical end point from quartz solubility measurements at 10 kbar. Earth Planet. Sci. Lett., 274:241-249.

Nicholls, J., 1980. A simple thermodynamic model for estimating the solubility of H_2O in magmas. Contrib. Mineral. Petrol. 74:211-220.

Nowak, M., Schreen, D., Spickenbom, K., 2004. Argon and CO_2 on the race track in silicate melts: A tool for the development of a CO_2 speciation and diffusion model. Geochim. Cosmochim. Acta 68:5127-5138.

Ochs, F.A. III, Lange, R.A., 1997. The partial molar volume, thermal expansivity, and compressibility of H_2O in $NaAlSi_3O_8$ liquid: new measurements and an internally consistent model. Contrib. Mineral. Petrol. 129:155-165.

Ochs, F.A. III, Lange, R.A., 1999. The density of hydrous magmatic liquids. Science 283:1314-1317.

Olafsson, M., Eggler, D.H., 1983. Phase relations of amphibole, amphibole-carbonate, and phlogopite-carbonate peridotite: petrologic constraints on the asthenosphere. Earth. Planet. Sci. Lett. 64:305-315.

O'Neill, H. St C., Palme, H., 1998. Composition of silicate Earth: implications for accretion and core formation. In I. Jackson (Editor) The Earth's Mantle, Composition, Structure and Evolution. Cambridge University Press, Cambridge, pp. 3-126.

Paillat, O., Elphick ,S., Brown, W.L., 1992. The solubility of water in $NaAlSi_3O_8$ melts: a re-examination of Ab-H_2O phase relationships and critical behaviour at high pressures. Contrib. Mineral. Petrol. 112:490-500.

Pan, V., Holloway, J.R., Hervig, R.L., 1991. The pressure and temperature dependence of carbon dioxide solubility in tholeiitic basalt melts. Geochim. Cosmochim. Acta 55:1587-1595.

Paonita, A., 2005. Noble gas solubility in silicate melts: a review of experimentation and theory, and implications regarding magma degassing processes. Annals Geophys. 48:647-669.

Papale, P., 1997. Thermodynamic modeling of the solubility of H_2O and CO_2 in silicate liquids. Contrib. Mineral. Petrol. 126:237-251.

Papale, P., 1999. Modeling of the solubility of a two-component H_2O+CO_2 fluid in silicate liquids. Am. Mineral. 84:477-492.

Papale, P., Moretti, R., Barbato, R., 2006. The compositional dependence of the saturation surface of H_2O + CO_2 fluids in silicate melts. Chem. Geol. 229:78-95.

Pawley, A.R., Holloway, J.R., McMillan, P.F., 1992. The effect of oxygen fugacity on the solubility of carbon-oxygen fluids in basaltic melt. Earth Planet. Sci. Lett. 110:213-225.

Petford, N., Kerr, R.C., Lister, J.R., 1993. Dike transport of granitoid magmas. Geology 21:845-848.

Pichavant, M., Holtz, F., McMillan, P.F., 1992. Phase relations and compositional dependence of H_2O solubility in quartz-feldspar melts. Chem. Geol. 96:303-319.

Pineau, F., Shilobreeva, S., Kadik, A., Javoy, M., 1998. Water solubility and D/H fractionation in the system basaltic andesite-H_2O at 1250 ° C and between 0.5 and 3 kbars. Chem. Geol. 147:173-184.

Patiño Douce, A.E, Johnston, A.D., 1991 Phase equilibria and melt productivity in the pelitic system: implications for the origin of peraluminous granitoids and aluminous granulites. Contrib. Mineral. Petrol. 107:202-218.

Porcelli, D.P., Ballentine, C.J., Wieler, R. (Editors), 2002. Noble Gases. Rev. Mineral. Geochem. 47.

Rapp, R.P., Watson, E.B., 1995. Dehydration melting of metabasalt at 8-32 kbar: implications for continental growth and crust-mantle recycling. J. Petrol. 36:891-931.

Romano, C., Dingwell, D.B., Behrens, H., Dolfi, D., 1996. Compositional dependence of H_2O solubility along the joins $NaAlSi_3O_8$-$KAlSi_3O_8$ and $NaAlSi_3O_8$-$LiAlSi_3O_8$ and $KAlSi_3O_8$-$LiAlSi_3O_8$. Am. Mineral. 81:452-461.

Rubey, W.W., 1951. Geologic history of seawater. Geol. Soc. Am. Bull. 62:1111-1148.

Rudnick, R.L., Fountain, D.M., 1995. Nature and composition of the continental crust: a lower crustal perspective. Rev. Geophys. 33:267-309.

Rudnick, R.L, and Gao, S., 2003. Composition of the Continental Crust. In: R.L. Rudnick (Editor), H.D. Holland, K.K. Turekian (Executive Editors), Treatise on Geochemistry, Volume 3, Elsevier, North Holland, pp.1-64.

Russell, S.S., Lee, M.R., Arden, J.W., Pillinger, C.T., 1995. The isotopic composition and origins of silicon-nitride from ordinary and enstatite chondrites. Meteoritics 30:399-404.

Saal, A.E., Hauri, E.H., Cascio, M.L., Van Orman, J.A., Rutherford, M.C., Cooper, R.F., 2008. Volatile content of lunar volcanic glasses and the presence of water in the Moon’s interior. Nature 454:192-195.

Salters, V.J.M., Stracke, A., 2004. Composition of the depleted upper mantle. Geochem. Geophys. Geosys. 5:doi:10.1029/2003GC000597.

Sandland, T.O., Du, L.-S, Stebbins, J.F., Webster, J.D., 2004. Structure of Cl-containing silicate and aluminosilicate glasses: A ^{35}Cl MAS-NMR study. Geochim. Cosmochim. Acta 68:5059-5069.

Sarda, P., Graham, D., 1990. Mid-ocean ridge popping rocks: implications for degassing at ridge crests. Earth Planet. Sci. Lett. 97:268-289.

Scaillet, B., Pichavant, M., 2005. A model of sulphur solubility for hydrous mafic

melts: application to the determination of magmatic fluid compositions of Italian volcanoes. Ann. Geophys. 48:671-698.

Scaillet, B., Macdonald, R., 2006. Experimental constraints on pre-eruption conditions of pantelleritic magmas: Evidence from the Eburru complex, Kenya Rift. Lithos 91:95-108.

Scaillet, B., Clemente, B., Evans, B.W., Pichavant, M., 1998. Redox control of sulfur degassing in silicic magmas. J. Geophys. Res. 103B:23937-23949.

Schaller, T., Dingwell, D.B., Keppler, H., Knöller, W., Merwin, L., Sebald, A., 1992. Fluorine in silicate glasses: a multinuclear nuclear magnetic resonance study. Geochim. Cosmochim. Acta 56:701-707.

Schmidt, B.C., Behrens, H., 2008. Water solubility in phonolite melts: Influence of melt composition and temperature. Chem. Geol. 256:259-268.

Schmidt, B.C., Holtz, F., Pichavant, M., 1999. Water solubility in haplogranitic melts coexisting with H_2O-H_2 fluids. Contrib. Mineral. Petrol.136:213-224.

Schneider, M.E., Eggler, D.H., 1986. Fluids in equilibrium with peridotite minerals: implications for mantle metasomatism. Geochim. Cosmochim. Acta 50:711-724.

Shaw, H.R., 1964. Theoretical solubility of H_2O in silicate melts: Quasi-crystalline models. Jour. Geol. 72:601-617.

Shaw, H.R., 1974. Diffusion of H_2O in granitic liquids: Part I. Experimental data; Part II. Mass transfer in magma chambers. In: W. Hofmann, B.J. Giletti, H.S. Yoder Jr., R.A. Yund (Editors), Geochemical Transport and Kinetics, Carnegie Institution of Washington, Washington, DC, pp. 139-170.

Shen, A., Keppler, H., 1995. Infrared spectroscopy of hydrous silicate melts to 1000 ° C and 10 kbar: Direct observation of H_2O speciation in a diamond-anvil cell. Am. Mineral. 80:1335-1338.

Shinohara, H., 2009. A missing link between volcanic degassing and experimental studies on chloride partitioning. Chem. Geol. 263:51-59.

Shinohara H., Iiyama J.T., Matsuo S., 1989. Partition of chlorine compounds between silicate melt and hydrothermal solutions. Geochim. Cosmochim. Acta 53:2617-2630.

Shishkina, T.A., Botcharnikov, R.E., Holtz, F., Almeev, R.R., Portnyagin, M.V., 2010. Solubility of H_2O- and CO_2-bearing fluids in tholeiitic basalts at pressures up to 500 MPa. Chem. Geol. 277:115-125.

Signorelli, S., Carroll, M.R., 2000. Solubility and fluid-melt partitioning of Cl in hydrous phonolitic melts. Geochim. Cosmochim. Acta 64:2851-2862.

Signorelli, S., Carroll, M.R., 2002. Experimental study of Cl solubility in hydrous

alkaline melts: constraints on the theoretical maximum amount of Cl in trachytic and phonolitic melts. Contrib. Mineral. Petrol. 143:209-218.

Silver, L.A., Stolper, E., 1985. A thermodynamic model for hydrous silicate melts. Jour. Geol. 93:161-178.

Silver, L.A., Stolper, E., 1989. Water in albitic glasses. J. Petrol. 30:667-709.

Silver, L.A., Ihinger, P.D., Stolper, E., 1990. The influence of bulk composition on the speciation of water in silicate glasses. Contrib. Mineral. Petrol. 104:142-162.

Simon, A.C., Ripley, E.M., 2011. The role of magmatic sulfur in the formation of ore deposits. . In: H. Behrens, J.D. Webster (Editors), Sulfur in Magmas and Melts: Its Importance for Natural and Technical Processes, Rev. Mineral. Geochem. 73:513-578.

Skjerlie, K.P., Patiño Douce, A.E., Johnston A.D., 1993. Fluid absent melting of a layered crustal protolith: implications for the generation of anatectic granites. Contrib. Mineral. Petrol. 114:365-378.

Smith, J.V., 1981. Halogen and phosphorus storage in the Earth. Nature 289:762-765.

Smith, J.V., Delaney, J.S., Hervig, R.L., Dawson, J.B., 1981. Storage of F and Cl in the upper mantle: geochemical implications. Lithos 14:133-147.

Spera, F.J., 1974. A thermodynamic basis for predicting water solubilities in silicate melts and implications for the low velocity zone. Contrib. Mineral. Petrol. 45:175-186.

Spera, F.J., Bergman, S.C., 1980. Carbon dioxide in igneous petrogenesis, I. Aspects of the dissolution of CO_2 in silicate liquids, Contrib. Mineral. Petrol. 74:55-66.

Stelling, J., Botcharnikov, R.E., Beermann, O., Nowak, M., 2008. Solubility of H_2O- and chlorine-bearing fluids in basaltic melt of Mount Etna at T = 1050-1250 ° C and P = 200 MPa. Chem. Geol. 256:102-110.

Stolper, E., 1982. The speciation of water in silicate melts. Geochim. Cosmochim. Acta 46:2609-2620.

Stolper, E. M., Holloway, J. R., 1988. Experimental determination of the solubility of carbon dioxide in molten basalt at low pressure. Earth Planet. Sci. Lett. 87:397-408.

Symonds R. B., Rose W. I., Bluth G. S., Gerlach, T. M., 1994. Volcanic gas studies, methods, results and applications. In: M.R. Carroll, J.R. Holloway (Editors), Volatiles in Magmas. Rev. Mineral. Geochem. 30:1-66.

Tamic, N., Behrens, H., Holtz, F., 2001. The solubility of H_2O and CO_2 in rhyoltic melts in equilibrium with a mixed CO_2-H_2O fluid phase. Chem. Geol. 174:333-

347.

Taylor, S. R., McLennan, S. M., 1985. The Continental Crust: Its Composition and Evolution. Blackwell, Oxford University Press, Oxford, 312 pp.

Taylor, S. R., McLennan, S.M., 1995. The geochemical evolution of the continental crust. Rev. Geophys. 33:241-265.

Tingle, T.N., 1987. An evaluation of the carbon-14 beta track technique: implications for solubilities and partition coefficients determined by beta track mapping. Geochim. Cosmochim. Acta 51:2479-2487.

Tomlinson, J.W., 1956. A note on the solubility of water in a molten sodium silicate. J. Soc. Glass. Tech. 40:25-31.

Tuttle, O.F., Bowen, N.L., 1958. Origin of granite in the light of experimental studies in the system $NaAlSi_3O_8$-$KAlSi_3O_8$-SiO_2-H_2O. Geol. Soc. Amer. Memoir 74.

Vetere, F., Botcharnikov, R.E., Holtz, F., Behrens, H., De Rosa, R., 2011. Solubility of H_2O and CO_2 in shoshonitic melts at 1250 ° C and pressures from 50 to 400 MPa: Implications for Campi Flegrei magmatic systems. J. Volcan. Geotherm. Res. 202:251-261.

Vielzeuf, D., Holloway, J.R., 1988. Experimental determinations of the fluid-absent melting relations in the pelitic system. Consequences for crustal differentiation. Con. Mineral. Petrol. 98:257-276.

Villemant, B., Boudon, G., 1998. Transition from dome-forming to plinian eruptive styles controlled by H_2O and Cl degassing. Nature 392:65-69.

Villemant, B., Boudon, G., 1999. H_2O and halogen (F, Cl, Br) behavior during shallow magma degassing processes. Earth Planet. Sci. Lett. 168:271-286.

Villemant, B., Boudon, G., Nougrigat, S., Poteaux, S., Michel, A., 2003. Water and halogens in volcanic clasts: tracers of degassing processes during plinian and dome-building eruptions. In: C. Oppenheimer, D.M. Pyle, J. Barclay (Editors), Volcanic Degassing. Geol. Soc. Lond. Spec. Pub., 213, pp. 63-79.

Wallace, P.J., 2005. Volatiles in subduction zone magmas: concentrations and fluxes based on melt inclusion and volcanic gas data. Jour. Volcan. Geotherm. Res. 140:217-240.

Wasserburg, G.J., 1957. The effects of H_2O in silicate systems. Jour. Geol. 65:15-23.

Wasserman, E., Wood, B., Brodhold, J., 1995. The static dielectric constant of water at pressures up to 20 kbar and temperatures to 1273 K: Experiment, simulations, and empirical equations. Geochim. Cosmochim. Acta 59:1-6.

Webster, J.D., 1990. Partitioning of F between H_2O and CO_2 fluids and a topaz rhyolite melt. Implications for mineralizing magmatic-hydrothermal fluids in

F-rich granitic systems. Con. Min. Petrol. 104:424-438.

Webster, J. D., 1992a. Fluid-melt interactions involving Cl-rich granites: experimental study from 2 to 8 kbar. Geochim. Cosmochim. Acta 56:659-678.

Webster, J.D., 1992b. Water solubility and chlorine partitioning in Cl-rich granitic systems: effects of melt composition at 2 kbar and 800 ° C. Geochim. Cosmochim. Acta 56:679-687.

Webster, J.D., Botcharnikov,R.E., 2011, Distribution of sulfur between melt and fluid in S-O-H-C-Cl-bearing magmatic systems at shallow crustal pressures and temperatures. In: H. Behrens, J.D. Webster (Editors), Sulfur in Magmas and Melts: Its Importance for Natural and Technical Processes, Rev. Mineral. Geochem. 73:247-283.

Webster, J.D., De Vivo B., 2002. Experimental and modeled solubilities of chlorine in aluminosilicate melts, consequences of magma evolution, and implications for exsolution of hydrous chloride melt at Mt. Somma-Vesuvius. Am. Mineral. 87:1046-1061.

Webster, J.D., Holloway, J.R., 1988. Experimental constraints on the partitioning of Cl between topaz rhyolite melt and H_2O and H_2O + CO_2 fluids: New implications for granitic differentiation and ore deposition. Geochim. Cosmochim. Acta 52:2091-2105.

Webster, J.D., Holloway, J.R., 1990. Partitioning of F and Cl between magmatic hydrothermal fluids and highly evolved granitic magmas. Geol. Soc. Am. Spec. Pap. 246: 21-34.

Webster, J.D., Mandeville, C.W., 2007. Fluid immiscibility in volcanic environments. In: A. Liebscher and C.A. Heinrich (Editors), Fluid-fluid Interactions, Rev. Mineral. Geochem. 65:313-362.

Webster, J.D., Rebbert, C.R., 1998. Experimental investigation of H_2O and Cl^- solubilities in F-enriched silicate liquids; implications for volatile saturation of topaz rhyolite magmas. Contrib. Mineral. Petrol. 132:198-207.

Webster, J.D., Kinzler, R.J., Mathez, E.A., 1999. Chloride and water solubility in basalt and andesite melts and implications for magmatic degassing. Geochim. Cosmochim. Acta 63:729-738.

Webster, J.D., Goldoff, B., Shimizu, N., 2011. C-O-H-S fluids and grantitic magma: how S partitions and modifies CO_2 concentrations of fluid-saturated felsic melt at 200 MPa. Contrib. Mineral. Petrol. In press: doi 10.1007/s00410-011-0628-1.

Webster J. D., Sintoni M. F., De Vivo, B., 2009a. The partitioning behavior of Cl, S, and H_2O in aqueous vapor-±saline-liquid saturated phonolitic and trachytic melts at 200 MPa. Chem. Geol. 263, 19-36.

Webster, J.D., Tappen, C.M., Mandeville, C.W., 2009b. Partitioning behavior of chlorine and fluorine in the system apatite-melt-fluid. II: Felsic silicate systems at 200 MPa. Geochim. Cosmochim. Acta 73:559-581.

Wedepohl, H., 1995. The composition of the continental crust. Geochim. Cosmochim. Acta 59:1217-1239.

Wilke. M., Klimm, K., Kohn, S., 2011. Spectroscopic studies on sulfur speciation in synthetic and natural glasses. In: H. Behrens, J.D. Webster (Editors), Sulfur in Magmas and Melts: Its Importance for Natural and Technical Processes, Rev. Mineral. Geochem. 73:41-78.

Williams-Jones, A.E., Heinrich, C.A., 2005. Vapor transport of metals and the formation of magmatic-hydrothermal ore deposits. Econ. Geol. 100:1287-1312.

Witham, F., Blundy, J., Kohn, S.C., Lesne, P., Dixon, J., Churakov, S.V., Botcharnikov, R., 2011. SolEx: A model for mixed COHSCl-volatile solubilities and exsolved gas compositions in basalt. Computers & Geosciences, doi:10.1016/j.cageo.2011.09.021 .

Wolf, M.B., Wyllie, P.J., 1991. Dehydration-melting of solid amphibolite at 10 kbar: Textural development, liquid interconnectivity and applications to the segregation of magmas. Mineral. Petrol. 44:151-179.

Yamashita, S., 1999. Experimental study of the effect of temperature on water solubility in natural rhyolite melt to 100 MPa. J. Petrol. 40:1497-1507.

Yardley, B.W.D., 1986. Is there water in the deep continental crust? Nature 323:111.

Zeng, Q., Stebbins, J.F., 2000. Fluorite sites in aluminosilicate glasses: high-resolution ^{19}F NMR results. Am. Mineral. 85:863-867.

Zhang, Y., (1999) H_2O in rhyolitic glasses and melts: measurement, speciation, solubility, and diffusion. Rev. Geophys. 37:493-516.

Zhang, Y., Zindler, A., 1993. Distribution and evolution of carbon and nitrogen in Earth. Earth. Planet. Sci. Lett. 117:331-345.

Table 1: Melt composition used in modeling the evolution of fluids during melting in the deep crust and ascent

S

Oxide	Wt. %
SiO_2	72.03
TiO_2	0.10
Al_2O_3	15.81
Fe_2O_3	0.19
FeO	1.93
MnO	0.19
MgO	1.16
CaO	1.93
Na_2O	3.86
K_2O	2.80
Total	100

Figure Captions

Figure 1: Solubility of water in melts of albitic composition and potassium feldspar composition at pressures from 50 to 800 MPa. Note the measurable differences in the solubility behavior for the two compositions, particularly at 500 MPa. Measurement uncertainties are approximately the size of the symbols. For further discussion please refer to the text. Data are from Behrens et al. (2001).

Figure 2: Comparison of the solubility of water in an albitic melt and in a melt of pure SiO_2. The lower water solubility in silica melt is hypothesized to be due to the lack of exchangeable cations (e.g., Na^+) in the theory of Burnham. Measurement uncertainties are approximately the size of the symbols. Please see text for a further discussion. Data are from Holtz et al. (2000).

Figure 3: Water solubility in haplogranitic melts as a function of pressure and temperature. The solubility is retrograde (lower solubility at high temperatures than at low) at low pressures, but changes to prograde by 500 MPa. Measurement uncertainties are approximately twice the size of the symbols. The data are from Holtz et al. (1995).

Figure 4: Water solubility in natural silicic composition melts. The term total in this and subsequent figures indicates the total concentration of a volatile and represents the sum of all species of that volatile dissolved in the melt. Both measured solubilities (data points) and the solubility modeled for the rhyolitic melt of Tamic et al. (2001) at 1000 °C using VOLATILECALC (Newman and Lowenstern, 2002) and the model of Papale et al. (2006) are plotted. Uncertainties in the measurements are similar to the size of the symbols. Data sources for Figures 4-8 are discussed in the text.

Figure 5: Water solubility in natural intermediate composition melts. Both measured solubilities (data points) and the solubility modeled for the andesitic melt of Hamilton et al. (1964) at 1100 °C using the model of Papale et al. (2006) are plotted. Uncertainties in the measurements are similar to the size of the symbols.

Figure 6: Water solubility in natural mafic composition melts. Measured solubilities (data points) and the the solubility modeled for the basaltic melt of Hamilton et al. (1964) at 1200 °C using the model of Papale et al. (2006) and the

water solubility for a basaltic melt with 49 wt.% SiO_2 calculated with VOLATILECALC (Newman and Lowenstern, 2002) are plotted. Uncertainties in the measurements are similar to the size of the symbols.

Figure 7: Carbon dioxide solubility in natural melt compositions. Measurement uncertainties are shown for the data of Pan et al. (1991). Carbon dioxide solubilities calculated by VOLATILECALC and by the Papale et al. model for a mid-ocean ridge basalt (MORB) at 1200 ° C are also plotted.

Figure 8: Compositions of H_2O and CO_2 in melts coexisting with a mixed volatile fluid at 200 and 500 MPa (Tamic et al., 2001), a basaltic melt at 200 and 500 MPa (Shishkina et al., 2010), and a shoshonitic melt at 200 and 400 MPa (Vetere et al., 2011). a) Volatile solubilities in rhyolitic melts (Tamic et al., 2001) coexisiting with a CO_2-H_2O fluid. b) Volatile solubilities in basaltic and shoshonitic melts (Tamic et al., 2001) coexisiting with a CO_2-H_2O fluid. The uncertainties in the measurements are similar to the size of the symbols. Open symbols are used for measurements at 200 MPa and filled symbols are used for 400-500 MPa measurements; the black, solid lines in both figures are fit to the data of Tamic et al. (2001) at 200 and 500 MPa. The red, dashed lines in both figures define the molar composition of the CO_2-H_2O fluid phase (if any) coexisting with the fluid-saturated melts (Tamic et al., 2001). The concentrations of H_2O and CO_2 in fluid-saturated rhyolitic and basaltic melts at 500 MPa calculated by VOLATILECALC are shown by the blue dash-dot line and black dotted line, respectively. Similar concentrations in a rhyolitic melt at 500 MPa calculated by the model of Papale et al. (2006) are shown by the blue dashed line. The black dash-dot and black dash-dot-dot lines are the concentrations of H_2O and CO_2 calculated by the Papale et al. (2006) model for the basaltic melt studied by Dixon et al. (2005) and the one investigated by Shishkina et al. (2010), respectively. Each of the measured or calculated solubility lines (either black or blue) defines a curve that is convex up; at concentrations of CO_2 and H_2O below the curves the melts are fluid-undersaturated and therefore a separate fluid phase does not exist. Please see the text for more discussion.

Figure 9: a) Compositions of H_2O and Cl in natural melts of various compositions coexisting with a fluid composed of H_2O and Cl at 200 MPa and different temperatures. Data are from Webster et al. (1999). b) Schematic behavior of Cl partitioning between silicate melt, aqueous fluid and a chloride brine at high temperatures and pressures. The Cl concentrations for sub-critical conditions are shown with the solid lines and the phase fields for the aqueous and brine phases coexisting with the silicate melt are divided by the horizontal dotted lines. The

Cl concentrations for supercritical conditions are shown with the dashed line. Please see text for further discussion.

Figure 10: Partitioning of chlorine between an aqueous fluid and basic to intermediate silicate melts with 5 000 ppm or less Cl and silicic melts with less than 500 ppm Cl as a function of pressure at experimental temperatures from ~800 to 1250 ° C. Uncertainties based upon fits to the concentrations of Cl in melts and fluids are displayed for some of the measurements. Where no uncertainties are plotted they are typically twice the size of the symbols. Many of the partition coefficients measured at 200 MPa have been displaced by up to ±15 MPa on the diagram in order to more clearly display the results. Please see the text for further discussion.

Figure 11: Concentrations of water and carbon dioxide in fluids coexisting with a rhyolitic melt at 800 MPa, 800 ° C calculated using the model of Papale et al. (2006). For CO_2 concentrations of 0.5 wt.% in the system composed of fluid+silicate melt no fluid phase exists, except when the water concentration is above approximately 9.5 wt%. Please see the text for further discussion of this model.

Figure 12: Water concentration in a silicic melt during ascent calculated with the model of Papale et al. (2006). The temperature in the model is held constant at 800 ° C and the system is closed to mass loss. Different combinations of water and carbon dioxide concentrations in the system were chosen based upon the results displayed in Figure 11. The carbon dioxide concentrations in the melts fall from approximately 5 000 ppm to 15 ppm with decreasing pressure. The conversion of pressure to depth was made assuming a mean crustal density of 2 700 kg m^{-3} in this and subsequent figures.

Figure 13: Compositions of H_2O-CO_2 fluids coexisting with a silicic melt during isothermal ascent of a rhyolitic melt calculated with the model of Papale et al. (2006). Please see the text for further discussion.

Figure 14: Chlorine concentration in the rhyoltic melt during ascent based upon the measurements of Shinohara et al. (1989). The fluid phase scavenges almost all of the chlorine from the melt and probably ore metals bound to chlorine. The effects of pressure on the partition coefficient seen in Figure 10 do not have a significant effect of the behavior of chlorine because at all conditions the modeled partition coefficient remains above 100.

Figure 15: Mass of the fluid phase exsolved from a silicic melt during ascent. The mass of the fluid phase increases significantly for magmas with low concentrations of volatiles during ascent, but the increase is less spectacular for magmas rich in volatiles because many volatiles exsolve at higher pressure. Nevertheless, magmas with larger concentrations of volatiles exsolve larger masses of fluids as required by the conservation of mass.

Figure 16: Magma volume as a function of pressure at 800 ° C. At high pressures, the fluid phase is minor and the volume of all the modeled rhyoltic volumes are similar. However, as pressure decreases and fluid exsolves from the melts, the volume becomes significant, particularly at pressures below approximately 200 MPa. This large volume increase may be responsible for the cracking of country rocks, loss of the volatile phase from the melt, and the formation of ore deposits (e.g., Burnham, 1979b).

Figure 17: Vesicularity of the modeled magmas as a function of pressure. Magmas with greater volatile concentrations exsolve more volatiles and achieve higher vesicularities than magmas with smaller volatile concentrations. The pressure range over which significant changes in the vesicularity occur is much larger for volatile-rich magmatic systems compared to systems with low-to-moderate volatile concentrations. The percolation threshold for spheres is at ~30 volume percent so that magmas with higher volatile concentrations reach this threshold and create an interconnected vesicle network at greater depth than magmas with low volatile concentrations.

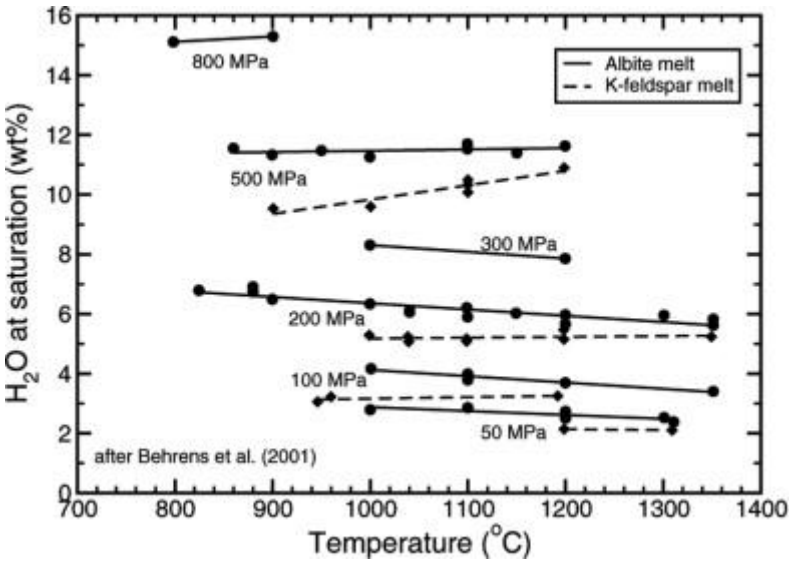

Fig. 1. Solubility of water in melts of albitic composition and potassium feldspar composition at pressures from 50 to 800 MPa. Note the measurable differences in the solubility behavior for the two compositions, particularly at 500 MPa. Measurement uncertainties are approximately the size of the symbols. For further discussion please refer to the text. Data are from Behrens et al. (2001).

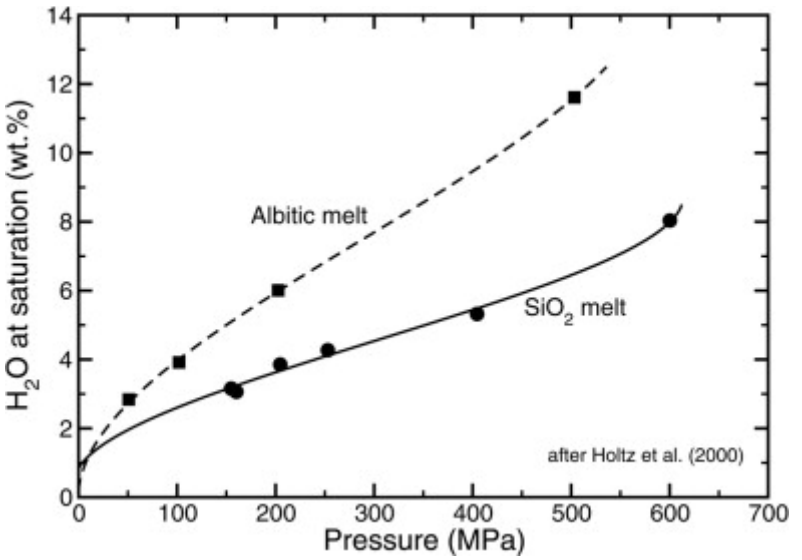

Fig. 2. Comparison of the solubility of water in an albitic melt and in a melt of pure SiO_2. The lower water solubility in silica melt is hypothesized to be due to the lack of exchangeable cations (e.g., Na^+) in the theory of Burnham. Measurement uncertainties are approximately the size of the symbols. Please see text for a further discussion. Data are from Holtz et al. (2000).

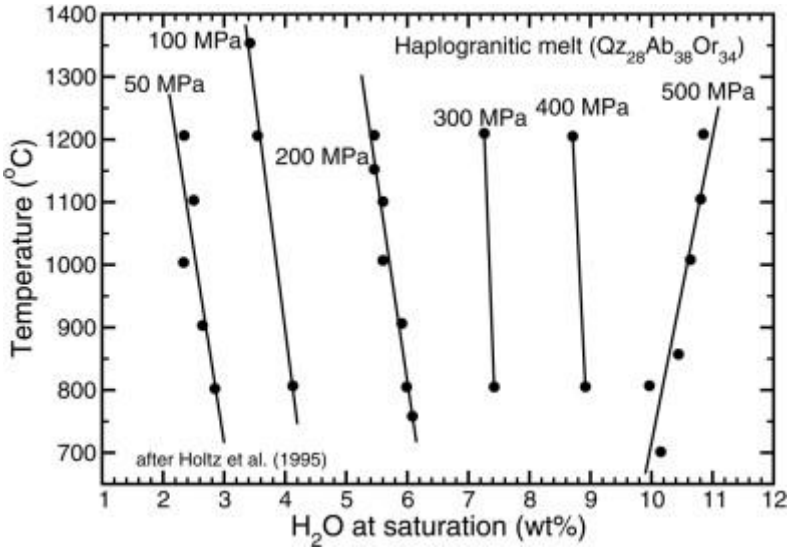

Fig. 3. Water solubility in haplogranitic melts as a function of pressure and temperature. The solubility is retrograde (lower solubility at high temperatures than at low) at low pressures, but changes to prograde by 500 MPa. Measurement uncertainties are approximately twice the size of the symbols. The data are from Holtz et al. (1995).

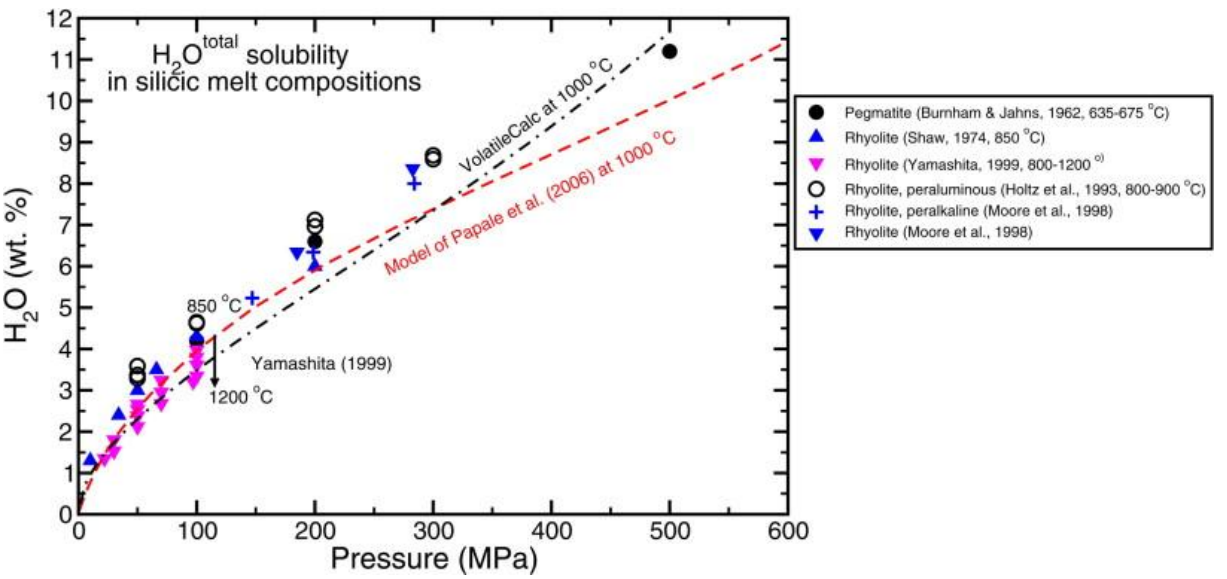

Fig. 4. Water solubility in natural silicic composition melts. The term total in this and subsequent figures indicates the total concentration of a volatile and represents the sum of all species of that volatile dissolved in the melt. Both measured solubilities (data points) and the solubility modeled for the rhyolitic melt of Tamic et al. (2001) at 1000 °C using volatilecalc (Newman and Lowenstern, 2002) and the model of Papale et al. (2006) are plotted. Uncertainties in the measurements are similar to the size of the symbols. Data sources for Fig. 4, Fig. 5, Fig. 6, Fig. 7 and Fig. 8 are discussed in the text.

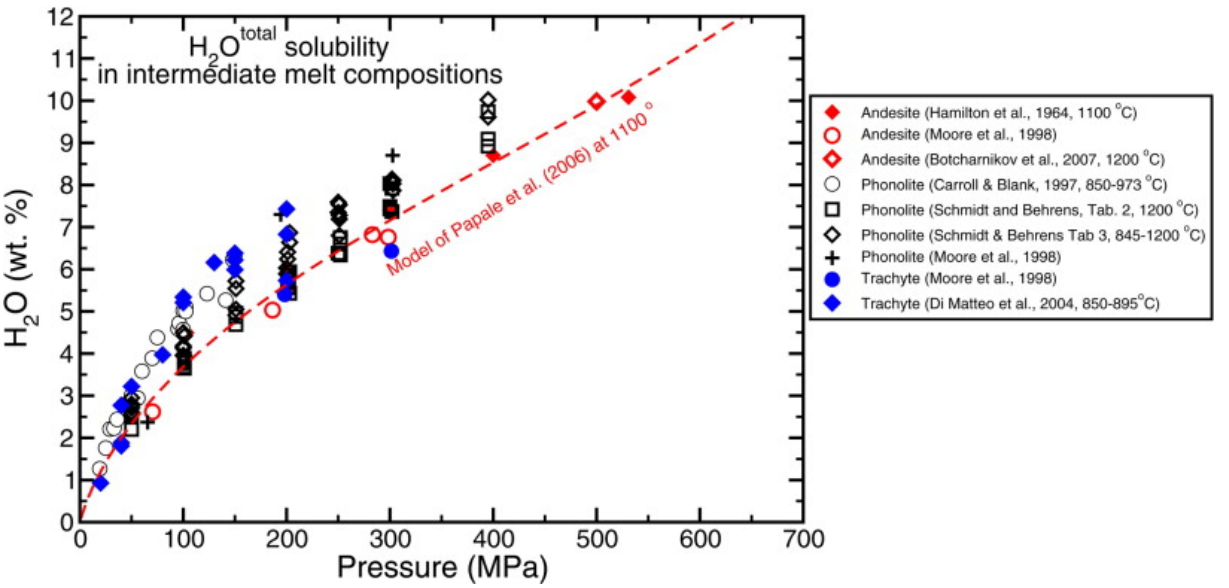

Fig. 5. Water solubility in natural intermediate composition melts. Both measured solubilities (data points) and the solubility modeled for the andesitic melt of Hamilton et al. (1964) at 1100 °C using the model of Papale et al. (2006) are plotted. Uncertainties in the measurements are similar to the size of the symbols.

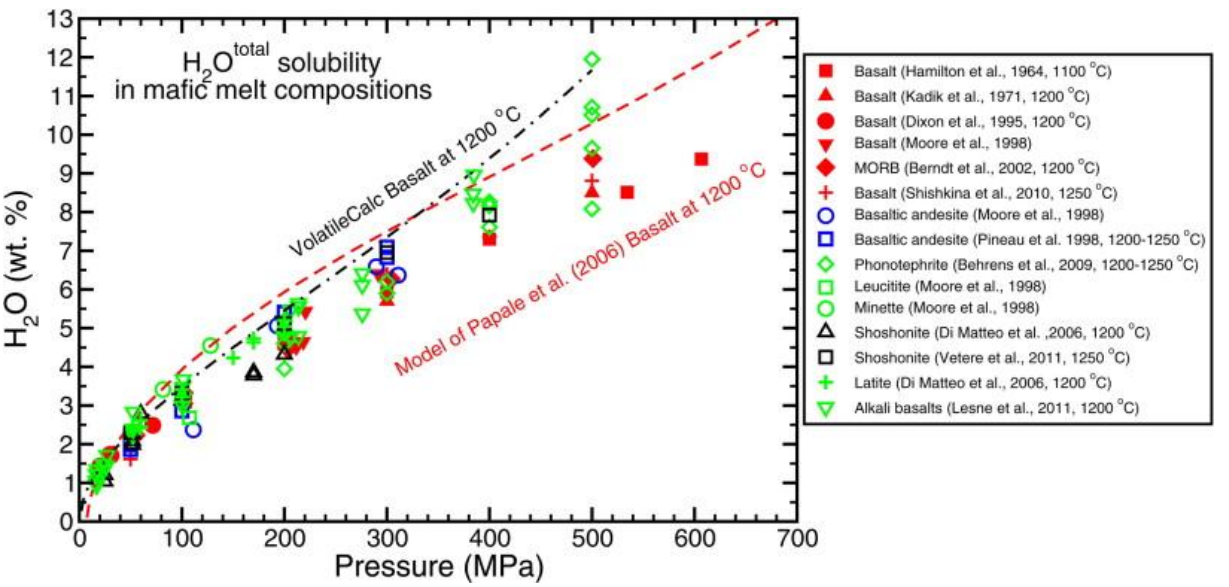

Fig. 6. Water solubility in natural mafic composition melts. Measured solubilities (data points) and the the solubility modeled for the basaltic melt of Hamilton et al. (1964) at 1200 °C using the model of Papale et al. (2006) and the water solubility for a basaltic melt with 49 wt.% SiO_2 calculated with volatilecalc (Newman and Lowenstern, 2002) are plotted. Uncertainties in the measurements are similar to the size of the symbols.

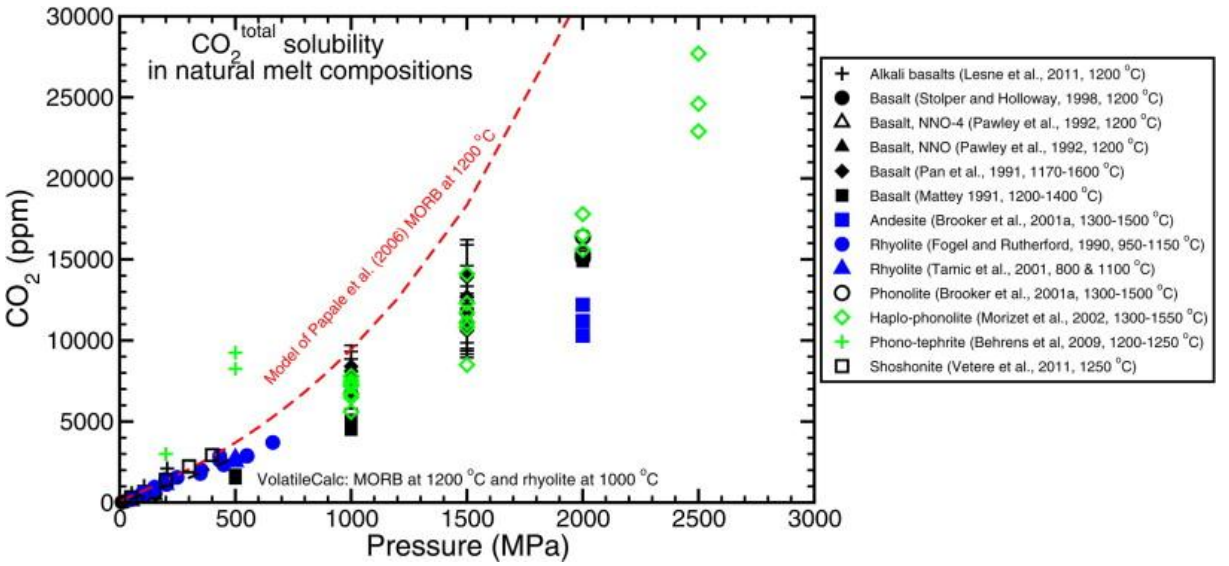

Fig. 7. Carbon dioxide solubility in natural melt compositions. Measurement uncertainties are shown for the data of Pan et al. (1991). Carbon dioxide solubilities calculated by volatilecalc and by the Papale et al. model for a mid-ocean ridge basalt (MORB) at 1200 °C are also plotted.

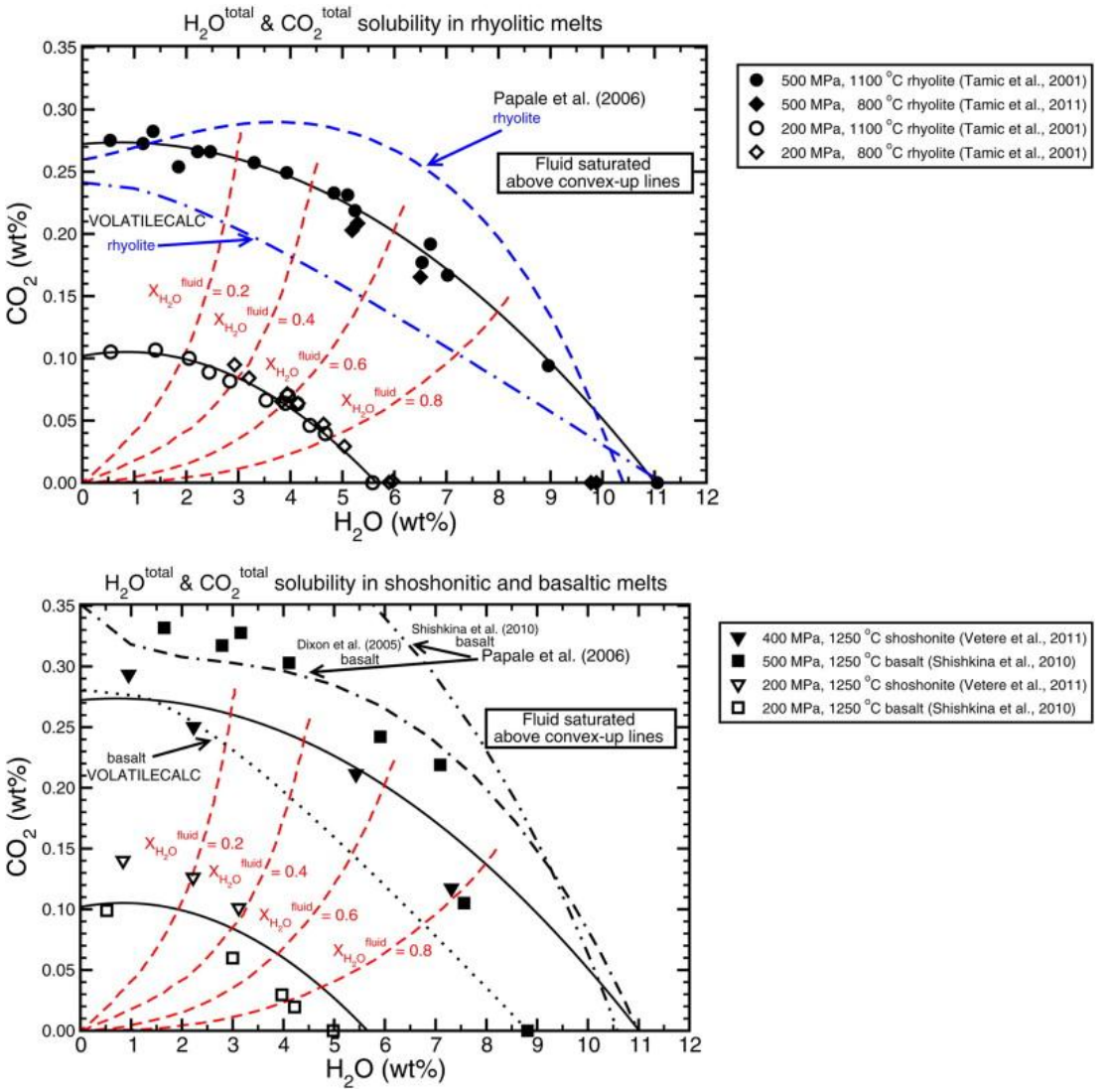

Fig. 8. Compositions of H_2O and CO_2 in melts coexisting with a mixed volatile fluid at 200 and 500 MPa (Tamic et al., 2001), a basaltic melt at 200 and 500 MPa (Shishkina et al., 2010), and a shoshonitic melt at 200 and 400 MPa (Vetere et al., 2011). a) Volatile solubilities in rhyolitic melts (Tamic et al., 2001) coexisiting with a CO_2-H_2O fluid. b) Volatile solubilities in basaltic and shoshonitic melts (Tamic et al., 2001) coexisiting with a CO_2-H_2O fluid. The uncertainties in the measurements are similar to the size of the symbols. Open symbols are used for measurements at 200 MPa and filled symbols are used for 400-500 MPa measurements; the black, solid lines in both figures are fit to the data of Tamic et al. (2001) at 200 and 500 MPa. The red, dashed lines in both figures define the molar composition of the CO_2-H_2O fluid phase (if any) coexisting with the fluid-saturated melts (Tamic et al., 2001). The concentrations of H_2O and CO_2 in fluid-saturated rhyolitic and basaltic melts at 500 MPa calculated by volatilecalc are shown by the blue dash-dot line and black dotted line, respectively. Similar concentrations in a rhyolitic melt at 500 MPa calculated by the model of Papale et al. (2006) are shown by the blue dashed line. The black dash-dot and black dash-dot-dot lines are the concentrations of H_2O and CO_2 calculated by the Papale et al. (2006) model for the basaltic melt studied by Dixon et al. (2005) and the one investigated by Shishkina et al. (2010), respectively. Each of the measured or calculated solubility lines (either black or blue) defines a curve that is convex up; at concentrations of CO_2 and H_2O below the curves the melts are fluid-undersaturated and therefore a separate fluid phase does not exist. Please see the text for more discussion.

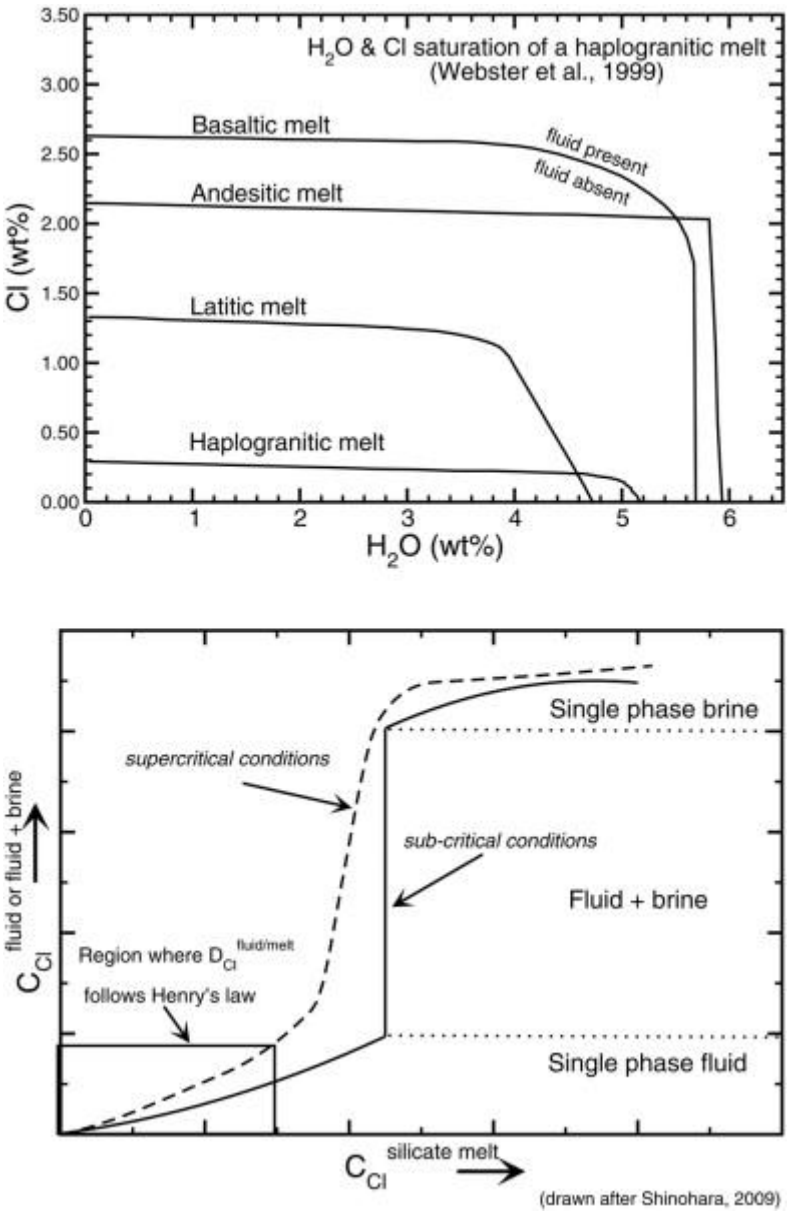

Fig. 9. a) Compositions of H_2O and Cl in natural melts of various compositions coexisting with a fluid composed of H_2O and Cl at 200 MPa and different temperatures. Data are from Webster et al. (1999). b) Schematic behavior of Cl partitioning between silicate melt, aqueous fluid and a chloride brine at high temperatures and pressures. The Cl concentrations for sub-critical conditions are shown with the solid lines and the phase fields for the aqueous and brine phases coexisting with the silicate melt are divided by the horizontal dotted lines. The Cl concentrations for supercritical conditions are shown with the dashed line. Please see text for further discussion.

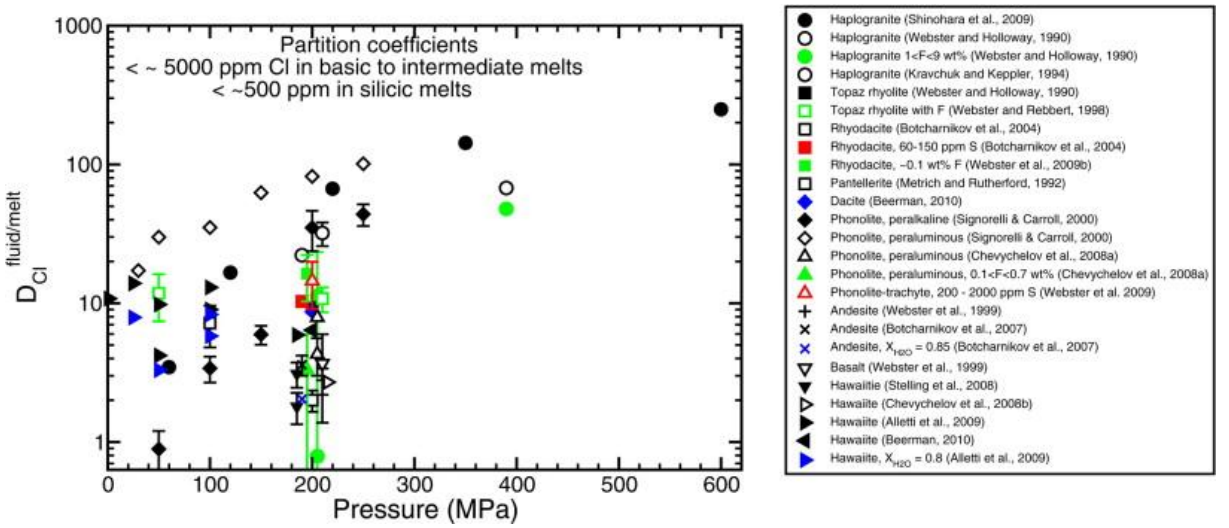

Fig. 10. Partitioning of chlorine between an aqueous fluid and basic to intermediate silicate melts with 5 000 ppm or less Cl and silicic melts with less than 500 ppm Cl as a function of pressure at experimental temperatures from ~ 800 to 1250 °C. Uncertainties based upon fits to the concentrations of Cl in melts and fluids are displayed for some of the measurements. Where no uncertainties are plotted they are typically twice the size of the symbols. Many of the partition coefficients measured at 200 MPa have been displaced by up to ± 15 MPa on the diagram in order to more clearly display the results. Please see the text for further discussion.

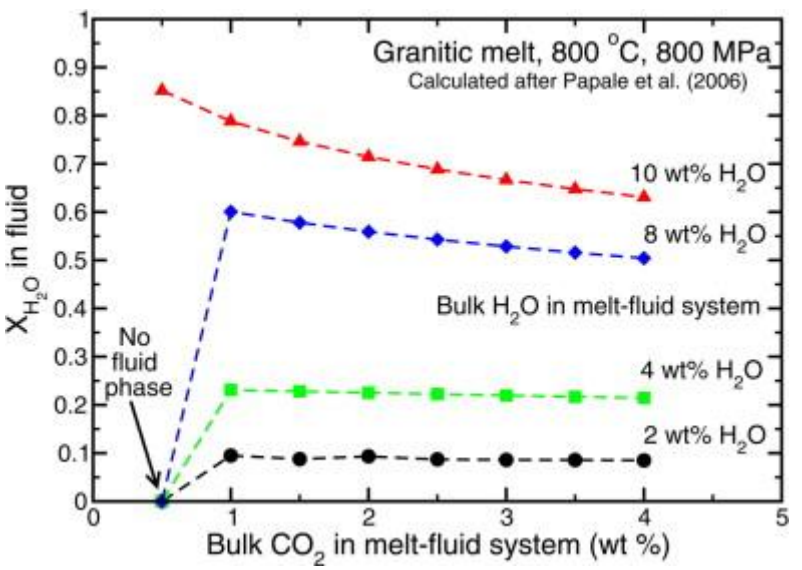

Fig. 11. Concentrations of water and carbon dioxide in fluids coexisting with a rhyolitic melt at 800 MPa, 800 °C calculated using the model of Papale et al. (2006). For CO_2 concentrations of 0.5 wt.% in the system composed of fluid + silicate melt no fluid phase exists, except when the water concentration is above approximately 9.5 wt%. Please see the text for further discussion of this model.

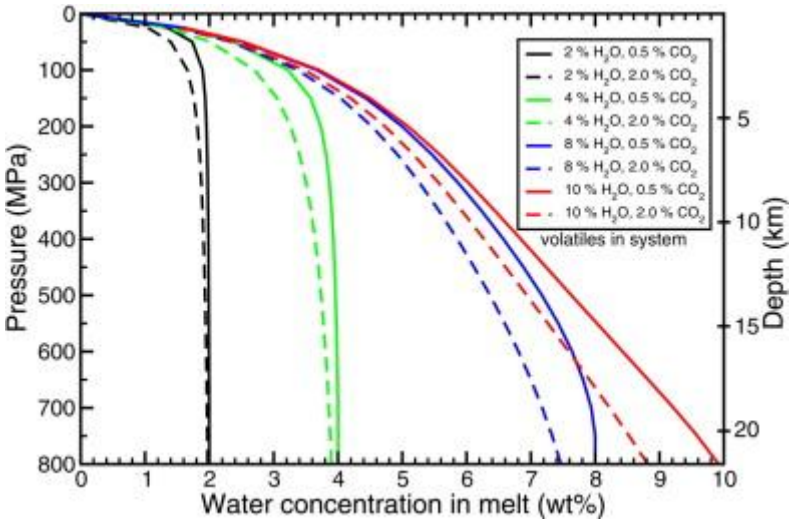

Fig. 12. Water concentration in a silicic melt during ascent calculated with the model of Papale et al. (2006). The temperature in the model is held constant at 800 °C and the system is closed to mass loss. Different combinations of water and carbon dioxide concentrations in the system were chosen based upon the results displayed in Fig. 11. The carbon dioxide concentrations in the melts fall from approximately 5 000 ppm to 15 ppm with decreasing pressure. The conversion of pressure to depth was made assuming a mean crustal density of 2 700 kg m^{-3} in this and subsequent figures.

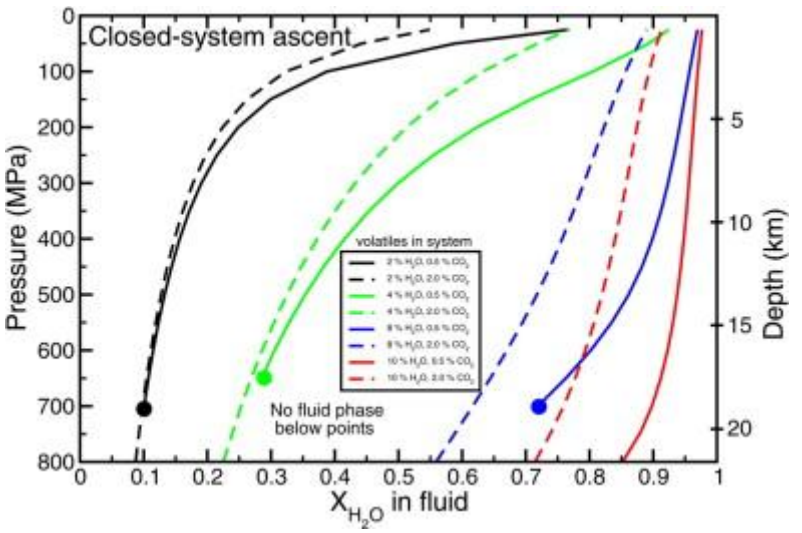

Fig. 13. Compositions of H_2O-CO_2 fluids coexisting with a silicic melt during isothermal ascent of a rhyolitic melt calculated with the model of Papale et al. (2006). Please see the text for further discussion.

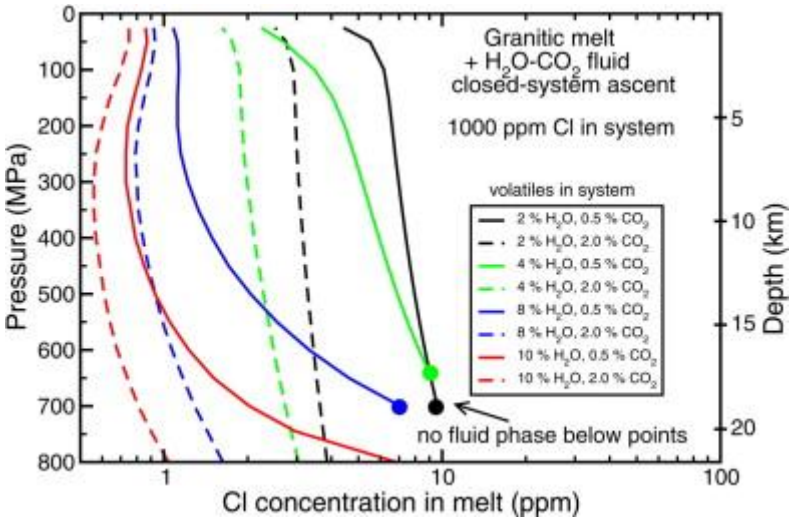

Fig. 14. Chlorine concentration in the rhyoltic melt during ascent based upon the measurements of Shinohara et al. (1989). The fluid phase scavenges almost all of the chlorine from the melt and probably ore metals bound to chlorine. The effects of pressure on the partition coefficient seen in Fig. 10 do not have a significant effect of the behavior of chlorine because at all conditions the modeled partition coefficient remains above 100.

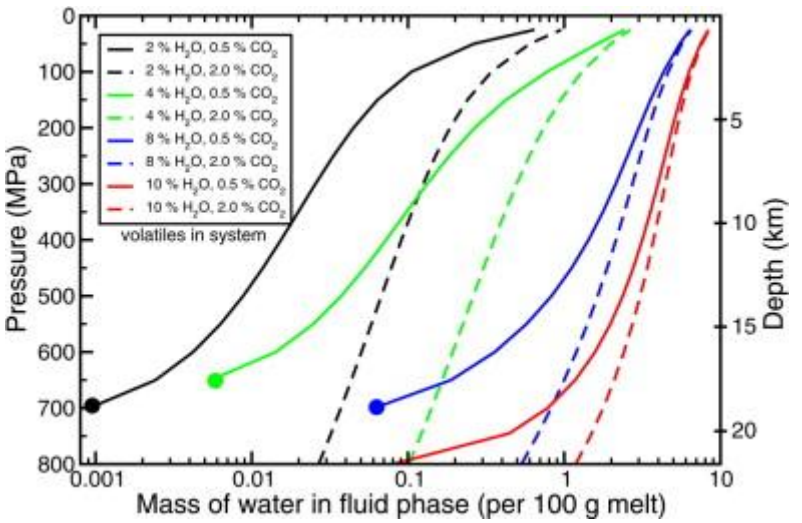

Fig. 15. Mass of the fluid phase exsolved from a silicic melt during ascent. The mass of the fluid phase increases significantly for magmas with low concentrations of volatiles during ascent, but the increase is less spectacular for magmas rich in volatiles because many volatiles exsolve at higher pressure. Nevertheless, magmas with larger concentrations of volatiles exsolve larger masses of fluids as required by the conservation of mass.

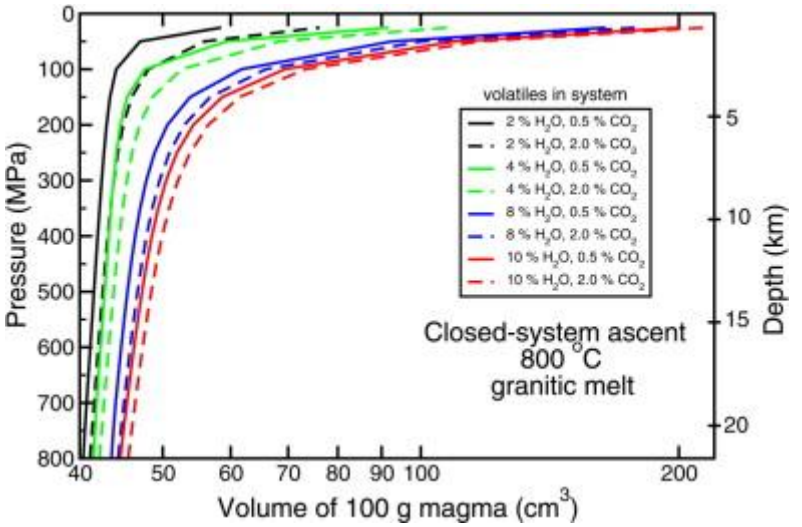

Fig. 16. Magma volume as a function of pressure at 800 °C. At high pressures, the fluid phase is minor and the volume of all the modeled rhyoltic volumes are similar. However, as pressure decreases and fluid exsolves from the melts, the volume becomes significant, particularly at pressures below approximately 200 MPa. This large volume increase may be responsible for the cracking of country rocks, loss of the volatile phase from the melt, and the formation of ore deposits (e.g., Burnham, 1979b).

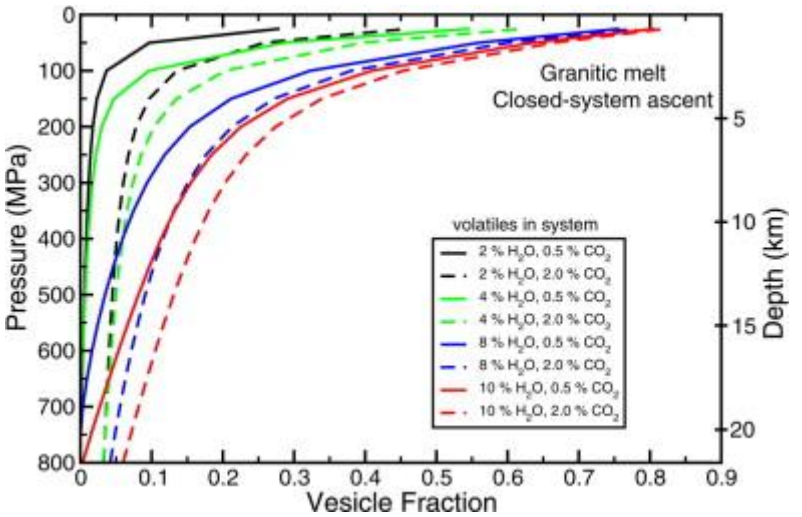

Fig. 17. Vesicularity of the modeled magmas as a function of pressure. Magmas with greater volatile concentrations exsolve more volatiles and achieve higher vesicularities than magmas with smaller volatile concentrations. The pressure range over which significant changes in the vesicularity occur is much larger for volatile-rich magmatic systems compared to systems with low-to-moderate volatile concentrations. The percolation threshold for spheres is at ~ 30 volume percent so that magmas with higher volatile concentrations reach this threshold and create an interconnected vesicle network at greater depth than magmas with low volatile concentrations.